Université de Montréal

Études des perméabilités membranaires des cellules de la macula densa

par

Mohamed Anuar Laamarti

Département de physiologie
Faculté de médecine

Thèse présentée à la faculté des études supérieures
En vue de l'obtention du grade de
Philosophiæ Doctor (Ph.D.)
en physiologie

Novembre 1997

Mohamed Anuar Laamarti

Université de Montréal

Faculté des études supérieures

Cette thèse intitulée :

Études des perméabilités membranaires des cellules de la macula densa

présentée par

Mohamed Anuar Laamarti

a été évaluée par un jury composé des personnes suivantes :

Président-rapporteur :	Michel Bergeron	Département de physiologie (Université de Montréal)
Directeur de recherche :	Jean-Yves Lapointe	Département de physique (Université de Montréal)
Membre du jury :	Jean-Louis Schwartz	Institut de biotechnologie (Montréal)
Examinateur externe :	Steven P. Nadler	Ottawa General Hospital (Université d'Ottawa)
Représentant du doyen :	René cardinal	Département de Pharmacologie (Université de Montréal)

SOMMAIRE

La rétroaction tubuloglomérulaire (RTG) est un mécanisme important dans le contrôle de la filtration glomérulaire et de l'hémodynamique rénale. Ce phénomène est relié aux cellules de la macula densa (MD) qui ont la capacité de détecter des changements dans la composition du liquide tubulaire et de transmettre cette information aux artérioles afférentes (AA) qui, en se contractant, diminuent le débit de filtration glomérulaire et augmentent la résistance hydraulique du rein. La nature du signal qui est envoyé des cellules de la MD vers les AA reste encore inconnue. On sait cependant que c'est une haute concentration de NaCl dans la lumière tubulaire qui déclenche la RTG, et que le cotransporteur $Na^+:K^+:2Cl^-$ est probablement le "sensor". Pour progresser dans l'étude de la RTG, une meilleure connaissance des cellules de la MD est absolument requise puisque c'est d'elles qu'origine le signal. La présente thèse a pour but de contribuer à une meilleure identification et à la caractérisation des propriétés membranaires des cellules de la MD.

Dans un premier temps, à l'aide de la technique de patch clamp en "single channel" nous avons mis en évidence une grande densité de canaux K^+ dans la membrane apicale. Nous montrons que ce type de canal est sensible au pH et au Ca^{2+} mais insensible à l'ATP. Dans un second temps, nous optons pour la technique de microperfusion de tubule isolé combinée à la microfluorimétrie. Nous démontrons ainsi la présence d'un échangeur $Na^+:H^+$ à la membrane apicale qui répond à toute variations de la concentration luminale de Na^+ et de NaCl ($[Na^+]_l$ et $[NaCl]_l$). Par ailleurs, en utilisant les effets secondaires du contransporteur $Na^+:K^+:2Cl^-$ sur le pH_i, nous

démontrons que ce transporteur s'équilibre lorsque $[NaCl]_l$ atteint 18 mM. Ainsi, nous concluons que dans les conditions physiologiques le cotransporteur produit une réabsorption de NaCl mais en opérant très près de son équilibre.

Dans un troisième temps, nous utilisons une méthode dont nous avons établi la faisabilité pour les cellules de la MD, et qui est basée sur l'utilisation de NH_4^+ pour déterminer l'amplitude de certains flux. Nous démontrons que le NH_4^+ entre dans les cellules par le cotransporteur $Na^+:K^+:2Cl^-$ et par un transporteur sensible au Ba^{2+}, et en sort, lors du retrait de NH_4^+ luminal, exclusivement sous forme de NH_3 et de H^+. Bien que la nature du transporteur sensible au Ba^{2+} n'ait pu être résolue de façon définitive, nous démontrons qu'elle ne correspond ni au canal K^+ ni à l'échangeur $K^+/(NH_4^+)H^+$. Ces études nous ont toutefois amené à présenter pour la première fois un modèle qui permet d'évaluer quantitativement les mesures de taux d'acidification (dpH_i/dt) et d'en tirer des mesures de flux. Grâce à ce modèle, nos données montrent que la membrane apicale est très perméable au NH_3 et, contrairement à ce qu'il a été admis jusqu'à présent, le flux de NH_4^+ n'est pas égal au flux de protons mesuré mais lui est plutôt 2 à 3 fois supérieur. Enfin, dans un dernier temps, nous avons montré que le cotransporteur a une haute affinité pour le Na^+ et pour le Cl^-. Nous avons aussi commencé à étudier les facteurs régulateurs de ce cotransporteur en observant une inhibition de 40 % du cotransport suite à l'augmentation de la $[Cl^-]_i$ par inhibition de sa sortie basolatérale (10 µM NPPB). De plus, l'ajout de dbAMPc + forskoline stimule la conductance basolatérale au Cl^- mais inhibe faiblement le cotransporteur apical.

En conclusion, nous considérons que ces études ont significativement contribué à l'amélioration de nos connaissances sur les cellules de la MD et à

la progression dans la compréhension de la RTG, puisque nous sommes maintenant en position de spéculer avec un peu plus de précision sur les effets secondaires d'une augmentation de $[NaCl]_l$.

TABLE DES MATIÈRES

LISTE DES FIGURES

LISTE DES ABRÉVIATIONS

AA	artériole afférente
AE	artériole efférente
ATP	adénosine triphosphate
BCECF	2',7'-bis-(2-carboxyethyl)-5(and-6) carboxyfluorescein
CCD	canal collecteur cortical
CMD	cellule de la macula densa
CNT	canal connecteur
COX	cyclooxygénase
DCT	tubule contourné distal
G	glomérule
GC-s	guanylate cyclase soluble
GFR	débit de filtration glomérulaire
20-HETE	acide 20-hydroxyeicosatetraenoique
MCD	canal collecteur médullaire
MD	macula densa
ME	mésangium extraglomérulaire
NO	oxyde nitrique
NOS	oxyde nitrique synthétase
NPPB	inhibiteur de canaux chlore
PCT	tubule contourné proximal
PG	prostaglandine
PLA_2	phospholipase A_2
PR	*pars recta* (partie droite du tubule proximal)

RAS	système rénine angiotensine
ROMK	canal K^+ à rectification entrante sensible à l'ATP
RTG	rétroaction tubuloglomérulaire
SNGFR	débit de filtation glomérulaire du néphron individuel
STP	stop flow pressure
TAL	branche ascendante large de l'anse de Henle
cTAL	branche ascendante large corticale de l'anse de Henle
mTAL	branche ascendante large médullaire de l'anse de Henle
Tx	thromboxane
Vm	potentiel membranaire

REMERCIEMENTS

J'adresse mes remerciements les plus sincères à Jean-Yves Lapointe, mon directeur de recherche, pour m'avoir accueilli dans son laboratoire, pour la formation scientifique acquise sous sa direction. Je le remercie grandement pour la confiance qu'il m'a accordée, son amitié et son appui soutenu tout le long de mes études supérieures.

Je remercie Bernadette Wallendorf, Pierre Bissonnette, Fairouz Jalal, Xing-Zhen Chen, Michael Coady et Emmanuelle Brochièro pour leur amitié et leur soutien.

Finalement, je tiens à remercier tous les membres du groupe de recherche en transport membranaire.

DEDICACE

À mon père qui nous a quittés

À Jamila, Malak et Doha.

A. INTRODUCTION

INTRODUCTION

Les reins sont constitués par la juxtaposition d'un système de tissu épithélial arrangé sous forme de tubule, les néphrons, et d'un système vasculaire spécialisé formé de deux réseaux de capillaires successifs permettant des échanges d'eau et d'électrolytes entre les deux compartiments. Chez l'homme adulte, chaque rein pèse environ 150 g et contient environ un million de néphrons; la longueur totale d'un néphron varie entre 20 et 44 mm. Macroscopiquement, on peut distinguer deux zones concentriques : le cortex, zone la plus superficielle, et la médullaire, plus profonde. La partie de la médullaire qui fait plus au moins saillie dans les cavités excrétrices est appelée papille. A chaque jour 150 à 180 litres de plasma sont filtrés par les glomérules, ce qui rend l'homme vulnérable à la déplétion volumique, et fortement dépendant du maintien d'un fort taux de réabsorption tubulaire. L'homéostasie du milieu intérieur est donc assurée par de multiples mécanismes qui maintiennent un équilibre entre la charge filtrée et le taux de réabsorption tubulaire. Chaque néphron comporte un glomérule, siège de la filtration glomérulaire, première étape de la formation de l'urine, et un tubule composé de plusieurs segments, définis par les caractères de l'épithélium qui les compose et par leur position dans le rein (Fig. 1). Une partie du tubule est constituée par une anse plus au moins longue, dite anse de Henle, s'enfonçant dans la médullaire et remontant ensuite dans le cortex. Dans tous les cas, la branche large ascendante de l'anse vient au contact du pôle vasculaire de son propre glomérule, formant ainsi l'appareil juxtaglomérulaire. Ce lieu est tout à fait particulier puisque c'est là que ce rejoignent les deux réseaux successifs de

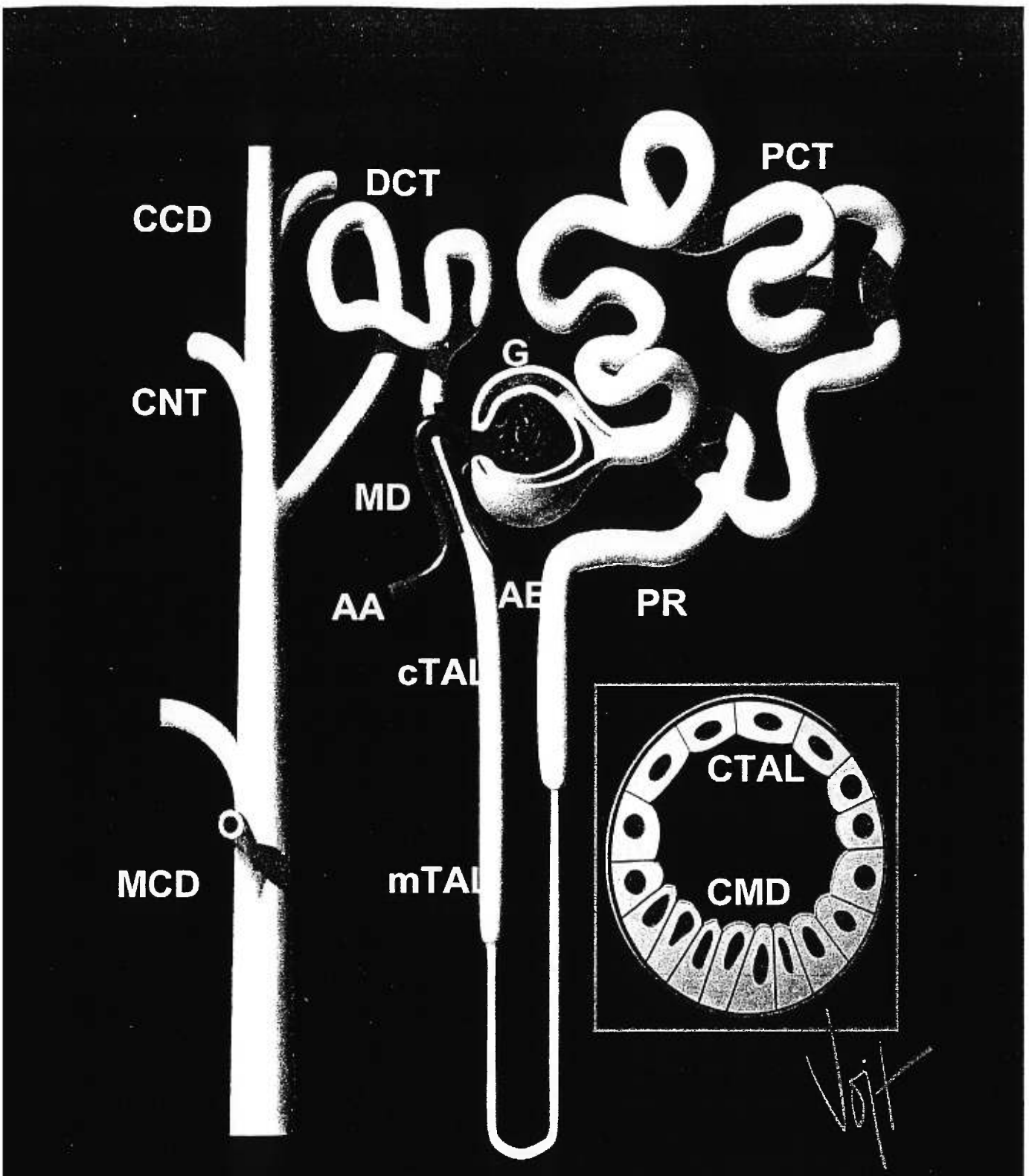

Figure 1. Description anatomique du néphron

http://www.vet.ohio-state.edu/docs/vojt/jpeg5.html

capillaires et c'est là que débute le néphron. A l'endroit exact où l'anse de Henle fait contact avec le glomérule, les cellules épithéliales de l'anse se transforment, s'épaississent et forme une plaque appelée macula densa (MD).

I. APPAREIL JUXTAGLOMÉRULAIRE

1. Anatomie

Au niveau du glomérule les artérioles afférente et efférente forment avec le tube distal un compartiment cunéiforme où l'on trouve trois types cellulaires qui sont particuliers à l'appareil juxtaglomérulaire (Fig.2). Premièrement on a les cellules de la macula densa qui bordent une partie de la paroi de l'anse de Henle. Ces cellules s'appuient en coussin sur un paquet étroit de cellules interstitielles spécialisées: les cellules Goormaghtigh ou encore appelées cellules du lacis. Du fait que ces cellules sont indistinctes des cellules mésangiales quant à leur structure fine (66) et du fait qu'elles se prolongent dans le mésangium, on les considère parfois comme étant des cellules mésangiales extraglomérulaires. Le troisième type de cellules de l'appareil juxtaglomérulaire, dites granulaires, est situé au milieu de la paroi de l'artériole afférente. Riches en grains de sécrétion, elles sont responsables de la production de rénine.

a. Macula densa

La macula densa est une plaque de cellules épithéliales (~30 cellules), située peu avant la transition entre l'anse large ascendante (TAL) et le tube contourné distal. Les cellules de la macula densa reposent sur une membrane basale épaisse et irrégulière qui s'appuie contre la couche de cellules mésangiales extraglomérulaires. Ces cellules sont en continuité (c'est-à-dire liées par "gap junctions") avec les cellules mésangiales intraglomérulaires et les cellules musculaires lisses des artérioles afférente et efférente. La surface de la macula densa s'étend souvent au delà des limites du mésangium extraglomérulaire (29).

Les cellules de la macula densa diffèrent des cellules tubulaires avoisinantes. Elles sont plus grandes que les cellules de l'anse large ascendante, possèdent un important noyau et leur membrane apicale est dépourvue de la glycoprotéine Tamm-Horsfall (2,149). Aussi, dans la plupart des cellules rénales, la membrane basolatérale forme des interdigitations dirigées vers l'intérieur et entre lesquelles on trouve une rangée de mitochondries. Ces interdigitations amplifient la surface de la membrane basolatérale et avec les mitochondries adjacentes augmentent la capacité de transport. Dans les cellules de la macula densa, ces interdigitations n'existent pas, mais on trouve des saillies de la membrane basolatérale à travers la membrane basale et dans l'espace occupé par les cellules mésangiales extraglomérulaires. Des études morphologiques (21) sur la membrane basale de la MD appuient cette observation. Cependant, l'existence de surface de contact spécialisée entre la MD et les cellules mésangiales extraglomérulaire n'a

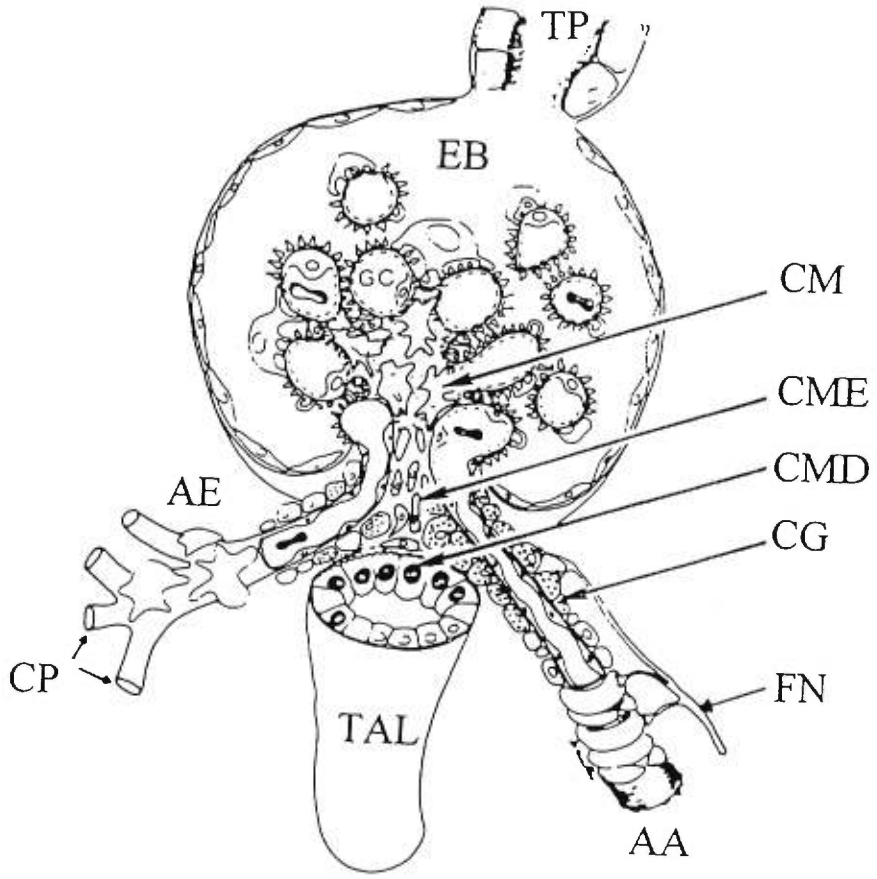

Figure 2. Structure de l'appareil juxtaglomérulaire. AA, artériole afférente; AE, artériole efférente; CME, cellule mésangiale extraglomérulaire; CMD, cellule de la macula densa; CG, cellule granulaire; MC, cellule mésangiale intraglomérulaire; TAL, branche ascendante large de l'anse de Henle; FN, fibre nerveuse; EB, espace de Bowman; TP, tubule proximal; CP, capillaire péritubulaire (tiré de Barajas 1997).

jamais été clairement démontrée. Bien que les gap junctions soient abondantes entre les cellules vasculaires, on ne les a jamais trouvées entre les cellules de la MD et les cellules mésangiales extraglomérulaires (3,153). Par rapport au noyau, l'appareil de Golgi est localisé du côté basal dans les cellules de la MD alors qu'il se trouve du côté apical dans toutes les autres cellules tubulaires rénales. Les mitochondries, bien que nombreuses, ne sont pas en contact avec la membrane basolatérale mais sont entièrement dispersées dans le cytosol (113). Les mesures microenzymatiques de la Na^+-K^+-ATPase rapportées par unité de volume cellulaire ont révélé une activité enzymatique faible (143), correspondant à 1/40 de celle trouvée dans la TAL (36). Des taux faibles de la Na^+-K^+-ATPase dans la membrane basale des cellules de la MD ont été aussi démontrés à l'aide d'anticorps monoclonaux contre l'enzyme (71). Cette faible activité Na^+-K^+-ATPasique a d'ailleurs été corrélée avec le faible niveau des enzymes du cycle de Krebs (79).

La différence la mieux établie de point de vue biochimique entre la MD et les cellules tubulaires avoisinantes se rapporte à l'activité du glucose-6-phosphate déshydrogènase (G6PD), l'enzyme qui dirige l'entrée du glucose dans la voie des pentoses (54). Des études microenzymatiques indiquent que l'activité de la G6PD dans la MD excède d'un facteur 2 celle mesurée dans le tubule proximal, et d'un facteur 3 celle mesurée dans le tubule distal (112). Chez certaines espèces l'activité anhydrase carbonique est plus élevée dans la MD que dans la TAL (87).

Une autre caractéristique morphologique et fonctionnelle des cellules de la MD concerne la perméabilité à l'eau. Comme il a été décrit précédemment, les cellules de la MD ne possèdent pas la protéine

Tamm-Horsfall, présente au niveau de la membrane apicale des cellules de l'anse large ascendante. Cette protéine pourrait être responsable de l'imperméabilité à l'eau de l'anse large ascendante (149). De larges espaces intercellulaires ont été observés entre les cellules de la MD (67,134). Ces espaces ressemblent à ceux observés entre les cellules du tube collecteur en présence d'un gradient osmotique et d'ADH (176). Cette ressemblance d'une part, et l'hypotonicité du liquide tubulaire qui passe au niveau de la MD d'autre part, laissent penser que les cellules de la MD seraient perméables à l'eau. Cette prédiction a trouvé un appui dans les travaux de Kaissling et Kriz (67) qui ont démontré un rétrécissement des espaces intercellulaires en présence de furosémide ou en hypertonicité luminale. Aussi, Kirk et coll. (77) ont démontré sur une préparation de tubule isolé que l'épaisseur de l'espace entre les cellules de la MD augmente lorsque le liquide tubulaire devient hypotonique. Aucun changement n'a été observé dans l'espace entre les cellules de l'anse large ascendante dans des conditions similaires. Ces études suggèrent que la MD constitue un îlot de cellules perméables à l'eau situé dans une anse large ascendante imperméable à l'eau.

b. Cellules mésangiales extraglomérulaires

Le mésangium extraglomérulaire (ME), localisé entre l'artériole afférente et l'artériole efférente, est en contact direct avec la MD. Les cellules mésangiales extraglomérulaire (cellules Goormaghtigh) sont de petite taille (151) et sont considérablement couplées par des gap junctions entre elles, avec les cellules mésangiales intraglomérulaires ainsi qu'avec les cellules

musculaires lisses des artérioles afférente et efférente (20,125,153). Il n'y a pas de gap junctions entre la MD et le ME ou les artérioles. L'anatomie et la position des cellules mésangiales extraglomérulaires nous donne la nette impression qu'il s'agirait de cellules réceptrices pouvant transmettre de l'information à partir de la MD jusqu'à l'AA, suite à la détection du signal luminal.

c. Cellules granulaires

Les cellules granulaires, encore appelées cellules épithélioïdes, sont localisées dans la paroi de l'artériole afférente, plus précisément dans la partie distale (juxtaglomérulaire). Ces cellules sont à l'origine des cellules musculaires lisses qui ont été complètement transformées. La présence d'un reticulum endoplasmique développé et de granules cytoplasmiques liées à la membrane est compatible avec une structure de cellules sécrétrices de protéines (66,85). En fait, ces cellules produisent la rénine. Toutefois, ce n'est pas le seul site de production car on retrouve cette hormone un peu plus loin dans les cellules intermédiaires de l'AA. Par ailleurs, dans les conditions de stimulation du RAS, on trouve la rénine tout au long de l'AA ; on pense que cette particularité est due à la transformation des cellules musculaires lisses en cellules granulaires sécrétrices de rénine et pauvres en myosine (155).

2. Rôle physiologique

Depuis l'identification de l'arrangement anatomique de l'appareil juxtaglomérulaire il y a environ 100 ans, plusieurs physiologistes ont tenté de décrire un éventuel mécanisme local de régulation du débit sanguin glomérulaire (43,94). Les premières théories concernant le rôle de cet arrangement anatomique très spécial sont apparues dans les années 60. La théorie de Thurau, énoncée en 1964 (156) contenait cinq propositions principales:

1) le taux de filtration glomérulaire d'un néphron unique (SNGFR) est influencé par la composition du liquide tubulaire qui passe devant les cellules de la MD.

2) le signal détécté par les cellules de la MD est la concentration luminale du Na^+ ($[Na]_l$) : une augmentation de $[Na]_l$ produisant une réduction de SNGFR.

3) le SNGFR varie en fonction des changements de résistance de l'AA.

4) le tonus vasculaire est contrôlé par le système rénine-angiotensine.

5) ce mécanisme est responsable de l'autorégulation du flux sanguin rénal et du taux de filtration glomérulaire.

Dès 1965, ces propositions ont été testées expérimentalement par Thurau et Schnermann (157) et l'existence d'une rétroaction négative du fluide distal sur le taux de filtration glomérulaire a été mise en évidence. Depuis, il s'est passé plus de trente années d'expérimentation qui ont permis d'appuyer solidement plusieurs de ces propositions (8,12) et d'apporter des nuances à certaines autres. Par exemple, on reconnait généralement aujourd'hui que la $[NaCl]_l$

(plutôt que $[Na^+]_l$) constitue le facteur détecté par les cellules de la MD. D'autre part, les cellules de la MD sont aussi responsables du déclenchement de la libération de rénine par les cellules granulées de l'AA (164), mais l'angiotensine qui sera ainsi générée est plutôt considérée comme un élément modulateur du signal envoyé par les cellules de la MD aux éléments contractiles de l'AA (108), la nature du signal étant toujours débattue (14,35,145).

a. sécrétion de rénine

La rénine est un enzyme protéolytique qui est libéré à partir des cellules granulaires de l'AA, suite à divers stimuli. Une fois dans la circulation, la rénine clive la liaison leucine-leucine de son substrat, l'angiotensinogène, pour former un décapeptide, l'angiotensine I, qui est biologiquement inactif. Deux résidus amino acide supplémentaire sont ensuite clivés par l'enzyme de conversion pour former un octapeptide actif, l'angiotensine II. Le système rénine-angiotensine joue un rôle vital dans la régulation de la pression sanguine et dans la régulation du volume du liquide extracellulaire par son effet sur le tonus vasculaire et le transport épithélial du tubule proximal (52,72). En général, la sécrétion de la rénine est gouvernée par trois mécanismes séparés: 1) le tonus sympathique; 2) le mécanisme de barorécepteur sensible aux altérations de la pression sanguine et 3) le mécanisme de rétroaction tubuloglomérulaire sensible aux changements de la composition du liquide tubulaire (52,72).

En 1939, Goormaghtigh a proposé pour la première fois que la libération de la rénine pourrait être influencée par la composition du liquide tubulaire au niveau de la MD. Quelques années plutard, Vander (164) a suggéré une relation inverse entre la [NaCl] au niveau de la MD et la sécrétion de rénine. Cependant, les études de microponctions (100) ont conduit à différentes conclusions: l'augmentation de la [NaCl] au niveau de la MD entraîne une augmentation de la sécrétion de la rénine. Aujourd'hui, grâce à la technique de microperfusion in vitro (88,150) il est définitivement admis que la sécrétion de rénine est inhibée par une augmentation de [NaCl] luminale.

Il existe maintenant suffisamment de preuves en faveur de l'hypothèse qui stipule que le signal détecté par la MD pour contrôler la sécrétion de rénine est le changement de transport de NaCl à travers le cotransporteur apical $Na^+:K^+:2Cl^-$, dont l'activité physiologique est surtout déterminée par la $[Cl^-]_l$ étant donné que les sites pour le Na^+ et le K^+ sont généralement saturés en conditions physiologiques.

b. Rétroaction Tubuloglomérulaire

La relation anatomique entre les cellules de la MD, la TAL, le mésangium extraglomérulaire, l'AA et le glomérule constitue une base morphologique pour le mécanisme de la rétroaction tubuloglomérulaire. Dans les conditions normales, une augmentation de la filtration glomérulaire entraîne une augmentation du débit luminal (53). L'augmentation du flux dans l'anse de Henle a pour conséquence une diminution de la réabsorption ionique par unité de volume de fluide tubulaire et donc une augmentation de la

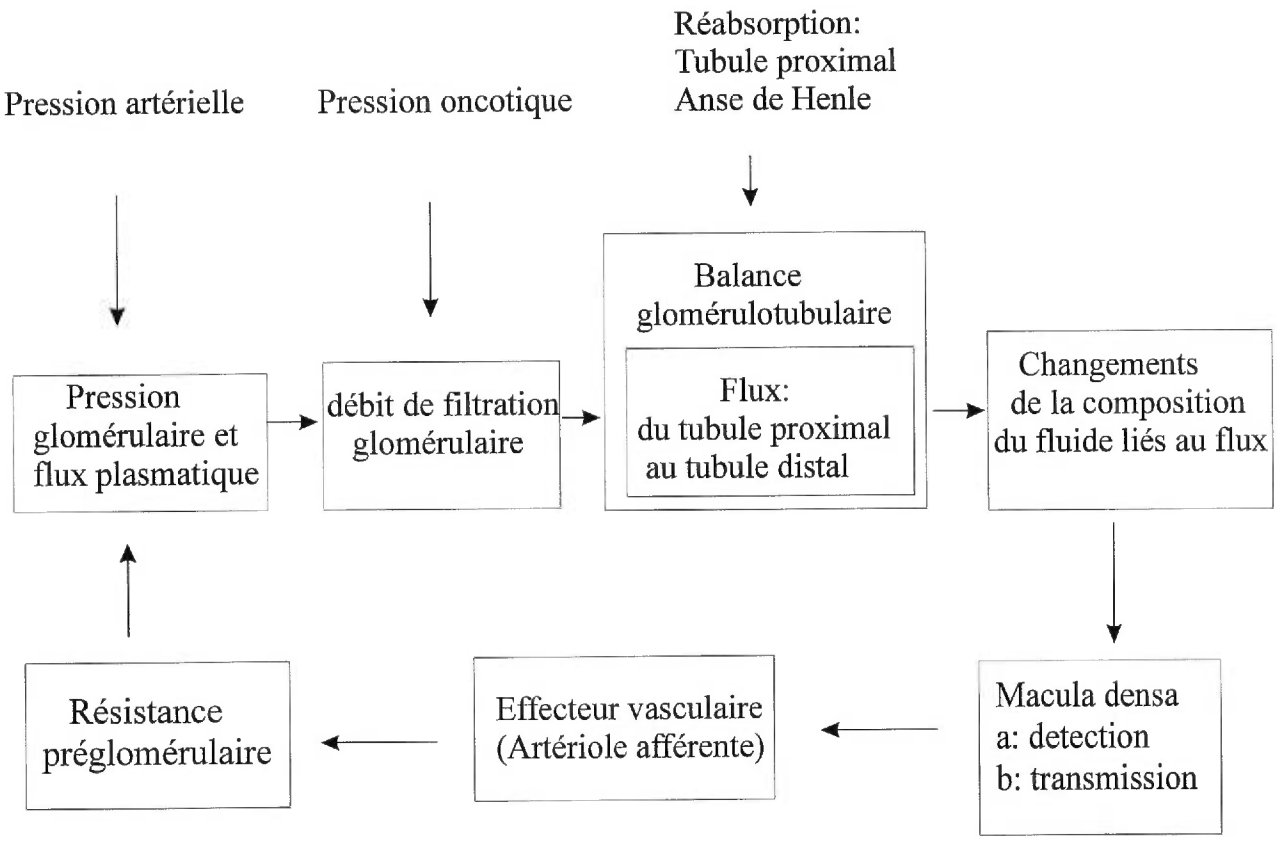

Figure 3. Schéma montrant les composantes du mécanisme de la rétroaction tubuloglomérulaire (traduit de Braam et coll. 1993)

concentration de Cl^- (6,145), de Na^+ (48) et de l'osmolarité (6). Ces changements sont détectés par la MD, qui réagit en modifiant le taux de libération d'une substance médiatrice "non identifiée" (109). Celle-ci entraîne la vasoconstriction de l'AA, diminue la filtration glomérulaire, et restaure les concentrations ioniques luminales au niveau de la MD. Le mécanisme de RTG est illustré à la Figure 3. La RTG peut être mesurée par la technique de microponction in vivo en perfusant de façon orthograde ou rétrograde l'anse de Henle. Dans le cas de la microponction orthograde, par exemple, on repère dans un premier temps les convolutions proximales et distales du même néphron à l'aide d'un colorant perfusé dans un tubule choisi au hasard. Dans un deuxième temps, on bloque le tubule proximal avec de l'huile et, à l'aide d'une pipette placée à proximité du glomérule, on mesure la pression dans la lumière du tubule proximal : "*stop flow pressure*" (SFP). Cette pression est équivalente à la pression qui règne dans les capillaires glomérulaires. Une troisième pipette est placée en amont de la goutte d'huile, qui sert à perfuser l'anse de Henle. Finalement, en faisant varier le taux de perfusion, on influence la composition ionique au niveau des cellules de la MD. La SFP mesurée dans ces conditions en fonction du taux de perfusion constitue la détermination classique de la RTG.

Sur une préparation de néphron juxtamédulaire, Casellas et Moore (28) ont démontré que la perfusion de la MD avec une solution de Ringer provoque une vasoconstriction localisée du segment de l'AA proche du glomérule; la réponse a été inhibée par le furosemide luminal. Dans des études de perfusion de l'AA et la MD, Ito et Carretero (61) ont démontré une vasoconstriction de la portion terminale de l'AA, lorsque la solution de perfusion de la MD fut

changée d'une solution hypotonique à une solution isotonique de NaCl. L'addition du furosemide bloque complètement la vasoconstriction de l'AA (28). Persson et coll. (123) ont aussi démontré que le calcium cytosolique de l'AA augmente lorsque les cellules de la MD sont exposées à une solution isotonique de NaCl. L'ensemble de ces résultats indique que le segment terminal de l'AA est la cible principale du signal de la RTG. Cependant, les études immunohistochimiques de Taugner et coll. (154) ont démontré que cette portion terminale de l'AA est pauvre en myosine et semble être non contractile. Jusqu'à date le problème n'est pas encore résolu, mais il est vraissemblable que la partie terminale de l'AA ne nécessite qu'une faible quantité de myosine pour se contracter.

Une question autour de laquelle un consensus s'est développé, c'est que l'augmentation de la résistance vasculaire de l'AA dépend de l'influx du calcium via les canaux Ca^{2+} voltage dépendants (28,110). Mitchell et Navar (98) ont démontré que les bloqueurs de canaux Ca^{2+} atténuent fortement la diminution de la pression glomérulaire et de la SNGFR consécutive à l'augmentation du flux luminal dans l'anse de Henle. Plus récemment, Ogasawara et coll. (115) ont démontré que le bloquage du canal Ca^{2+} par la nifedipine empêche la réponse vasoconstrictrice à la perfusion intra-artérielle de NaCl hypertonique. Ce résultat renforce davantage l'hypothèse du rôle des canaux Ca^{2+} voltage dépendants dans le mécanisme de la RTG.

Une relation entre la concentration de NaCl luminale et le SNGFR a été observée pour la première fois par Schnermann et Wright (135) dans leur étude de microponction orthograde. Cependant, cette hypothèse n'a pas été

admise à l'unanimité. Pour la vérifier, l'anse de Henle a été perfusée de façon rétrograde à partir du tubule distal. Dans ces conditions où la composition ionique au niveau de la MD est identique à celle du liquide de perfusion, le SNGFR varie inversement avec la $[NaCl]_l$ (136). L'implication du NaCl dans la RTG a été renforcée lorsque Wright et Schnermann (177) ont démontré une inhibition de la RTG par le furosémide. Cette observation a été à l'origine de l'hypothèse du transport de NaCl par le cotransporteur $Na^+:K^+:2Cl^-$ comme étape initiale de la génération de la RTG.

Dans des études de microperfusion rétrograde, Schnermann et coll (136) ont obtenu des indications suggérant que l'initiation du signal de la RTG dépend de la présence de Cl^- et non pas du Na^+. Cette différence est due au fait que le cotransporteur $Na^+:K^+:2Cl^-$ a une forte affinité au Na^+ et une faible affinité au Cl^- (46). Ainsi, dans les solutions dépourvues de Na^+, il entre suffisamment de cet ion pour saturer le cotransporteur.

Plutard, Seney et Wright (148) ont démontré que la RTG nécessite la présence simultanée de Na^+ et de Cl^- , et que la réponse maximale est obtenue à 60 mM de NaCl. De plus, lorsque le Na^+ est complètement retiré de la solution de perfusion, aucune réponse de la RTG n'a été observée, et ceci même en présence de 60 mM de Cl^-. De la même façon, Boberg et al (18,19) arrivent à la même conclusion, à savoir un effet synergique de Na^+ et de Cl^- sur la RTG.

D'autres chercheurs ont longtemps défendu l'idée que c'était l'osmolarité qui était en fait détectée (6,7,106,107). Cette hypothèse est supportée par d'autres études (67,77) qui ont indiqué que les cellules de la MD sont perméables à l'eau.

Kirk et coll (77), en utilisant la technique de tubule perfusé, ont évalué la sensibilité des cellules de la MD aux changements de l'osmolarité. La réduction de l'osmolarité luminale entraîne une dilatation des espaces intercellulaires latérales et une légère augmentation de l'épaisseur des cellules de la MD. Ce résultat, suggère que la MD soit perméable à l'eau. Gonzalez et coll (38,39) ont observé un faible flux d'eau à travers les cellules de la MD. Dans la mesure où ce segment est perméable à l'eau, le flux d'eau varierait en fonction du gradient osmotique transépithélial. Ainsi, dans les conditions où le liquide tubulaire est hypotonique, un flux net d'eau se produirait à partir de la lumière tubulaire, à travers les espaces latérales dans l'interstitium du complexe juxtaglomérulaire.

La taille des espaces latéraux entre les cellules de la MD semble aussi dépendre des fonctions de transport de ces cellules. Cette notion a reçu un appui considérable par l'étude chez le rat où on a montré une réduction de la largeur de ces espaces à la suite d'un traitement au furosémide (96).

Aujourd'hui, cette idée de l'osmolarité comme signal détecté par les cellules de la MD a été largement abandonnée même s'il est devenu clair, chez d'autres types cellulaires, que le cotransporteur $Na^+:K^+:2Cl^-$ est stimulé par l'hypertonicité (86,165). Dans les cellules de la MD il n'est pas encore établi que le cotransporteur $Na^+:K^+:2Cl^-$ est sensible à la tonicité. Si tel est le cas, les changements de l'osmolarité luminale affecteraient la RTG à travers le cotransporteur et raviverait l'hypothèse de l'osmolarité.

A la suite de l'activation du mécanisme par lequel la MD détecte le signal luminal, un signal, fort probablement de nature chimique, est envoyé

vers les cellules contractiles de l'AA. Dans une série d'expériences de microperfusion rétrograde, Bell et coll (8,9,11) ont démontré que l'addition d'ionophore à calcium dans le liquide de perfusion aboutit à une activation de la RTG. D'autres études indiquent que les agents qui inhibent la libération du Ca^{2+} à partir des réserves intracellulaires, tel que le TMB-8, atténuent fortement la réponse de la RTG (9). Cette inhibition peut d'ailleurs être inversée par l'addition d'un ionophore à calcium (9). Dans d'autres études utilisant des solutions de perfusion sans Ca^{2+} ou contenant un agent chélateur (EGTA), il a été démontré que l'influx de Ca^{2+} dans les cellules de la MD n'est pas nécessaire pour une réponse normale de la RTG, et que celle-ci est insensible à la trifluoperazine, c'est-à-dire probablement indépendante de la calmoduline (10). Cependant, les antagonistes de la calmoduline retardent le retour aux valeurs contrôle du stop-flow pressure (SFP) après cessation de la perfusion luminale (10).

Il existe un désacord autour de l'hypothèse qui implique le Ca^{2+} intracellulaire comme voie de transmission de signal à partir de la MD. En effet, Bell et coll (12) ont montré que le passage d'une solution de perfusion hypotonique à une solution isotonique conduit à une augmentation réversible de Ca^{2+} dans les cellules de la MD. Par contre, Salomonsson et coll (129) ont observé de faibles diminutions de $[Ca^{2+}]_i$ suite à une augmentation de [NaCl] du fluide luminal.

Alternativement, le signal envoyé par les cellules de la MD pourrait ne pas être de nature chimique mais plutôt de nature électrique. L'augmentation de la [NaCl] luminale entraîne une dépolarisation, alors que la diminution de la

[NaCl] luminale ou l'application de la furosémide entraîne une hyperpolarisation (82,132). Curieusement, il y a un parallélisme précis entre la relation du SFP en fonction de [NaCl] luminale d'une part et celle du potentiel membranaire basolatéral en fonction de $[NaCl]_l$ d'autre part (13). Ainsi, le changement du potentiel membranaire basolatéral pourrait participer à la communication transcellulaire du signal de la rétroaction tubuloglomérulaire. Cette possibilité est d'autant plus intéressante qu'il a été démontré que l'étape finale de la RTG est une entrée de Ca^{2+} dans les cellules contractiles par l'intermédiaire de canaux Ca^{2+} avtivés par une dépolarisation (98). L'étape critique qui fait défaut dans cette hypothèse est la nature du mode de transmission de cette dépolarisation entre les cellules MD et les cellules du ME puisque aucune gap junction n'a été observé entre ces deux types de cellules.

Beaucoup d'agents paracrines susceptibles d'être impliquer dans la RTG ont été testés. Initiallement, il a été suggéré que l'angiotensine II est le médiateur de la réponse de la RTG (159,160,161). Cependant, ce concept s'est avéré indéfendable, car la sécrétion de la rénine, qui conduit à la formation d'angiotensine, diminue lorsque la [NaCl] luminale augmente (108,150). Maintenant il semble clair que l'angiotensine II n'est pas directement impliquée dans la réponse de RTG (55,97,142), mais il est à souligner que l'angiotensine II exerce un rôle modulateur important en augmentant la sensibilité de la RTG à la concentration luminale de NaCl, ce qui permet à ce mécanisme d'adapter sa réponse à différentes conditions de balance hydro-sodique.

L'adénosine a été souvent évoquée comme médiateur de la RTG (116,137,152). La formation d'adénosine dépendrait du taux d'utilisation d'ATP dans le tubule proximal, l'anse de Henle et les cellules de la MD. L'adénosine ainsi produite exercerait un effet vasoconstricteur sur l'artériole afférente via les récepteurs adénosine de type A_1 des cellules de muscles lisses. L'ATP extracellulaire peut fonctionner aussi comme un agent paracrine (26,58), en agissant via les récepteurs purinergiques de type P_2 (99) de l'AA.

Les métabolites de l'acide arachidonique ont été aussi impliqués dans la modulation de l'activité de la RTG (33,140,141,173,174). L'administration systémique d'inhibiteurs de la cyclooxygénase atténue la réponse de la rétroaction tubuloglomérulaire (140,138). Cependant, la perfusion de l'anse de Henle avec l'acide arachidonique (33), PGE_2 et $PGF_{2\alpha}$ (122) ou des analogues de thromboxane (173,174) augmente la réponse de RTG. Les métabolites de la cytochrome P-450 semblent également impliqués dans le mécanisme du RTG (180).

Des études récentes ont démontré que l'oxyde nitrique (NO) peut être aussi un important modulateur de la sensibilité de la RTG (162,175). Mundel et coll. (102), Wilcox et coll. (175), et Tojo et coll. (163) ont rapporté que l'isoforme NOS I (la forme neuronale de l'enzyme) est spécifiquement localisé dans les cellules de la MD. L'inhibition de NOS par la N-methyl-L-arginine (L-NMA) réduit la pression du stop-flow et augmente la réponse de RTG (175). Ito et Ren (63) ont observé que l'addition de L-NMA conduit à la constriction de l'AA seulement lorsque le tubule a été perfusé avec une

solution de NaCl isotonique et non avec une solution hypotonique. Ces données suggèrent que lorsque les cellules de la MD sont exposées à des [NaCl] élevées, la libération de NO atténuerait par son effet vasodilatateur la réponse de la RTG.

Il apparaît donc de plus en plus clair que, comme c'est souvent le cas en transmission de signal biologique, le signal de la RTG est multiple et qu'il implique l'émission simultanée d'une substance vasoconstrictrice (inconnue) et d'une substance vasodilatatrice comme le NO. De plus, de nombreuses autres substances pourraient exercer des effets modulateurs variés.

3. Importance de la rétroaction tubuloglomérulaire dans l'autorégulation du flux sanguin rénal

Plusieurs organes sont capables de maintenir le débit sanguin relativement constant en dépit des changements de la pression de perfusion. Il s'agit d'un phénomène d'autorégulation. Dans le rein, ce mécanisme est démontré au mieux dans des conditions expérimentales où celui-ci est isolé et perfusé, donc dénervé et en l'absence d'hormones (31,156). Des variations de pression de perfusion entre 60 et 160 mmHg modifient peu le débit sanguin rénal et le débit de filtration glomérulaire (105). L'existence d'une autorégulation du débit de filtration glomérulaire pour un domaine de pression artérielle identique à celui de l'autorégulation du débit sanguin rénal a conduit au concept d'une autorégulation commune, dépendant des variations des résistances vasculaires préglomérulaires. Les études de microponctions des néphrons superficiels accessibles à la surface du rein chez le rat Wistar (127)

ont permis de mesurer les déterminants du débit sanguin glomérulaire et de la filtration glomérulaire individuelle. Les mesures confirment que le débit sanguin glomérulaire est maintenu principalement par la résistance de l'artériole afférente.

Deux mécanismes ont été proposés pour expliquer l'autorégulation du débit sanguin rénal et de la filtration glomérulaire: le mécanisme myogénique et la RTG.

a. Réponse myogénique

L'augmentation de la pression de perfusion responsable d'un étirement de la paroi vasculaire et de l'artériole afférente entraînerait immédiatement une vasoconstriction réduisant le diamètre de cette artériole, et maintenant à peu près le débit sanguin rénal, malgré l'augmentation de la pression de perfusion. Cette réponse myogénique est abolie par la papavérine (30) qui provoque une paralysie des muscles lisses. Elle est aussi inhibée par le verapamil qui bloque les canaux calciques. Il est donc vraisemblable que l'étirement provoque une ouverture de canaux calciques permettant l'entrée de calcium dans les cellules musculaires lisses, ce qui provoque leur contraction.

b. Rétroaction tubuloglomérulaire

Dans la RTG, les cellules de la MD détectent les changements de [NaCl] luminale qui résultent des changements de SNGFR. Les premières preuves expérimentales en faveur de l'hypothèse de la RTG ont été fournies

par les travaux de Navar et coll. (103). Chez le chien et le rat, les SNGFR mesurés en absence de RTG, (c'est-à-dire lorsque le liquide tubulaire est recueilli au niveau du tubule proximal) diminuent significativement lorsque la pression artérielle passe de 140 à 100 mmHg. Par contre, les SNGFR mesurés en présence d'une RTG fonctionnelle (c'est-à-dire lorsque le liquide tubulaire est recueilli à partir du tubule distal) ne varient pas.

La réponse myogénique et la RTG interagissent au niveau de l'AA (144). Ainsi, le degré de contribution de chaque mécanisme à l'autorégulation peut varier selon les conditions physiologiques. Par exemple, la RTG est essentiellement responsable de l'autorégulation lors d'un régime pauvre en sels, alors que la réponse myogénique devient plus importante dans un régime riche en sels ou en expansion volumique.

Dans le cas d'une expansion volumique, [NaCl] au niveau de la MD augmente. Selon le mécanisme de la RTG, une telle élévation de NaCl provoquerait une vasoconstriction de l'AA et diminuerait en conséquence le taux de filtration glomérulaire. Cependant, l'expansion volumique ne change pas le taux de filtration glomérulaire et parfois même l'augmente. Une telle contradiction montre jusqu'à quel point le mécanisme de la RTG est un mécanisme flexible qui change de sensibilité en fonction de l'état du volume du liquide corporel (120,147). Bien que ce mécanisme n'ait pas été tout à fait défini, la diminution des niveaux circulants d'angiotensine II semble jouer un rôle important (124).

On sait depuis longtemps que l'AA est le site effecteur principal de la RTG qui est, comme on vient de le voir, impliquée dans la régulation du débit

sanguin rénal. Il existe cependant une controverse sur la portion de l'AA qui réagit aux stimuli de la MD. D'un côté on prétend que le segment tout à fait terminal est incapable de se contracter à cause de sa faible teneur en myosine (154). D'autres part, d'autres auteurs ont des observations qui supportent un rôle important pour cette portion terminale (161,139). Ito et coll. (61,63) ont démontré que le segment terminal de l'AA est la cible principale de la RTG, la portion proximale étant réservée à la réponse myogénique (62,65).

II. TECHNIQUES EMPLOYÉES POUR ÉTUDIER FONCTIONNELLEMENT LES CELLULES DE LA MACULA DENSA

La technique de microponction a été la première approche utilisée pour rechercher l'existence d'une relation fonctionnelle entre le tube distal et le glomérule. En 1965 Thurau et Schnermann (157) ont fourni le premier support expérimental en faveur de cette relation. Dans cette étude, les changements de diamètre du tubule proximal ont été utilisés comme indicateur des changements de SNGFR. L'injection de solutions à fortes [NaCl] dans le segment superficiel le plus distal du tubule proximal de rat anesthésié a été souvent suivi par un collapse du tubule proximal. Ce comportement a été interprété comme signifiant une forte réduction du taux de filtration glomérulaire. Thurau et Schnermann (157,158) ont conclu en la présence d'un mécanisme de régulation rétroactif. Postérieurement, Gottschalk et Leyssac (44) ont confirmé cette observation, mais ils ont attribué ce collapse tubulaire à un artefact (c'est-à-dire une fuite du liquide au niveau du tubule proximal).

Bien que cette technique ait fourni plusieurs observations qualitatives, la démonstration définitive de l'existence d'un mécanisme de contrôle rétroactif a nécessité une méthode expérimentale plus contrôlée et plus quantitative.

Dès 1970, la technique de microponction in vivo appliquée par Schnermann et coll. (135) a ouvert une nouvelle voie d'étude de la RTG. Cette technique permet de contrôler simultanément la vitesse du flux au niveau de l'anse de Henle, la composition du liquide tubulaire et la mesure du taux de filtration dans le même néphron. On commence par repérer les convolutions proximales et distales appartenant au même néphron en injectant un colorant dans la lumière tubulaire proximale. Puis on bloque le tubule proximal avec une colonne d'huile ou de cire et on mesure la pression luminale dans le tubule proximal. Il s'agit de la SFP qui approche la pression présente dans les capillaires glomérulaires et dans l'espace de Bowman. A l'aide d'une autre pipette de verre, on perfuse l'anse de Henle de façon orthograde à partir de la dernière convolution proximale superficielle. La composition de la solution utilisée est généralement similaire à celle de la solution luminale à la fin du tubule proximal (solution isotonique de NaCl). C'est en jouant sur le taux de perfusion que l'on influencera la composition de la solution atteignant les cellules de la MD c'est-à-dire à la suite de la réabsorption effectuée par l'anse de Henle. L'existence de la RTG a été établie expérimentalement chez le rat (6,135,178), le chien (104) et l'amphiume (121). Les réponses de la RTG sont généralement évaluées en mesurant le SNGFR, le SFP et la pression capillaire glomérulaire. Chez le rat, la perfusion orthograde ou rétrograde avec une solution isotonique de Ringer réduit de 30-60% le SNGFR et de 20-30% le

SFP. Sur la base de ces données, il a été conclu que la fonction glomérulaire est influencée par la RTG.

Depuis 1976, la RTG est étudiée in vivo chez le rat en microperfusant de façon rétrograde l'anse de Henle (à partir de la première convolution superficielle du tubule distal) et en mesurant le taux de perfusion proximal ou la SFP. On a montré assez clairement que : 1) le remplacement complet du Cl^- bloquait la génération de la RTG (145); 2) la RTG déclenchée par 6mM de Cl^- était amplifiée par la présence de Na^+ et vice versa (18); 3) la RTG est bloquée par les diurétiques de l'anse comme le furosémide et le bumétanide (118,145).

Les techniques de microponction in vivo ont apporté beaucoup de renseignements sur la RTG. Cependant, le mécanisme physiologique réel permettant aux cellules de la MD de jouer leur rôle dans la RTG n'a pu être déterminé par cette technique. Dans chaque néphron, cette petite plaque de cellules est enfoncée dans le cortex où elle n'est pas accessible à la microponction. En 1984 et 1985, il est devenu possible d'isoler et de perfuser in vitro la portion large ascendante de l'anse de Henle contenant la MD et le glomérule qui lui est attaché (24,77). Cette approche permet de visualiser les cellules de la MD et de tirer des conclusions concernant les caractéristiques fonctionnelles spécifiques des cellules de la MD.

Un moyen d'obtenir des informations spécifiques sur la sensibilité des cellules de la MD est de les visualiser à fort grossissement (1200×) en utilisant le microscope à contrast différentiel d'interférence (76). On a démontré que la diminution de la pression osmotique luminale entraîne d'une part une augmentation de l'épaisseur des espaces latéraux intercellulaires entre les

cellules de la MD et d'autre part une augmentation de l'épaisseur des cellules de la MD. Ces résultats ont permis de suggérer que les cellules de la MD étaient perméables à l'eau.

En 1988, Bell et coll. (12) dans une étude préliminaire ont combiné la technique de perfusion de tubule isolé à celle de la fluorescence en utilisant le Fura 2 (sonde fluorescente sensible au Ca^{2+}). Cette technique a permis de tester directement dans la MD l'effet de la composition du liquide tubulaire sur l'activité du calcium cytosolique. De la même façon, en 1990 l'équipe de Persson en Suède (128) a mesuré la $[Cl^-]_i$ dans les cellules de la MD à l'aide de la sonde SPQ (6-methoxy-1-(3-sulphonato-propyl)quinolinium). De notre coté nous avons mesuré le pH_i avec la sonde BCECF (2',7'-bis-(2-carboxyethyl)-5 (and -6) carboxyfluorescein) et établi la présence d'un échangeur Na^+:H^+ au niveau de la membrane apicale des cellules de la MD (32).
En 1987 (150), cette technique de microperfusion in vitro a rendu possible l'étude directe du contrôle de la sécrétion de rénine par les cellules de la MD, et ceci en absence de toute influence nerveuse et hémodynamique. On a montré que la sécrétion de rénine est stimulée par une diminution de $[Cl^-]$ luminal au niveau de la MD.

Une autre approche pour étudier la façon dont les changements de la composition du liquide tubulaire pourraient affecter la fonction des cellules de la MD est de mesurer les propriétés électriques de ces cellules. Puisque cette technique implique l'empalement de cellules individuelles avec des microélectrodes, il a été possible d'obtenir des informations sur certaines voies

de transport au niveau des membranes apicale et basolatérale. Ainsi, en 1989 notre laboratoire (13) a montré qu'une augmentation de $[NaCl]_l$ produisait une dépolarisation. Au cours de la même année, le laboratoire de Schlatter (132) a démontré un effet hyperpolarisant du furosémide luminal. Enfin, les deux laboratoires ont prouvé l'existence d'un cotransporteur $Na^+:K^+:2Cl^-$ sensible à la furosémide (82,132). En 1991, notre laboratoire a démontré la présence d'une grande conductance Cl^- dans la membrane basolatérale (83).

En 1993, Schlatter (133) a appliqué pour la première fois sur la MD, la technique de patch-clamp en configuration "whole cell". On a obtenu des valeurs de potentiel intracellulaire plus reproductibles que celles obtenues avec des microélectrodes. En 1994, nous avons aussi appliqué aux cellules de la MD la technique de patch-clamp, mais en "single channel", dans le but d'identifier les canaux présents dans la membrane apicale. Nous avons trouvé une grande densité de canaux K^+ (56).

III. MODÈLE DE CELLULE DE LA MACULA DENSA

Étant donné leur nombre restreint et leur difficulté d'accès et d'isolation, les propriétés des cellules de la MD sont restées inconnues jusqu'à la fin des années 80 où, essentiellement, on ne disposait que de deux données: les cellules de la MD ont une faible densité de la Na^+/K^+-ATPase (5,143) et elles ont probablement un cotransporteur $Na^+:K^+:2Cl^-$ sensible au furosémide puisque la RTG peut être bloquée par les diurétiques de l'anse (177). En 1985, suite à la démonstration par Kirk et coll. (77) qu'il était possible de disséquer

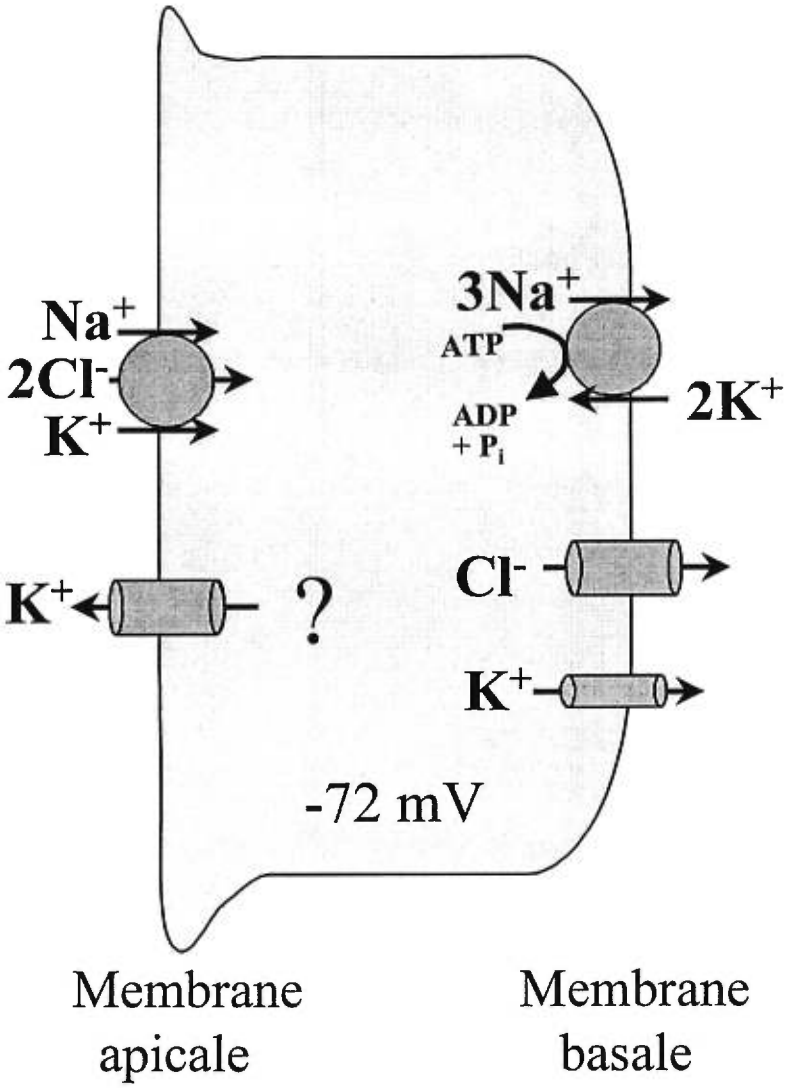

Figure 4. Modèle de cellule de la macula densa en 1993.

chez le lapin des TAL avec leur glomérule attaché, notre laboratoire, en collaboration avec le Dr P.D. Bell, s'est attaqué à l'étude des cellules de la MD. À partir des études de notre laboratoire (12,13,82,83) et des études d'autres chercheurs (132,133), voici l'idée que nous nous faisions des cellules de la MD en 1993, au moment où le travail de cette thèse a commencé (Fig. 4). Au niveau de la membrane apicale il existe un cotransporteur $Na^+:K^+:2Cl^-$ sensible à la furosémide (82,132). La présence d'un canal K dans la membrane apicale a été suggérée. A la membrane basolatérale, une faible activité Na^+/K^+-ATPasique a été rapportée (5,143). Notre équipe a aussi démontré une forte conductance au Cl^- au niveau basolatérale (83). La valeur moyenne de potentiel membranaire (Vm) rapportée par Schlatter (133), en présence d'une $[NaCl]_l$ de 140 mM est de -72 mV. Ce fort potentiel suggérait un fort gradient K^+ et une cellule largement perméable à cet ion.

IV. PROJET DE RECHERCHE

Il est très clair que nous avons un grand besoin de mieux connaître les propriétés des cellules de la MD pour pouvoir progresser dans l'identification du signal de la RTG. En particulier, il existe un grand vide dans la connaissance des phénomènes se produisant entre l'augmentation du transport apical de NaCl par les cellules de la MD et la contraction de l'artériole afférente. Les travaux récents d'électrophysiologie réalisés dans notre laboratoire (13,82,83) ainsi que dans le laboratoire de Schlatter et coll. (132) ont montré une grande similarité du transport de Na^+, de K^+ et de Cl^- dans les cellules de la MD et les cellules de la TAL. Ainsi, il a été suggéré que la

membrane apicale des cellules de la MD possède un canal K^+, puisque ce canal est présent dans la membrane apicale des cellules de TAL. Cependant, l'existence d'une telle conductance K^+ n'avait pas encore été déterminée expérimentalement dans les cellules de la MD au moment de commencer ce travail. Une des raisons est la difficulté d'interpréter les changements du potentiel membranaire basolatéral qui se produisent suite à la variation de $[K^+]_l$, car le changement du K^+ luminal peut influencer le potentiel membranaire à travers la conductance K^+ et/ou indirectement à travers le contransporteur $Na^+:K^+:2Cl^-$ et la $[Cl^-]_i$. Par conséquent, une approche directe était nécessaire afin de déterminer si vraiment une conductance K^+ existe au niveau de la membrane apicale. En microdissection, nous avons trouvé qu'il est possible d'enlever la partie de TAL qui cache les cellules de la MD et d'exposer la membrane apicale de ces cellules. Cette procédure permet d'utiliser la technique de patch-clamp et d'observer directement les canaux ioniques de la membrane apicale. Nous avons alors dans un premier temps (premier article) tenté de mettre en évidence les canaux, éventuellement sélectifs au K^+, présents dans la membrane apicale des cellules de la MD.

L'existence du $Na^+:H^+$ dans la membrane apicale et basolatérale des cellules de TAL et son rôle dans la régulation du pH_i, nous a incités à rechercher, dans une deuxième étape, en collaboration avec le laboratoire du Dr P.D. Bell de l'Université d'Alabama à Birmingham, si un tel échangeur existe aussi dans les cellules de la MD. Nous nous sommes alors intéressés à la présence de l'échangeur $Na^+:H^+$, particulièrement au niveau de la membrane apicale car dans les conditions normales, $[NaCl]_l$ peut varier de 20 à 60 mM

selon l'amplitude du transport de NaCl par le TAL (145). Notre technique est basée sur la mesure du pH_i avec la sonde fluorescente sensible au pH le 2',7'-bis-(2-carboxyethyl)-5 (and -6) carboxyfluorescein (BCECF).

Dans une troisième étape, nous nous sommes intéressés à la détermination de la concentration de NaCl luminale qui permet d'équilibrer le cotransporteur $Na^+:K^+:2Cl^-$ apical pressenti comme le mécanisme de détection à l'origine du signal de la RTG. De plus, grâce aux effets secondaires sur le pH_i produits par l'entrée de Na^+ par le cotransporteur, nous avons pu estimer son affinité pour le Cl^- luminal.

Bien que ces expériences de fluorescence pour déterminer le pH_i nous aient permis d'obtenir indirectement beaucoup de renseignements sur les concentrations ioniques intracellulaires et sur certaines caractéristiques du cotransporteur apical, ces données, bien que précieuses, restent un peu fragiles puisque la détermination de l'activité du cotransporteur apical est bien indirecte (une chaîne de trois événements: effet du transport sur $[Na^+]_i$, de $[Na^+]_i$ sur l'échangeur $Na^+:H^+$ et de l'échangeur $Na^+:H^+$ sur le pH_i). Nous avons alors établi pour les cellules de la MD, la faisabilité d'une méthode plus directe pour déterminer les flux à travers le cotransporteur apical. Cette méthode est basée sur le fait que le NH_4^+ peut se substituer au K^+ dans divers transporteurs et canaux incluant le cotransporteur $Na^+:K^+:2Cl^-$ et affecter directement le pH_i en se dissociant en $NH_3 + H^+$.

Du fait que la technique de NH_4^+/NH_3 permet de mesurer efficacement le flux de NH_4^+ à travers le contransporteur $Na^+:K^+:2Cl^-$, il est possible de déterminer les paramètres cinétiques et les mécanismes de régulation de ce cotransporteur. C'est d'ailleurs ce que nous avons fait dans l'article 5.

V. CONTRIBUTION PERSONNELLE AUX DIFFÉRENTS TRAVAUX RÉALISÉS DANS CETTE THÈSE

Article n° 1 : Basic properties and potential regulators of the apical K^+ channel in macula densa cells.

J'ai participé à la révision du manuscrit et aux expériences demandées lors de la révision par les arbitres au sujet de l'effet du Ca^{2+} cytosolique et de pH_i sur l'activité du canal K^+.

Article n° 2 : Evidence for apical sodium proton exchange in macula densa cells

Nous avons travaillé cet article en collaboration avec le Dr P.D. Bell. J'ai fourni les séries d'expériences qui ont démontré que l'échangeur $Na^+:H^+$ était toujours actif même aux pH_i relativement élevés atteint en présence de furosémide. J'ai contribué à la rédaction et la révision de l'article.

Article n° 3 : *Activation of $Na^+:K^+:2Cl^-$ cotransport by luminal chloride in macula densa cells*

J'ai participé à la rédaction et à la révision de l'article. J'ai aussi confirmé les résultats expérimentaux sur l'effet de $[Cl^-]_l$ sur le pH_i par l'intermédiaire du cotransporteur $Na^+:K^+:2Cl^-$.

Article n° 4 : *Determination of NH_4^+/NH_3 fluxes across apical membrane of macula densa cells : a quantitative analysis*

Toutes les expériences ont été réalisées par moi-même. La rédaction et la révision de l'article ont été faites par moi et mon directeur de recherche.

Article n° 5 : *Transport and regulatory properties of the apical $Na^+:K^+:2Cl^-$ cotransporter of the macula densa cells*

J'ai réalisé toutes les expériences et j'ai participé à côté de mon directeur de recherche à la rédaction et la révision de l'article.

B. RÉSULTATS

PREMIER ARTICLE

Basic Properties And Potential Regulators Of The Apical K^+ Channel In Macula Densa Cells

Hurst A.M, J.Y. Lapointe, Laamarti M.A. and P.D. Bell

Basic Properties and Potential Regulators of the Apical K^+ Channel in Macula Densa Cells

A. M. HURST, J.-Y. LAPOINTE, A. LAAMARTI, and P. D. BELL*

From the Groupe de Recherche en Transport Membranaire, Université de Montréal, Montréal, Québec HC3J7; and *Nephrology Research and Training Center, Departments of Medicine and Physiology, University of Alabama at Birmingham, Birmingham, Alabama, 35294

ABSTRACT These studies examine the properties of an apical potassium (K^+) channel in macula densa cells, a specialized group of cells involved in tubuloglomerular feedback signal transmission. To this end, individual glomeruli with thick ascending limbs (TAL) and macula densa cells were dissected from rabbit kidney and the TAL covering macula densa cells was removed. Using patch clamp techniques, we found a high density (up to 54 channels per patch) of K^+ channels in the apical membrane of macula densa cells. An inward conductance of 41.1 ± 4.8 pS was obtained in cell-attached patches (patch pipette, 140 mM K^+). In inside-out patches (patch pipette, 140 mM; bath, 5 mM K^+), inward currents of 1.1 ± 0.1 pA (n = 11) were observed at 0 mV and single channel current reversed at a pipette potential of −84 mV giving a permeability ratio (P_K/P_{Na}) of over 100. In cell-attached patches, mean channel open probability (*N.Po*, where N is number of channels in the patch and *Po* is single channel open probability) was unaffected by bumetanide, but was reduced from 11.3 ± 2.7 to 1.6 ± 1.3 (n = 5, $p < 0.02$) by removal of bath sodium (Na^+). Simultaneous removal of bath Na^+ and calcium (Ca^{2+}) prevented the Na^+-induced decrease in *N.Po* indicating that the effect of Na^+ removal on *N.Po* was probably mediated by stimulation of Ca^{2+} entry. This interpretation was supported by studies where ionomycin, which directly increases intracellular Ca^{2+}, produced a fall in *N.Po* from 17.8 ± 4.0 to 5.9 ± 4.1 (n = 7, $p < 0.02$). In inside-out patches, the apical K^+ channel was not sensitive to ATP but was directly blocked by 2 mM Ca^{2+} and by lowering bath pH from 7.4 to 6.8. These studies constitute the first single channel observations on macula densa cells and establish some of the characteristics and regulators of this apical K^+ channel. This channel is likely to be involved in macula densa transepithelial Cl^- transport and perhaps in the tubuloglomerular feedback signaling process.

INTRODUCTION

Within each cortical thick ascending limb (TAL) glomerulus complex, specialized cells, called macula densa cells, reside in the TAL on the side of the tubule that is

Address correspondence to Dr. P. D. Bell, Departments of Medicine and Physiology, 865 Sparks Center, UAB Station, University of Alabama at Birmingham, Birmingham, AL 35294.

J. GEN. PHYSIOL. © The Rockefeller University Press · 0022-1295/94/06/1055/16 $2.00
Volume 103 June 1994 1055–1070

closest to the glomerulus (Schnermann and Briggs, 1985). This close association between macula densa cells and vascular components of the juxtaglomerular apparatus forms the anatomical basis for the physiological response observed during flow rate changes in the loop of Henle (Barajas, 1981); i.e., increases in TAL tubular fluid flow rate result in elevations in luminal [NaCl] at the macula densa and decreases in glomerular filtration rate (Schnermann, Ploth, and Hermle, 1976). Macula densa cells are thought to sense a change in composition of tubular fluid and to initiate signals that alter vascular resistance. This response is known as tubuloglomerular feedback (Briggs, 1981; Wright, 1981; Bell, Franco-Guevera, Abrahamson, Lapointe, and Cardinal, 1988; Schnermann and Briggs, 1985).

Experimental evidence regarding the nature of the tubuloglomerular feedback mechanism has come largely from in vivo micropuncture studies (Briggs and Schnermann, 1987; Schnermann and Briggs, 1985). It was not until 1985 that the macula densa cells could be directly visualized during microperfusion of an individually dissected TAL with associated glomerulus (Kirk, Bell, Barfuss, and Ribadeneira, 1985; Skott and Briggs, 1987). In 1988, electrophysiological techniques utilizing microelectrodes were combined with the isolated perfused macula densa preparation to examine transport properties of macula densa cells (Bell et al., 1988). This work, as well as other microelectrode studies, (Bell, Lapointe, and Cardinal, 1989; Schlatter, Salmonsson, Persson, and Greger, 1989; Lapointe, Bell, and Cardinal, 1990; Lapointe, Bell, Hurst, and Cardinal, 1991) provided evidence for an electroneutral $Na^+/K^+/2Cl^-$ cotransporter at the apical membrane of macula densa cells, a large basolateral conductance for Cl^- and a much smaller basolateral conductance for K^+.

The scheme for ion transport in macula densa cells is similar in many respects to that proposed for TAL cells. There does, however, appear to be differences between the two cell types. With the addition of furosemide, a faster membrane potential response time is observed in TAL compared to macula densa cells (Schlatter, Salmonsson, Persson, and Greger, 1989; and unpublished observation, Lapointe, Cardinal and Bell). In addition, there may be differences in the affinity of the apical cotransporter for Na^+ and Cl^- between macula densa and TAL cells (Lapointe et al., 1990). In spite of these differences, the proposal has been made that macula densa cells transport Na^+, Cl^- and K^+ in a manner which is similar to cells of the TAL. This has, in part, lead to the suggestion that macula densa cells possess an apical K^+ conductance since this channel is present in the apical membrane of TAL cells. The existence of such an apical K^+ conductance, however, has not been determined experimentally in macula densa cells. One reason for this is the inherent difficulty of interpreting changes in basolateral membrane potential with alterations in luminal $[K^+]$ because changes in luminal K^+ may influence membrane potential through the K^+ conductance and/or indirectly through the cotransporter and intracellular $[Cl^-]$. Therefore, a more direct approach was required in order to determine if an apical K^+ conductance existed in macula densa cells. Using the isolated macula densa-glomerulus-TAL unit, we found that it was possible to remove the TAL which covers the macula densa plaque thus exposing the apical membrane of macula densa cells. This allowed us to use patch clamp techniques to investigate directly the conductive properties of the apical membrane of macula densa cells. Our results provide evidence for the existence of a high density of K^+ channels in the apical membrane of

macula densa cells. We report the basic characteristics of this channel; conductance, selectivity, voltage dependence, and the effects of different potential regulators of channel activity. This knowledge allowed us to compare the properties and regulation of this K^+ channel with what is known for the apical K^+ channel of cortical TAL and provided some insight into the issue of similarities in transport characteristics between macula densa and TAL cells. In addition, an understanding of the characteristics and regulation of this apical K^+ channel may help in elucidating the mechanisms involved in the generation of tubuloglomerular feedback signals.

METHODS

Tubule Preparation

Studies were performed using kidneys obtained from New Zealand white rabbits. The renal artery was cannulated and the left kidney perfused with 30 ml of chilled preservation fluid (Na_2HPO_4, 56 mM; NaH_2PO_4, 13 mM; sucrose, 140 mM) (Pirie and Potts, 1985). Transverse slices were cut and placed in chilled preservation fluid. Mid-cortical TAL's with attached glomeruli were isolated by dissection at a magnification of 80 with sharpened forceps. That portion of the TAL covering the macula densa plaque was carefully removed by dissection to expose the apical membrane of macula densa cells (Fig. 1). An individual macula densa-glomerulus-TAL unit was then transferred to a chamber which was mounted on the stage of an inverted microscope. The glomerulus was stabilized with a glass holding pipette in such a position that the apical membrane of macula densa cells was clearly visible and accessible to a patch pipette. The bathing solution exchange time was on the order of 30 s. All experiments were performed at room temperature and the composition of the solutions used are shown in Table I.

TABLE I

Composition of Solutions Used for Cell-Attached and Inside-out Experiments

	Pipette	Ringer	0Na	0Na/0Ca	0Ca EGTA	0Ca
NaCl	0	135	0	0	135	135
KCl	140	5	5	5	5	5
NMDG	0	0	135	135	0	0
$CaCl_2$	2	2	2	0	0	0
$MgCl_2$	1	1	1	1	1	1
HEPES	5	5	5	5	5	5
EGTA	0	0	0	0	1.5	0
glucose	5	5	5	5	5	5
mannitol	0	0	0	2	0	0

The pH of each solution was adjusted to pH 7.4 by titration of HEPES with either KOH for the pipette solution or NaOH for all the other solutions.

Patch Clamping

A Narishige PP-83 two stage patch pipette puller was used to fabricate patch pipettes from hematocrit capillary tubes (Fisher Scientific Co., Pittsburgh, PA). Standard patch clamp techniques (Hamill, Marty, Neher, Sakmann, and Sigworth, 1981) were used to record channel currents which were amplified with a List (LM-EPC7, FRG) patch clamp amplifier and recorded

onto video tape, following pulse code modulation (Neurodata DR-384), for later analysis. Unless stated otherwise, all experiments were performed at a pipette potential of 0 mV.

Data Analysis

Data analysis was performed using PClamp software (version 5.5.1, Axon Instruments, Inc., Foster City, CA). Channel currents were low pass filtered at 500 Hz (Frequency Devices) and digitized at 1 kHz via a TL-1 DMA Labmaster interface (Axon Instruments, Inc.) using an 386 IBM compatible PC.

Mean channel open probability ($N.Po$) was calculated from the following equation:

$$N.Po = \langle I \rangle / i$$

where N is the number of channels in the patch, Po is the single channel open probability, $\langle I \rangle$ is the mean current and i is the single channel current. In patches with a high level of channel activity, recording times in the order of 4 s were sufficient to determine $N.Po$ whereas longer recording times (up to 60 s) were needed whenever channel activity was low. This calculation makes the assumption that the leak current is minimal at a pipette potential of 0 mV. This assumption is supported by the finding that, in 10 patches where channel activity decreased to zero during an experimental maneuver, the current measured at a pipette potential of 0 mV was only -0.27 ± 0.07 pA (inward current). In experiments where $N.Po$ was measured during changes in the applied potential, we assumed that leak current was linearly related to voltage. All acceptable recordings had a minimum seal resistance of 10 giga Ohms as estimated from the current measured at the reversal potential of the channel. Under these conditions, the contribution of leak current to the determination of $N.Po$ at, for example, +20 mV (cell-attached patches), was $< 10\%$. Channel conductance was estimated from linear regression analysis of single channel current-voltage curves. Voltage applied to the pipette (Vp) is referenced to the bath potential ($Vp - V_{bath}$). In cell-attached patches, potential across the patch is equal to the cell membrane potential minus Vp whereas in inside-out patches, the potential across the patch is simply equal to minus Vp.

Solutions

In all experiments, a high K^+ solution was used in the patch pipette (Table I). The composition of the bathing solutions are also shown in Table I. In some experiments, the following drugs were added to the Ringer solution: 5 μM bumetanide, 5 μM ionomycin, 0.1 mM dibutyryl cyclic AMP + 1 μM forskolin and 2 mM ATP. In some inside-out patch experiments, pH of the 0 Ca^{2+} solution (without EGTA) was adjusted to pH 6.8 with HCl. Care was taken to adjust the pH of the final solution to pH 7.4 by addition of small amounts of NaOH, KOH (pipette solution) or HCl (0 Ca^{2+} solution without EGTA). All chemicals were purchased from Sigma Chemical Co., (St. Louis).

Statistics

Data are presented as mean ± SEM. Because control and experimental values were always obtained in the same patch, statistical analysis was performed using the paired t test. Data in Fig. 8 were analyzed using the Wilkinson Rank Test.

RESULTS

Fig. 1 is a photograph of a macula densa preparation used for patch clamp experiments. As shown in the example, macula densa cells are clearly visible and the apical membrane is directly exposed to the bathing solution because the TAL which

covered the plaque has been pulled away. The preparation was steadied at the bottom of the chamber by gently applying pressure to the glomerulus with a glass pipette. Using this arrangement, the success rate of seal formation with a seal resistance higher than 10 GΩ (assuming a voltage-independent open probability, see below) was 38% in 363 attempts.

Conductance, Selectivity and Voltage Dependence

A high density of a single type of K^+ channels was observed on the apical membrane of macula densa cells. A single patch could contain up to 54 simultaneously open channels. There was, however, a considerable variation in *N.Po* values obtained in

FIGURE 1. Photograph of exposed macula densa plaque (at *arrow*), thick ascending limb and attached glomerulus. The diameter of the macula densa cells is ~20 μM.

these studies. The most likely explanation for this finding is that the density of K channels may vary from cell to cell or that there may be uneven distribution of channels within the apical membrane. Fig. 2 shows the current-voltage relationship for the channel we observed in cell-attached (Fig. 2 *A*) and inside-out patches (Fig. 2 *B*), in the presence of a high K^+ pipette solution and the control Ringer's bathing solution. In cell-attached patches, inward currents of 2.8 ± 0.3 pA (n = 6) were observed at 0 mV pipette potential. Average inward conductance of the channel was 41.1 ± 4.8 pS (n = 6) and, as estimated by extrapolation, the single channel current would reverse at a pipette potential of −86 mV. This is consistent with a high intracellular [K^+] and the presence of a K^+ selective channel.

Measurements of channel selectivity were performed in inside-out patches with a K^+ gradient of 140 mM to 5 mM (pipette to bath). Patches were excised into a Ca^{2+} free Ringer solution containing EGTA (see section entitled; Modulators of K^+ channel activity in inside-out patches) and single channel inward currents of 1.1 ± 0.1 pA (n = 11) were observed at a Vp of 0 mV and the reversal potential estimated by extrapolation was −84 mV. From the reversal potential, a permeability ratio (P_K/P_{Na}) of greater than 100 can be estimated, indicating a highly K^+ selective channel. However, conductance of the channel in inside-out patches was only 17.9 ± 2.4 pS (n = 8), a value which was approximately half of that obtained in cell-attached patches. A part of this decrease in channel conductance could be due to the dependence of the conductance for inward currents on cytosolic [K^+] as predicted by the constant field equation. However, this effect is greatest at the reversal potential

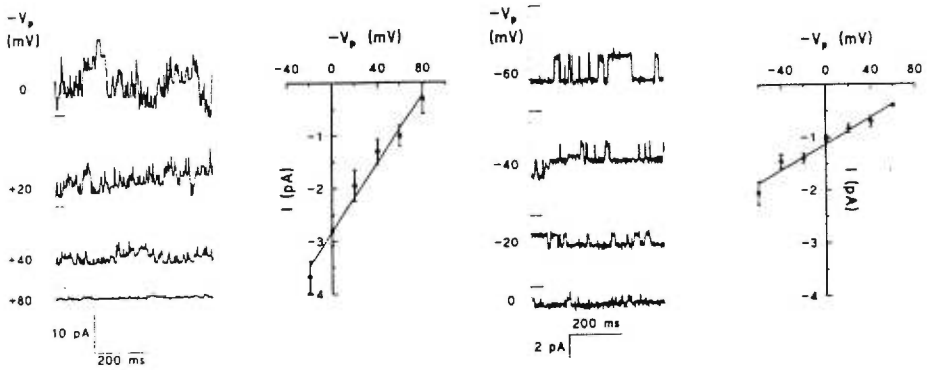

FIGURE 2. (*A*) On the left is an example of the current recordings at different pipette potentials obtained from cell-attached patches with high K^+ in the pipette and the bath containing normal Ringer solution. The graph on the right is the *I-V* relationship and the solid line is a linear regression fit of the data. Downward deflection and negative currents represent inward currents (pipette to cell) and the horizontal lines represent the zero current level from which channel currents (and some leak current) have been measured. (*B*) On the left is an example of the current-voltage relationship from inside-out patches with high K^+ in the pipette and 0 Ca^{2+} Ringer + EGTA in the bath. On the right is the *I-V* relationship and the solid line is a linear regression fit of the data.

and should be small at potentials where the channel conductance was measured. It is also possible that the decrease in conductance in inside-out patches, could be due to the absence of important cytosolic regulators of channel permeability in the inside-out configuration. Finally, there is the possibility that the channels seen in excised patches are different from the channels in cell-attached configuration. We believe that this is a rather unlikely explanation as it requires a peculiar combination of rapid activation and deactivation of the channels upon excision. In addition, the Ca sensitivity (see below) seen in both configurations argues against this possibility.

The macula densa apical K^+ channel does not appear to be very voltage dependent in either cell-attached or inside-out configuration (Fig. 3). To reduce the error associated with leak current, paired measurements of *N.Po* were performed over a relatively narrow voltage range. In cell-attached patches (left side of Fig. 3), *N.Po* was

11.5 ± 2.0 in the absence of an applied potential and did not change significantly *N.Po* = 12.2 ± 2.9 (n = 6, $p > 0.6$) over a 40 mV depolarization. *N.Po* was consistently less in inside-out patches (right side of Fig. 3) compared to cell-attached patches, further suggesting that the inside-out configuration resulted in a modification of the channel or a loss of cytosolic regulators. In the absence of an applied potential *N.Po* was 5.3 ± 1.0, and did not change significantly (5.1 ± 1.0 [n = 3, $p > 0.7$]) with the application of a 20 mV depolarization.

Effects of Bumetanide on K⁺ Channel Activity

Previous work on apical K^+ channels in the frog diluting segment (Hurst and Hunter, 1992), a preparation which has been used as a model for the mammalian TAL, found that loop diuretics such as furosemide can alter K^+ channel activity indicating some form of indirect coupling between K^+ channel and $Na^+/K^+/2Cl^-$ cotransporter. Because the apical membrane of macula densa cells also contains both K^+ channel and $Na^+/K^+/2Cl^-$ cotransporter (Bell et al., 1989; Schlatter et al., 1989; Lapointe et al., 1990) it was of interest to determine if bumetanide altered the activity of K^+ channels in macula densa cells. This $Na^+/K^+/2Cl^-$ transporter in macula densa cells is sensitive to loop diuretics and it has been shown that furosemide inhibits feedback responses (Wright and Schnermann, 1974).

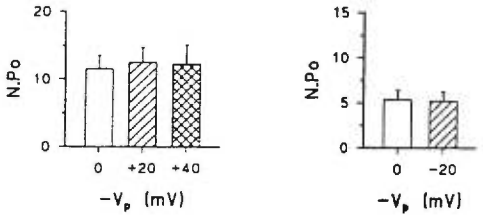

FIGURE 3. (*Left*) Dependence of channel open probability (*N.Po*) on voltage in cell-attached patches. (*Right*) Dependence of channel open probability (*N.Po*) on voltage in inside-out patches.

In cell-attached patches, 5 μM of the loop diuretic bumetanide was added to the Ringer solution. In six experiments, addition of bumetanide did not significantly alter *N.Po*. Under control conditions, *N.Po* was 15.2 ± 5.3 and 14.4 ± 6.8 ($p > 0.2$) in the presence of bumetanide.

Effect of Na⁺ and Ca²⁺ on K⁺ Channel Activity

In other cell-attached patch experiments, the effects of replacement of bath Na^+ with *n*-methyl-D-glucamine (see Table I, $0Na^+$) on macula densa K^+ channel activity was assessed. (It should be noted that pH of the $0Na^+$ solution was adjusted to pH 7.4 with NaOH, therefore the $0Na^+$ solution contained ~3 mM Na^+) Fig. 4 shows a typical record from a cell-attached patch illustrating the decline in channel activity during removal of bath Na^+. As summarized on the left side of Fig. 5, *N.Po* fell significantly from 11.3 ± 2.7 to 1.6 ± 1.3 (n = 5, $p < 0.02$) during removal of bath Na^+.

Removal of Na^+ from the bathing solution may have multiple effects on macula densa cells including alterations in intracellular concentrations of other electrolytes. We hypothesized that one effect of Na^+ removal might be an increase in macula

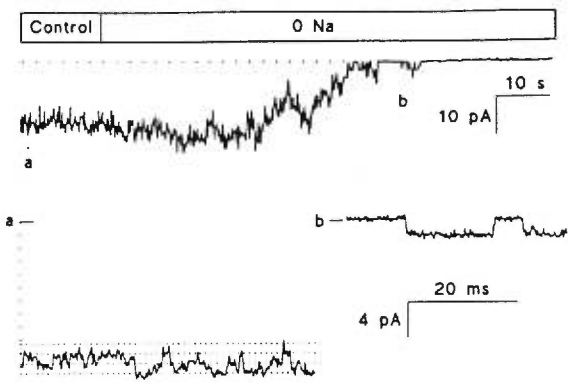

FIGURE 4. Representative recording showing the effect of elimination of bath Na^+ on channel activity (*top record*). The lower records are on an expanded time base and were taken from the places indicated by *a* and *b* in the upper record. In *a*, the solid line is the closed channel current level; in *b* there is only one channel open. Downward deflections are channel opening events and represent current flow from pipette to cell.

densa intracellular [Ca^{2+}] perhaps through Ca^{2+} entry via a Na^+:Ca^{2+} exchanger. The increase in cytosolic [Ca^{2+}] would, in turn, be responsible for the decline in K^+ channel activity. If so, then inhibition of channel activity during Na^+ removal would be dependent upon the presence of external Ca^{2+}. The right side of Fig. 5 shows that K^+ channel activity did not significantly change during simultaneous removal of Na^+ and Ca^{2+} from the bath solution. In control experiments *N.Po* was 21.9 ± 5.5, whereas in 0 Na^+/0 Ca^{2+} *N.Po* was 21.1 ± 7.2 ($n = 5$, $p > 0.8$). This result clearly shows that the decrease in K^+ channel activity during Na^+ removal is dependent upon the presence of external Ca^{2+}.

To characterize further the effect of intracellular Ca^{2+} on K^+ channel activity, experiments were performed in which intracellular [Ca^{2+}] was elevated using the Ca^{2+} ionophore, ionomycin. Fig. 6 shows that ionomycin (5 μM) addition in the presence of 2 mM Ca^{2+} in the bathing solution, produced substantial deceases in channel activity from cell-attached patches. Mean *N.Po* in the absence of ionomycin was 17.8 ± 4.0 and decreased significantly to 5.9 ± 4.1 ($n = 7$, $p < 0.02$) in the presence of ionomycin.

The Effect of Cyclic AMP on Macula Densa K^+ Channels

A close association often exists between intracellular Ca^{2+} and cyclic AMP signaling systems such that cyclic AMP can modulate Ca^{2+}-mediated events (Rasmussen and

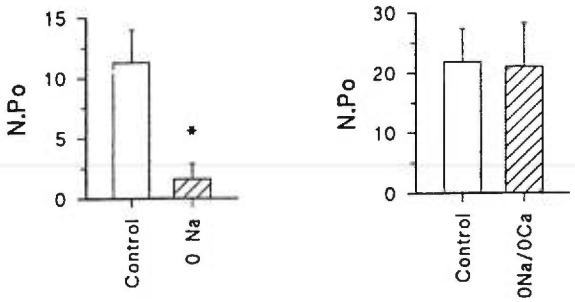

FIGURE 5. (*Left*) The effect of Na^+ removal on average *N.Po* in cell-attached patches. *Indicates significance at the 5% level. (*Right*) The effect of simultaneous removal of Na^+ and Ca^{2+} from the bath on average *N.Po* in cell-attached patches.

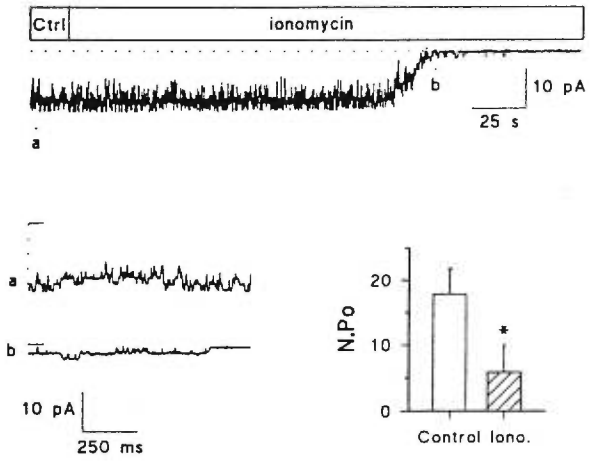

FIGURE 6. Representative tracing showing inhibition of K^+ channel activity with 5 μM ionomycin. (*Left*) The lower traces (*a* and *b*) are expanded time base records taken from the upper trace at the positions marked. The solid line under trace *a* is the closed channel current level and in *b*, there is only one channel open. Downward deflections are channel opening events and represent current flow from the pipette to the cell. (*Right*) Presents average data obtained in these experiments. *Indicates significance at the 5% level.

Barrett, 1984). Also, agents that increase cell cyclic AMP levels previously have been shown to significantly inhibit the transmission of tubuloglomerular feedback signals (Bell, 1985, 1987). In cell-attached patches, macula densa cell cyclic AMP content was increased by addition of dibutyryl cyclic AMP (0.1 mM) and forskolin (1 μM), an activator of adenylate cyclase. In three experiments, addition of dibutyrl cyclic AMP plus forskolin had no effect on K^+ channels; control *N.Po* was 29.4 ± 6.9 compared to 25.1 ± 8.0 ($p > 0.2$) in the presence of dibutyryl cyclic AMP + forskolin.

Modulators of K^+ Channel Activity in Inside-out Patches

To elucidate further the regulation of macula densa K^+ channel, experiments were performed using inside-out patches. Because channel activity may be inhibited by Ca^{2+}, patches were initially excised into a Ca^{2+}-free Ringer solution containing

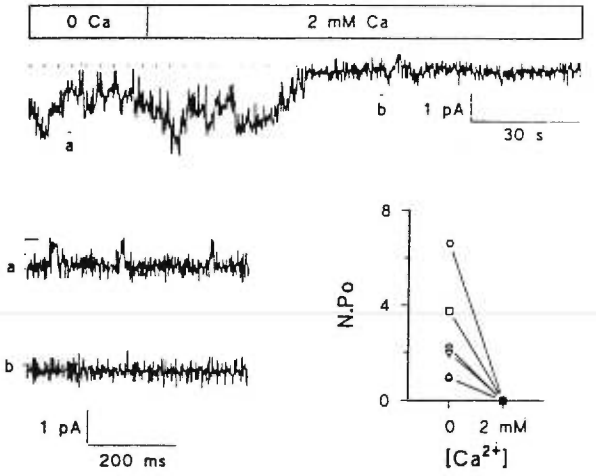

FIGURE 7. Representative tracing showing the effects of bath Ca^{2+} on channel activity in an inside-out patch. (*Left*) Traces *a* and *b* are expanded time base records of the upper trace taken from the place indicated. The solid line in *a* is the closed channel current level and in *b*, all channels are closed. Downward deflections are channel opening events and represent current flow from pipette to bath. (*Right*) The effect of 2 mM Ca^{2+} on *N.Po* in six experiments.

EGTA. As previously discussed, inside-out patches exhibited lower channel activity compared to that obtained in cell-attached patches but this lower channel activity was routinely observed to be stable for a few minutes (2–4 min). This length of time was sufficient to discriminate between rapid effects (10–20 s), responses to experimental manipulations and channel rundown. Fig. 7 shows an example and summarizes K^+ channel activity during addition of Ca^{2+} (2 mM) to the bath solution. In six experiments, *N.Po* under control conditions averaged 2.7 ± 0.9 and decreased to zero ($p < 0.03$) in each experiment with addition of Ca^{2+}. Reactivation of channel activity by removal of bath Ca^{2+} was unsuccessful at least over a 4-min recovery period.

Recent work has indicated that there may be physiological changes in macula densa cell pH during alterations in luminal [NaCl] (Fowler, Lapointe, and Bell, 1991). In addition, other studies have shown that certain renal K^+ channels are

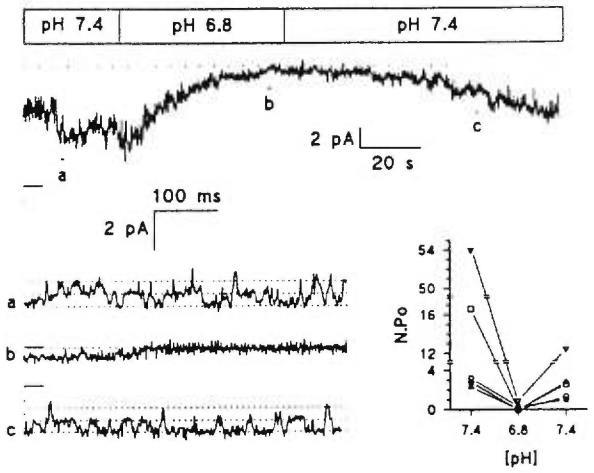

FIGURE 8. Representative recording depicting the effect of bath acidification on channel activity in inside-out patches is shown in the upper portion of this figure. (*Left*) Expanded time-base records taken from the place indicated: (*a*) during control (pH 7.4); (*b*) at pH 6.8; and (*c*) after return to pH 7.4. Solid lines above the traces (*a* and *c*) are the closed channel current levels and in *b* there is no channel activity. Downward deflections are channel opening events and represent current flow from pipette to cell. (*Right*) Individual data obtained in inside-out patches during changes in bath pH.

sensitive to changes in pH (Hurst and Hunter, 1989; Beck, Hurst, Lapointe, and Laprade, 1993; Bleich et al., 1990). Therefore, studies were performed in inside-out patches to determine if the macula densa apical K^+ channel was sensitive to pH. As shown in the tracing (Fig. 8), there was a fall in channel activity with a reduction in bath pH from 7.4 to 6.8 that was partially reversible upon return of bath pH to 7.4. Data from individual experiments are shown in the lower right hand corner of Fig. 8. In this group, there was a large variability in initial *N.Po* values. Nevertheless, in each experiment lowering bath pH resulted in a substantial fall in *N.Po* to values which were at or near zero. Because of the initial variability in *N.Po*, these data were analyzed with a Wilkinson Rank Test which revealed a highly significant decrease in *N.Po* upon reducing bath pH ($p < 0.001$).

A number of recent studies have shown that certain K^+ channels are sensitive to ATP including the K^+ channel found on the apical membrane of TAL cells (Wang et

al., 1990; Bleich et al., 1990). In inside-out patches we tested for ATP sensitivity of the macula densa K^+ channel. Control *N.Po* was 1.9 ± 0.7 and addition of 2 mM disodium ATP to the 0 Ca^{2+} (no EGTA) bathing solution did not produce a significant change in *N.Po*, 1.6 ± 0.6 ($n = 3$, $p > 0.2$).

DISCUSSION

In the present study we report that the apical membrane of macula densa cells contains a high density of K^+ selective channels. Careful removal of the TAL covering the macula densa cells enabled us to perform patch clamp experiments on this previously inaccessible region of the nephron. A similar approach, but using collagenase, was recently used to measure cell potential in whole cell recordings (Schlatter, 1993). The abundance of K^+ channels and high rate of successful seal formation allowed us to document certain biophysical properties of the channel and to determine the effect of some potential regulators. In addition, careful examination of the recordings revealed the presence of another smaller channel (single-channel

TABLE II

Comparison of K^+ Channels in Macula Densa and TAL Cells

	Macula densa	Thick ascending limb		
	Apical Rabbit*	Apical Rabbit‡	BLM Rabbit§	Apical Rat‖
G (pS) room temperature	41	22	35	—
G (pS)37°C	—	27	—	60
Vdep	No	No	Yes	No
Ca^{2}	Yes	No	No	Yes
pH	Yes	No	N/D	Yes
ATP	No	Yes	N/D	Yes

Abbreviations: BLM, basolateral membrane; G, conductance; Vdep, voltage dependence; N/D, not determined.

*Present study; ‡Wang, White, Geibel, and Giebisch, 1990; §Hurst, Duplain, and Lapointe, 1992; ‖Bleich, Schlatter, and Greger, 1990.

current of 0.7 pA at zero mV pipette potential in cell attached patches) with an unknown specificity. It was present in less than 10% of the patches and was most evident under conditions where *N.Po* of the K^+ channel was reduced to zero. Additional studies will be necessary to identify and characterize this other apical channel. Nevertheless, the results with the macula densa apical K^+ channel allowed us to compare the characteristics of this channel with the properties reported for K^+ channels in the TAL, to speculate on the involvement of an apical K^+ channel in transepithelial transport by macula densa cells and to discuss the possible role of this K^+ channel in the tubuloglomerular feedback signal transmission.

Comparison of the Macula Densa and TAL K^+ Channels

As shown in Table II, the apical K^+ channel of macula densa cells exhibits characteristics which are different from those already identified for the K^+ channel on either the apical membrane of rat (Bleich et al., 1990) or rabbit TAL (Wang et al., 1990) or even on the basolateral membrane of rabbit TAL (Hurst et al., 1992). One

difference between macula densa and TAL K^+ channels is the higher incidence and abundance of channels observed in macula densa compared with TAL cells. The density of K^+ channels in the TAL appears to be extremely low (Bleich et al., 1990; Wang et al., 1990; Hurst et al., 1992) as indicated by a very low success rate for recording channel activity from giga Ohm patches. Whereas in macula densa cells, gigaohm seal formation was successful 38% of the time and of these, 75% exhibited channel activity with nearly all recordings exhibiting multiple channels.

There also seems to be differences in the conductance of various renal K^+ channels. In the cell-attached configuration with a high K^+ solution in the patch pipette, the macula densa cell K^+ channel has an inward conductance of 41 pS (room temperature) compared to 60 pS (37°C) in rat (Bleich et al., 1990) and 22 pS (room temperature) in rabbit (Wang et al., 1990). Voltage sensitivity of the renal K^+ channel has only been demonstrated in cell-attached patches of rabbit TAL basolateral membrane where this K channel was found to open with membrane depolarization. The apical membrane channels of rat and rabbit TAL as well as the apical K^+ channel of macula densa cells are voltage insensitive (Wang et al., 1990; Bleich et al., 1990) in cell attached patches while in the rat, the apical K^+ channel is apparently sensitive to voltage in inside-out patches (Bleich et al., 1990). In macula densa cells, the K^+ channel remains voltage insensitive (at least over the range of voltages tested) after the membrane patch has been pulled away from the cell and an inside-out patch is formed.

The regulation of the macula densa cell K^+ channel is also different from that of the K^+ channels in TAL. In rabbit, both apical (Wang et al., 1990) and basolateral (Hurst et al., 1992) K^+ channels are insensitive to changes in cell $[Ca^{2+}]$, however, the apical K^+ channel in rat TAL (Bleich et al., 1990) is inhibited by millimolar $[Ca^{2+}]$. In addition to its direct inhibitory effect, the presence of Ca^{2+} renders the channel less sensitive to ATP by a factor of ~ 10. In macula densa cells, the K^+ channel appears to be sensitive to Ca^{2+} but not to ATP. The pH sensitivity of the K^+ channel varies with species; in rabbit the apical K^+ channel is not sensitive to pH (Wang et al., 1990), whereas in rat, the channel activity was reduced with a decrease in pH (Bleich et al., 1990). In macula densa cells, the channel is almost completely inhibited by acidification to a pH of 6.8.

In summary, the macula densa apical K^+ channel presents a distinct set of characteristics in terms of pH, Ca^{2+}, ATP and voltage sensitivity with respect to either rat or rabbit apical TAL channels. The fact that single channel conductances in cell-attached configuration are not the same further suggests that the K channels in these three tissues are different.

Macula Densa Apical K^+ Channels

In the TAL, an apparent low density of apical K^+ channels recycles K^+ across the luminal membrane (Greger, 1985). This provides for a continuous source of luminal fluid K^+ which permits sustained flux through the $Na^+/K^+/2Cl^-$ and generation of a lumen positive potential that drives paracellular reabsorption. Therefore, apical K^+ channels play an essential role in transepithelial transport in TAL. In macula densa cells, it is not clear whether the abundance of apical K^+ channels serves the same function. Under normal conditions, NaCl transport by the TAL has substantially

reduced luminal [NaCl] before the macula densa. Therefore, the magnitude of transepithelial NaCl transport by macula densa cells is probably small. Also, because of the small size of the macula densa plaque, relative to the TAL, luminal $[K^+]$ is most likely "set" by the upstream TAL. These considerations suggest that luminal K^+ recycling may not the primary role of the apical K^+ channel in macula densa cells.

In recent studies we have found that vectorial transport by macula densa cells is reabsorptive when luminal NaCl is in the range of 20–150 mM (luminal K^+ = 10 mM) (Lapointe, J. Y., A. Laamarti, A. M. Hurst, B. C. Fowler, and P. D. Bell, manuscript in preparation). One criteria for continued reabsorption at the lower range of luminal [NaCl]'s is the ability of these cells to reduce intracellular chloride ($[Cl^-]_i$) to low levels when NaCl transport is reduced. Using the fluorescent probe SPQ, previous work (Salomonsson, Gonzalez, Westerlund, and Persson, 1991*b*; Salomonsson et al., 1993) estimated macula densa $[Cl^-]_i$ at 6–28 mM in the presence of luminal furosemide; indicating that macula densa cells are capable of achieving a low $[Cl^-]_i$. In previous studies, we reported that macula densa cells have a single conductive pathway for Cl^- which is located at the basolateral membrane (Lapointe et al., 1991). Cl^- exit through this conductive pathway is driven by cell membrane potential since there is a large chemical gradient favoring Cl^- entry. Because basolateral K^+ conductance is small (Lapointe et al., 1991), it is likely that the apical K^+ channels play a major role in maintaining a cell negative membrane potential which controls the rate of Cl^- exit. This interpretation is indeed supported by the experimental observation that addition of 1 mM barium to a 20 mM NaCl luminal solution depolarized basolateral membrane potential by 15 to 30 mV ($n = 4$; unpublished observations). Thus, by controlling cell membrane potential, the apical K^+ channel would be responsible for "setting" macula densa steady state $[Cl]_i$ which, in turn, would influence NaCl transport since ionic flux through the cotransporter is inversely related to $[Cl]_i$. Because tubuloglomerular feedback responses are inhibited by furosemide (Wright and Schnermann, 1974), ionic flux through the Na^+:K^+:$2Cl^-$ cotransport may be involved in the initiation of the tubuloglomerular feedback signaling process. Macula densa apical K^+ channels could play an important role in feedback signal transmission process by indirectly modulating this flux.

Because $[Ca^{2+}]_i$ and pH appear to regulate channel activity it is interesting to consider how these two systems could modulate channel activity during tubuloglomerular feedback responses. Observations reported in the present study suggest the presence of a basolateral Na^+:Ca^{2+} exchanger because replacing Na^+ in the bathing solution resulted in inhibition of the apical K channel only in the presence of external Ca^{2+}. If a Na^+:Ca^{2+} exchanger exists at the basolateral membrane of macula densa cells then increases in Na^+:K^+:$2Cl^-$ would increase $[Ca^{2+}]_i$ through both an increase in $[Na]_i$ and cellular depolarization (Schlatter et al., 1989; and Lapointe et al., 1990). However, the direction and magnitude of changes in macula densa $[Ca^{2+}]_i$ with alterations in luminal [NaCl] and osmolality is not clear. This is, in part, due to technical issues involved in the measurement of Fura 2 fluorescence during changes in cell volume (Bell et al., 1988; Salomonsson 1991*a*). In addition, the sensitivity of the macula densa apical K^+ channel to $[Ca^{2+}]_i$ in situ is not known. In three preliminary experiments using Fura 2 to measure $[Ca^{2+}]_i$, we found that removing extracellular Na increased macula densa $[Ca^{2+}]_i$ by only 70 to 150 nM. This same

maneuver resulted in a decrease in N.Po from 11.3 to 1.6 (see Fig. 5) suggesting that the channel may be sensitive to changes in $[Ca^{2+}]_i$ within the physiological range. Additional studies will be needed to establish the relationship between cytosolic calcium concentration, K channel activity and the tubuloglomerular feedback mechanism.

Recent studies have provided evidence for a $Na^+:H^+$ exchanger located on the apical membrane of macula densa cells. Using the fluorescent probe BCECF to monitor changes in macula densa pH, an amiloride-sensitive alkalinization was obtained with increases in luminal $[Na^+]$ or [NaCl] (Fowler et al., 1991). When luminal [NaCl] was increased from 25 to 150 mM, pH in macula densa cells increased from 7.15 to 7.30. In the present study, we found that reductions in bath pH from 7.4 to 6.8 completely inhibited the macula densa K^+ channel using inside-out patches. Further studies are needed to determine if increases in cell pH from a baseline of 7.15 to 7.30 would result in activation of the K^+ conductance. However, there is some doubt that changes in pH within this range will alter channel activity. The addition of furosemide or bumetanide to the lumen alkalinize macula densa cells presumably by reducing $[Na]_i$ and increasing $Na^+:H^+$ exchange. However, in the present studies, addition of bumetanide did not alter K^+ channel activity. If this observation is confirmed, then it would suggest that variations in luminal fluid [NaCl] between 20 and 150 mM would not alter K^+ channel activity, at least through changes in cell pH. This would then allow $[Cl]_i$ to change as a function of prevailing luminal fluid [NaCl] which may be important in providing a constant tubuloglomerular feedback signal.

In summary, we report the first single channel observations on a renal cell type involved in the regulation of single nephron glomerular filtration rate. A high density of Ca^{2+} and pH sensitive K^+ channels have been found in the apical membrane of macula densa cells. This channel, which appears to be different from K^+ channels in other renal epithelia, is likely to be involved in the control of membrane potential, basolateral Cl^- flux and influx through the $Na^+:K^+:2Cl^-$. By controlling these processes, the apical K^+ channel may serve an important modulator role in the transmission of tubuloglomerular feedback signals.

This work was funded by the a research grant from NIH (DK 32032) and the Kidney Foundation of Canada. A. M. Hurst is a British SERC-NATO postdoctoral fellow.

Original version received 19 March 1993 and accepted version received 19 January 1994.

REFERENCES

Barajas, L. 1981. The juxtaglomerular apparatus: anatomical considerations in feedback control of glomerular filtration rate. *Federation Proceedings.* 40:76–86.

Beck, J. S., A. M. Hurst, J. Y. Lapointe, and R. Lapade. 1993. Regulation of basolateral K^+ channel in proximal tubule studied during continuous microperfusion. *American Journal of Physiology.* 264: F494–F501.

Bell, P. D. 1985. Cyclic AMP-calcium interaction in the transmission of tubuloglomerular feedback signals. *Kidney International.* 28:728–732.

Bell, P. D. 1987. Calcium antagonists and intrarenal regulation of glomerular filtration rate. *American Journal of Nephrology.* 7(Suppl. 1):24–31.

Bell, P. D., M. Franco-Guevera, D. R. Abrahamson, J. Y. Lapointe, and J. Cardinal. 1988. Cellular mechanisms for tubuloglomerular feedback signalling. *In* The Juxtaglomerular apparatus. A. E. G. Persson, and U. Boberg, editors. Elsevier Science Publishers, New York. 63–77.

Bell, P. D., J. Y. Lapointe, and J. Cardinal. 1989. Direct measurement of basolateral membrane potentials from cells of the macula densa. *American Journal of Physiology.* 257:F463–F468.

Bleich, M., E. Schlatter, and R. Greger. 1990. The luminal potassium channel of the thick ascending limb of Henle's loop. *Pfluegers Archives.* 415:449–460.

Briggs, J. 1981. The macula densa sensing mechanism for tubuloglomerular feedback. *Federation Proceedings.* 40:99–103.

Briggs, J. P., and J. Schnermann. 1987. The tubuloglomerular feedback mechanism: functional and biochemical aspects. *Annual Review of Physiology.* 49:251–273.

Fowler, B. C., J-Y. Lapointe, and P. D. Bell. 1991. Influence of luminal NaCl transport on macula densa intracellular pH. *Journal of the American Society of Nephrology.* 2:736. (Abstr.)

Greger, R. 1985. Ion transport mechanisms in thick ascending limb of Henle's loop of mammalian nephron. *Physiological Reviews.* 65:760–797.

Hamill, O. P., A. Marty, E. Neher, B. Sakmann, and F. J. Sigworth. 1981. Improved patch clamp techniques for high resolution current recording from cells and cell free membrane patches. *Pfluegers Archives.* 391:85–100.

Hurst, A. M., M. Duplain, and J-Y. Lapointe. 1992. Basolateral membrane potassium channels in rabbit cortical thick ascending limb (CTAL). *American Journal of Physiology.* 263:F262–F267.

Hurst, A. M., and M. Hunter. 1992. Apical membrane potassium channels in frog diluting segment stimulation by furosemide. *American Journal of Physiology.* 262:F606–614.

Hurst, A. M., and M. Hunter. 1989. Apical K channels of frog diluting segment: inhibition by acidification. *Pflügers Archiv.* 415:115–117.

Kirk, K. L., P. D. Bell, D. W. Barfuss, and M. Ribadeneira. 1985. Direct visualisation of the isolated and perfused macula densa. *American Journal of Physiology.* 248:F890–F894.

Lapointe, J. Y., P. D. Bell, A. M. Hurst, and J. Cardinal. 1991. Basolateral ionic permeabilities of macula densa. *American Journal of Physiology.* 260:F856–F860.

Lapointe, J. Y., P. D. Bell, and J. Cardinal. 1990. Direct evidence for apical Na^+:$2Cl^-$:K^+ cotransport in macula densa cells. *American Journal of Physiology.* 258:F1466–F1469.

Pirie, S. C., and D. J. Potts. 1985. Application of cold flush preservation to in vitro microperfusion studies of kidney tubules. *Kidney International.* 28:982–984.

Rasmussen, H., and P. Q. Barrett. 1984. Calcium messenger system: an integrated view. *Physiological Reviews.* 64:938–984.

Salomonsson, M., E. Gonzalez, M. Kornfield, and A. E. G. Persson. 1993. The cytosolic chloride concentration in macula densa and cortical thick ascending limbs. *Acta Physiologica Scandinavica.* 147:305–313.

Salomonsson, M., E. Gonzalez, P. Westerlund, and A. E. G. Persson. 1991*a*. Intracellular cytosolic free calcium concentration in the macula densa and in ascending limb cells at different luminal concentrations of sodium chloride and with added furosemide. *Acta Physiologica Scandinavica.* 142:283–290.

Salomonsson, M., E. Gonzalez, P. Westerlund, and A. E. G. Persson. 1991*b*. Chloride concentration in macula densa and cortical thick ascending limb cells. *Kidney International Supplement.* 32:S51–S54.

Schlatter, E., M. Salomonsson, A. E. G. Persson, and R. Greger. 1989. Macula densa cells sense luminal NaCl concentration via furosemide sensitive Na^+,K^+,$2Cl^-$ cotranport. *Pfluegers Archives.* 414:286–290.

Schlatter, E. 1993. Effect of various diuretics on membrane voltage of macula densa cells. Whole-cell patch-clamp experiments. *Pflugers Archives.* 423:74–77.

Schnermann, J., and J. Briggs. 1985. Function of the juxtaglomerular apparatus: local control of glomerular hemodynamics. *In* The Kidney: Physiology and Pathophysiology. Seldin, D. W., and G. Giebisch, editors. Raven Press, New York. 669–697.

Schnermann, J., D. W. Ploth, and M. Hermle. 1976. Activation of tubuloglomerular feedback by chloride transport. *Pfluegers Archives.* 362:229–240.

Skott, O., and J. P. Briggs. 1987. Direct demonstration of macula densa-mediated renin secretion. *Science.* 237:1618–1620.

Wang, W., S. White, J. Geibel, and G. Giebisch. 1990. A potassium channel in the apical membrane of rabbit thick ascending limb of Henle's loop. *American Journal of Physiology.* 258:F244–F253.

Wright, F. S., and J. Schnermann. 1974. Interference with feedback control of glomerular filtration rate by furosemide, triflocin and cyanide. *Journal of Clinical Investigation.* 53:1695–1708.

Wright, F. S. 1981. Characteristics of feedback control of glomerular filtration rate. *Federation Proceedings.* 40:87–92.

DEUXIÈME ARTICLE

Evidence for apical sodium proton exchange in macula densa cells

Fowler B.C., Chang Y.S., Laamarti M.A., Higdon M., Lapointe J.Y., and

P.D. Bell

Kidney International, Vol. 47 (1995), pp. 746–751

Evidence for apical sodium proton exchange in macula densa cells

BETH C. FOWLER, YOON-SIK CHANG, ANOUAR LAAMARTI, MICHAEL HIGDON, JEAN-YVES LAPOINTE, and P. DARWIN BELL

Nephrology Research and Training Center, Departments of Medicine and Physiology, University of Alabama at Birmingham, Birmingham, Alabama, USA, and Membrane Transport Research Group, University of Montreal, Montreal, Quebec, Canada

Evidence for apical sodium proton exchange in macula densa cells. These studies were performed to determine if changes in luminal sodium chloride concentration ([NaCl]) might alter macula densa intracellular pH. Isolated thick ascending limbs with attached glomeruli were bathed in a 150 mM NaCl Ringer's solution and perfused *in vitro* with a 25 mM NaCl solution; N-methyl-D-glucamine cyclamate was used to substitute for NaCl. Macula densa cells were loaded with BCECF and intracellular pH was monitored using a microscope based-dual excitation photometer system. Control intracellular pH for all experiments in which tubules were initially perfused with 25 mM NaCl averaged 7.22 ± 0.06; $N = 28$. Increasing luminal [NaCl] from 25 to 150 mM elevated macula densa pH by 0.15 ± 0.03 ($N = 6$; $P < 0.05$) while increasing just luminal [Na] from 25 to 150 mM alkalinized macula densa cells by 0.17 ± 0.05 ($N = 6$; $P < 0.05$). In addition, there was a highly significant linear relationship between luminal [Na] and intracellular pH between 25 and 150 mM NaCl. Other studies were performed to assess the effects of amiloride, an inhibitor of Na:H exchange, on macula densa intracellular pH. Addition of amiloride, to the 25 mM NaCl perfusate acidified macula densa cells by 0.09 ± 0.03 ($N = 6$; $P < 0.001$) and significantly attenuated the increase in pH obtained when luminal [NaCl] was raised from 25 to 150 mM. Other studies evaluated the effects of inhibition of Na:2Cl:K cotransport on macula densa pH. Furosemide (50 μM) alkalinized macula densa pH by 0.11 ± 0.02 ($N = 5$; $P < 0.01$) in the presence of 25 mM NaCl in the lumen whereas amiloride entirely reversed the furosemide-induced alkanization in these cells. These results demonstrate that changes in either luminal [NaCl] or furosemide-sensitive NaCl transport can alter macula densa intracellular pH presumably by varying the Na gradient across the apical membrane. The results of these studies are consistent with the existence of an apical Na:H antiporter in macula densa cells.

Macula densa cells, located at the point of contact between cortical thick ascending limb and glomerulus, are an integral component of the tubuloglomerular feedback mechanism [1]. This feedback mechanism is thought to involve detection of changes in luminal fluid composition by macula densa cells and transmission of information to afferent arteriolar smooth muscle cells. Tubuloglomerular feedback signals produce changes in renal vascular resistance which are responsible for alterations in glomerular filtration rate (GFR) [2–6]. Tubuloglomerular feedback may be a major factor in linking single GFR with tubular reabsorption as well as in the autoregulation of renal blood flow and GFR.

Received for publication July 8, 1994
and in revised form October 10, 1994
Accepted for publication October 10, 1994

To gain further insights into this mechanism, recent studies have utilized isolated segments of cortical thick ascending limbs (CTAL's) with attached glomeruli and *in vitro* tubular perfusion techniques. This approach, coupled with electrophysiological techniques, has provided the means of defining and examining certain transport characteristics of macula densa cells [7–11]. For example, it was found that basolateral membrane potential (Vbl) of macula densa cells depolarized by approximately 30 mV in response to increases in luminal fluid sodium chloride concentration ([NaCl]) from 20 to 150 mM [9, 10]. Further studies by our laboratories [8] and others [10, 11] demonstrated that Vbl was sensitive to the addition of furosemide to the lumen, suggesting that NaCl movement across the luminal membrane occurred, at least in part, through a Na:2Cl:K cotransporter. Although no evidence was obtained for apical electrogenic conductances for Na or Cl [8], recent studies using patch clamp techniques and previous electrophysiological studies [10] have identified the presence of apical potassium channels that are sensitive to changes in cytosolic pH and calcium [12]. Finally, other studies utilizing microelectrodes have identified a basolateral Cl conductance that may participate in the regulation of Vbl through transport related changes in intracellular [Cl] [7, 10].

In other renal epithelia, including proximal tubule and thick ascending limb, a Na:H exchanger has been identified in both apical and basolateral membranes and it is generally recognized that this exchanger plays an important role in the control of intracellular pH [13–22]. It was therefore of interest to determine if such an exchanger also existed in macula densa cells. We were particularly interested in the presence of an apical Na:H transporter since under normal conditions, luminal [NaCl] can vary within the range of 20 to 60 mM due to flow dependent changes in NaCl transport by the thick ascending limb [5, 23, 24]. Therefore, the existence of a luminal Na:H exchanger might lead to a mechanism in which macula densa cells, through changes in intracellular pH, would be sensitive to physiological alterations in luminal [Na]. The purpose of these studies was to directly measure macula densa intracellular pH using the fluorescent probe BCECF during alterations in luminal fluid [NaCl].

Methods

Experiments were performed using kidneys obtained from female New Zealand white rabbits weighing 0.5 to 1 kg maintained on Purina Rabbit Chow. Saggital slices of kidney were

placed in a dissection dish containing Ringer's solution composed of (in mM): 148 NaCl, 5 KCl, 1 $MgSO_4$, 1.6 Na_2HPO_4, 0.4 NaH_2PO_4, 1.5 $CaCl_2$ and 5 D-glucose. Glomeruli with thick ascending limbs were isolated and transferred to a chamber containing Ringer's solution which was mounted on an Leitz Fluovert inverted microscope with quartz optics as described previously [25, 26]. The thick ascending limb was cannulated and perfused with Ringer's solution. The bathing solution was continuously aerated with 100% O_2 and the solution in the chamber was exchanged at a rate of 1 ml/min. Temperature was maintained at 37°C. Luminal solutions were modified by isosmotically replacing Na with N-methyl-D-glucamine and Cl with cyclamate (Sigma Chemical Co., St. Louis, MO, USA) in order to achieve a [Na] or [Cl] of between 25 and 150 mM. All solutions were adjusted to a pH of 7.4. In some experiments, 50 μM furosemide (Elkins-Sinn, Inc., Cherry Hill, NJ, USA) and/or 1 mM amiloride (Sigma Chemical Co.) were added to the perfusion solution.

Intracellular pH of macula densa cells was measured with dual excitation wavelength fluorescence microscopy (Photon Technologies, Inc., Princeton, NJ, USA) using the fluorescent probe, 2',7'-bis-(2-carboxyethyl)-5 (and -6) carboxyfluorescein acetoxymethyl ester (BCECF-AM; Molecular Probes Inc., Eugene, OR, USA) dissolved in dimethylsulfoxide. Excitation monochrometers were set at 500 and 440 nm and light entering the microscope was alternated between these two wavelengths by a computer controlled chopper assembly. Fluorescent emissions were restricted by a 10 nm bandpass filter centered at 530 nm. An adjustable optical photometer sampling window was positioned over the macula densa cells and emitted photons were detected by a Leitz photometer that was modified for photon counting. Magnification was 400× using an Olympus 40× UVF lens. Fluorescence measurements were performed at a rate of 20 points/sec, and data were stored and processed using PTI software [25, 26].

Macula densa cells were loaded with dye by adding BCECF-AM (10 μM) to the 25 mM NaCl luminal perfusate. Tubules were perfused with BCECF-AM while monitoring macula densa BCECF fluorescence at both excitation wavelengths. Loading of macula densa cells with BCECF-AM generally required 5 to 10 minutes, at which time cps for both wavelengths stabilized at values that were at least ten times greater than background fluorescence. Background fluorescence was subtracted from each channel. BCECF-AM was removed from the lumen and a period of 10 to 15 minutes was allowed to elapse before measurements were performed.

BCECF ratios were converted to pH units using an intracellular calibration procedure similar to that reported by Alpern [27] and Chaillet and Boron [28]. Macula densa cells were loaded with BCECF and then perfused and bathed with a solution containing (in mM) 120 KCl, 1.0 MgCl, 1.5 Na_2HPO_4, 25 HEPES and 14 μM of the K/H ionophore nigericin (Sigma Chemical Co.). For both the bath and luminal solutions, pH was adjusted in increments of 0.4 pH units between 6.4 and 8.0. The relationship between pH and ratio was linear between pH of 6.4 to 8.0. Ratios obtained at each pH and experimental ratios were converted to pH by interpolation.

Experimental studies consisted of only the manipulation of the luminal solution while maintaining the composition of the bathing solution constant. For these studies, the BCECF ratio was monitored for approximately 100 seconds during perfusion with the control Ringer's solution in which both [Na] and [Cl] were 25 mM. After a stable control period was obtained, the luminal perfusate was switched to one containing a different [NaCl] and/or drug and the ratio was monitored for an additional 100 to 300 seconds or until a steady state value was obtained. The perfusate was then returned to the 25 mM Ringer's solution and a recontrol value obtained. All pH values reported in these studies are steady state changes in intracellular pH.

Data are expressed as mean ± SE. Statistical significance was established using Student's paired *t*-test or linear regression analysis. Significance was accepted at $P < 0.05$.

Results

Using BCECF, the overall average macula densa intracellular pH in these studies was 7.22 ± 0.06 ($N = 28$) in the presence of 25 mM luminal NaCl and 150 mM NaCl in the bathing soution. The first series of studies were performed to determine the effects of luminal [NaCl] on macula densa intracellular pH. An example of such an experiment is shown in Figure 1A. In response to an increase in luminal [NaCl] from 25 to 150 mM, there was a rapid alkalinization of macula densa cells. This increase in cellular pH was sustained and reversible upon the return of luminal [NaCl] to 25 mM. Figure 1B illustrates that the same general pattern of response was obtained if only Na was elevated from 25 to 150 mM, and also demonstrates the reversibility of this response upon return of luminal [Na] to 25 mM. These studies are summarized in Figure 2. Macula densa pH increased by 0.15 ± 0.03 ($N = 6$; $P < 0.01$) in response to an increase in luminal [NaCl] from 25 to 150 mM and by 0.17 ± 0.05 ($N = 6$; $P < 0.05$) when Na was elevated to 150 mM at constant luminal Cl. The relationship between luminal [Na] and intracellular pH is shown in Figure 3. In each of six experiments there was a progressive increase in macula densa cell pH as luminal NaCl was increased from 25 to 150 mM. The relationship between pH and luminal [Na] was $y = 0.003(x) + 7.024$ with an r value of 0.996 based on linear regression analysis.

If the alkalinization obtained with increases in luminal [Na] or [NaCl] was due to Na:H exchange, then it should be sensitive to amiloride. This issue was addressed in the next series of studies which are summarized in Figure 4. As shown on the left side of Figure 4, addition of amiloride (1 mM) to the perfusate acidified macula densa cells by 0.09 ± 0.03 ($P < 0.001$) in the presence of 25 mM luminal [Na]. It also blunted the increase in pH obtained with an elevation in luminal [NaCl]. ΔpH in response to increased luminal [NaCl] from 25 to 150 mM was 0.33 ± 0.08 without amiloride and was significantly reduced (0.21 ± 0.06; $P < 0.02$) in the presence of amiloride in the lumen.

Previously, we and others [8, 10] have concluded that NaCl transport by macula densa cells involves a furosemide sensitive Na:2Cl:K transporter. It was therefore of interest to determine if addition of luminal furosemide affected macula densa intracellular pH. Presumably this could occur through changes in intracellular [Na] which then would alter Na:H exchange. As shown in Figure 5, addition of 50 μM furosemide to the 25 mM NaCl luminal perfusate resulted in a significant alkalinization of these cells. The ΔpH due to this maneuver was 0.11 ± 0.02 ($N = 5$; $P < 0.01$). If the alkalinization induced by furosemide was due to Na:H exchange then it should be sensitive to amiloride. As shown in Figure 5, 1 mM amiloride reversed furosemide-induced alkalinization and significantly acidified macula densa cells by 0.26 ± 0.04 ($N = 5$; $P < 0.04$) in the continued presence of furosemide.

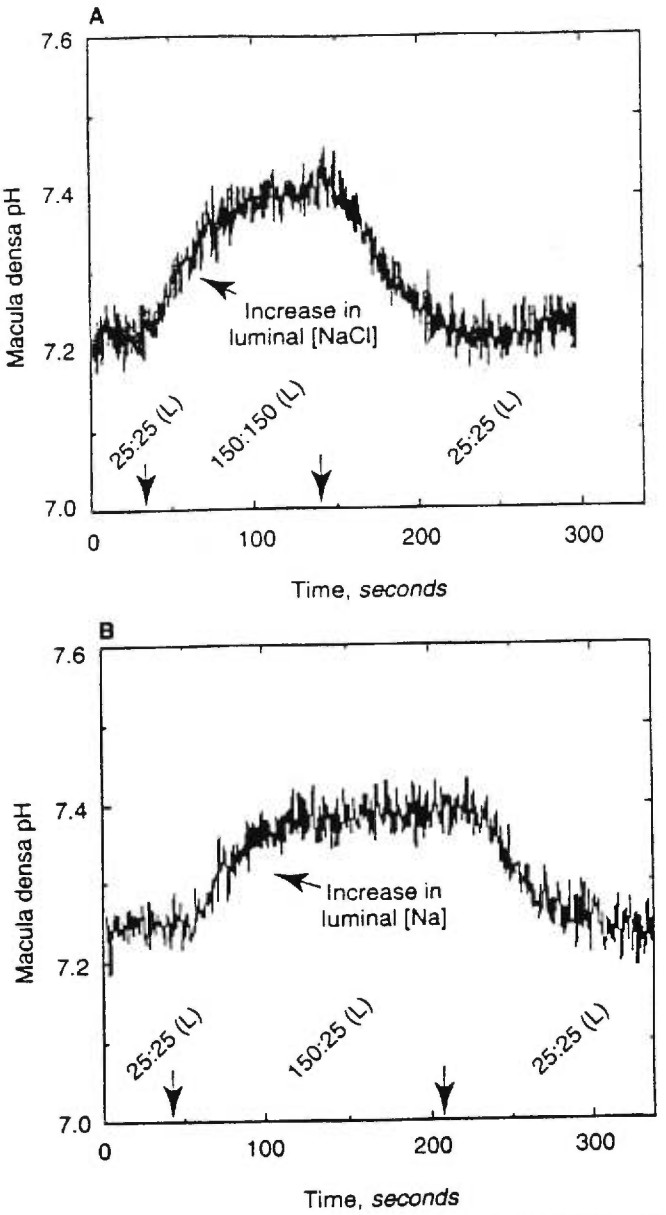

Fig. 1. *Examples of the effects of increases in luminal [NaCl]* (**A**) *or just [Na]* (**B**) *on macula densa intracellular pH.*

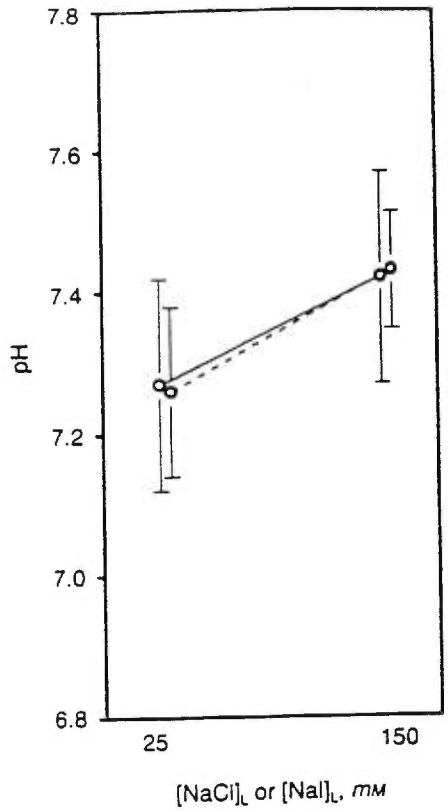

Fig. 2. *Summary of the effect of increasing luminal [NaCl] or just [Na] on macula densa cell pH.* As shown, there was no significant difference between the effects of NaCl (–O–) or Na (--O--) at constant luminal [Cl].

Discussion

The present studies measured intracellular pH in macula densa cells using the fluorescent probe BCECF. Initial measurements of intracellular pH were performed in the presence of 25 mM NaCl in the lumen and 150 mM NaCl in the bathing solution. Luminal [NaCl] at the macula densa is thought to be in the range of 20 to 60 mM so that pH measurements obtained at a low luminal [NaCl] may reflect macula densa intracellular pH under physiological conditions. We found that intracellular pH in macula densa cells averaged 7.22, a value similar to that obtained in a variety of epithelial and non-epithelial cells [14].

Macula densa intracellular pH was sensitive to changes in luminal fluid [NaCl]. In response to an increase in luminal [NaCl] from 25 to 150 mM, there was an increase in pH that was sustained and reversible upon return to the 25 mM NaCl luminal perfusate. In addition, nearly identical increases in intracellular pH were obtained when Na alone was increased from 25 to 150 mM. The most straightforward interpretation of this data is that, like other renal epithelia, the macula densa cells possess an apical Na:H exchanger [15–17, 19, 22]. As will be discussed in the accompanying paper [29], an increase in luminal [Cl] can acidify macula densa cell pH when luminal [Na] is kept constant at 20 mM. It should be carefully noted that this is exactly opposite to the alkalinization obtained with increases in either luminal Na or NaCl. Further experiments show that this acidification, with a specific increase in luminal [Cl], is due to a stimulation of Na:2Cl:K contransport which presumbly increases intracellular [Na] and thereby decreases proton efflux through the apical exchanger at constant low luminal [Na]. However, when luminal [Na] or [NaCl] was elevated to 150 mM in the present study, there would be a continued large gradient for Na entry through the Na:H exchanger inspite of Na:2Cl:K contransport-induced changes in intracellular [Na].

In other experiments, we found a linear increase in macula densa cell pH when luminal [NaCl] was varied between 25 to 150 mM. We were particularly interested in the fact that changes macula densa cell pH were linear when luminal [NaCl] was varied

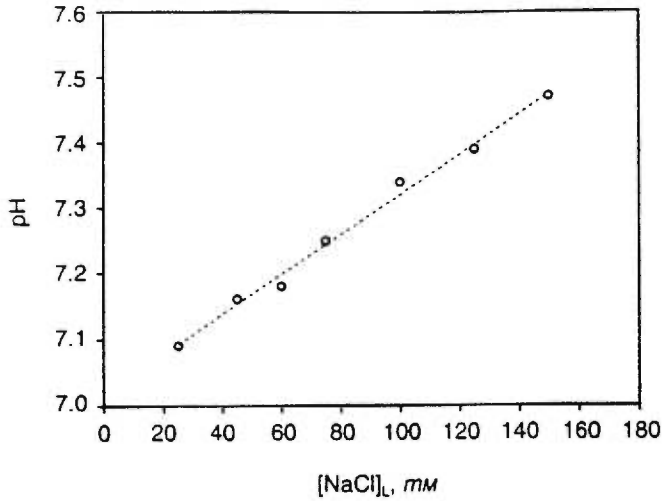

Fig. 3. *Summary of the relationship between luminal [NaCl] and macula densa cell pH.* [NaCl] was set at 25, 45, 60, 75, 100, 125, and 150 mM and osmolality of the solution was kept constant with N-methyl-D-glucamine. Data were analyzed using linear regression analysis. Experiments were performed in 6 different preparations. All 7 different [NaCl] were tested in each preparation.

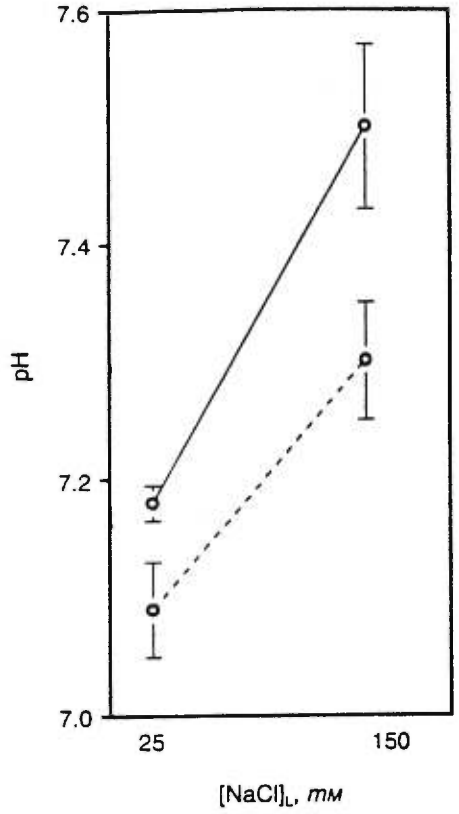

Fig. 4. *The effects of amiloride (1 mM) on baseline macula densa pH and in the response of these cells to increases in luminal [NaCl].* Control (–O–) and amiloride (--O--) studies were performed in 6 paired experiments.

between 25 and 75 mM. Since variations in [NaCl] within this range may represent normal fluxations in luminal [NaCl] at the macula densa [23, 24], these results suggest that macula densa cellular pH may vary in response to normal physiological changes in luminal [NaCl].

It is now well established that a number of epithelial tissues possess apical and/or basolateral forms of the Na:H exchanger. In renal epithelia, the Na:H exchanger is either restricted to the apical membrane such as in proximal tubular cells [19] or is present in both apical and basolateral membrane as in LLC-PK1 cells and TAL [20, 21, 30]. In most cells, the basolateral exchanger has generally been found to have a high affinity for amiloride and its analogs [30, 31] and is most likely the ubiquitous "housekeeping" form of the exchanger (NHE-1) [32]. A distinct isoform of the Na:H exchanger family, NHE-3, was found to be exclusively expressed in kidney and intestine and displays an amiloride affinity that is about two orders of magnitude lower than that of NHE-1 [33–35]. In all likelihood this form of the exchanger is expressed at the apical membrane of renal and intestinal epithelial cells. In macula densa cells, 150 mM luminal Na alkalinized macula densa cells and even a large concentration of amiloride (1 mM) reduced the elevation in pH by only 36% (see Figure 4; ΔpH of 0.21 vs. 0.33 pH with increased luminal NaCl in the presence and absence of amiloride, respectively). For comparison, the apical exchanger of rat proximal tubules is inhibited by 31 to 33% in the presence of 0.9 mM amiloride and 152 mM Na [21, 36]. While amiloride was found to act as a competitive inhibitor with a K_i of 33 μM for the basolateral exchanger of proximal tubule [36]. In the medullary TAL, both apical and basolateral exchangers appear to be quite sensitive to amiloride with 0.5 mM amiloride inhibiting 80 to 90% of exchange activity in the presence of symmetrical 140 mM Na solution. A low amiloride K_i of 10.6 μM (Recalculation of the amiloride K_i based on the data in Fig. 8 of Kikeri et al, using a K_m^{Na} of 113.2 mM as reported in the same paper gives a value of 6 μM which is even lower than the reported value of 10.6 μM.) was found for the apical exchanger of the medullary TAL which approaches the range of K_i reported for NHE-1 [20, 33]. This indicates that the macula densa cells possess an apical Na:H exchanger which is resistant to amiloride and, in this characteristic, is similar to the exchanger reported for the brush border membrane of proximal tubules and dissimilar to the apical medullary TAL exchanger.

In other studies, we found that, in the presence of 25 mM luminal NaCl, administration of furosemide resulted in sustained alkalinization of macula densa cells. As stated earlier, these results suggest that alterations in furosemide-sensitive Na:2Cl:K cotransport can alter the pH of these cells. Presumably this occurs, through a furosemide inhibition of NaCl cotransport, a fall in intracellular [Na] and a stimulation of Na entry and proton exit through the apical Na:H exchanger. As discussed in the accompanying paper [29] this lends support to the notion that, in the presence of 25 mM [NaCl], macula densa cells are absorbing NaCl. That the effects of furosemide occur through the Na:H exchanger was further supported by the finding that furosemide-induced alkalinization was sensitive to amiloride. The addition of amiloride completely reversed the alkalinization obtained with furosemide.

The results of these studies suggest that macula densa pH can be influenced by at least two processes. First, macula densa pH is sensitive to alterations in luminal [Na]. Low flow rate through the thick ascending limb would be associated with low luminal [Na]

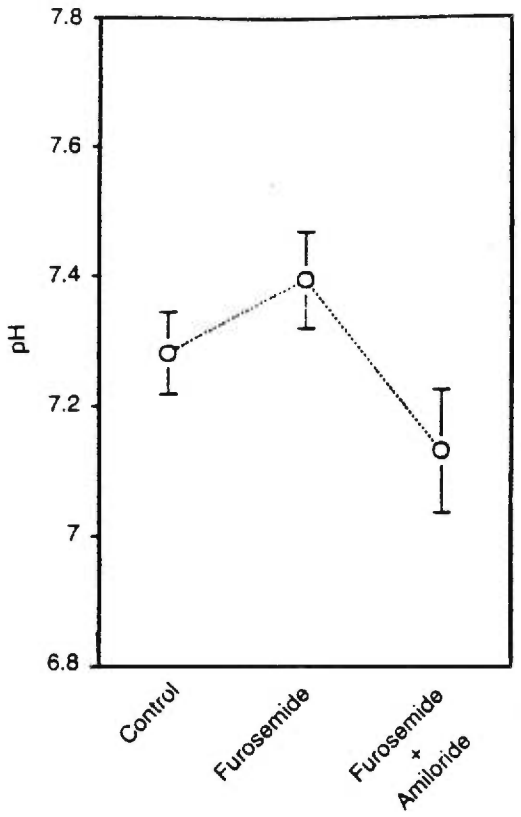

Fig. 5. *The effects of 50 μM furosemide added to the perfusate on macula densa pH.* Furosemide alkalinized macula densa cells while the addition of 1 mM amiloride reversed the furosmide-induced alkalinization and substantially acidified these cells. Experiments were performed in 6 different preparations.

and acidified macula densa cells while high low flow rates would produce high luminal [Na] and alkalinized macula densa cells. Second, macula densa cell pH can be influenced by Na:2Cl:K transporter induced changes in intracellular [Na]. Under physiological conditions, an increase in cotransport resulting from elevated luminal [NaCl] would lead to an increase in intracellular [Na] and a reduced Na gradient across the exchanger. Enhanced NaCl cotransport may tend to reduce or counteract the alkalinization obtained by a specific increase in luminal [Na]. Therefore the net effect of increased luminal [NaCl] would be determined by the resultant Na gradient across the macula densa cell. Interestingly, changes in luminal or cellular K might have an effect on cell pH due to the effects of K on cotransport.

The results of these studies help to further define the transport characteristics of macula densa cells. Recent evidence suggests that the apical membrane contains a Na:2Cl:K cotransporter and a K channel while the basolateral membrane has a predominant chloride conductance. The results of these studies now indicate that these cells contain an apical Na:H exchanger that can alter intracellular pH in response to changes in luminal [Na]. Although its role in tubuloglomerular feedback awaits to be defined, it is interesting that this exchanger links changes in luminal [NaCl] with intracellular pH, a clearly important intracellular messenger system.

Acknowledgments

This work was supported by National Institutes of Health Grant DK-32032, NIH Training Grant DK-07545 and the Kidney Foundation of Canada. We thank Clay Isebell for technical support and Martha Yeager for secretarial assistance.

Reprint requests to P. Darwin Bell, Ph.D., University of Alabama at Birmingham, UAB Station, 865 Sparks Center, Birmingham, Alabama 35294, USA.

References

1. Barajas L: The juxtaglomerular apparatus: Anatomical considerations in the feedback control of glomerular filtration rate. *Fed Proc* 40:78–86, 1981
2. Bell PD, Franco M, Navar LG: Calcium as a mediator of tubuloglomerular feedback. *Ann Rev Physiol* 49:275–293, 1987
3. Bell PD, Franco M, Abrahamson DR, Lapointe J-Y, Cardinal J: Cellular mechanisms for tubuloglomerular feedback signaling, in *The Juxtaglomerular Apparatus*, edited by AEG Persoon, U Boberg, Amsterdam, Elsevier, 1988, pp 63–77
4. Briggs JP, Schnermann J, Scott O: Macula densa transport: Direct and indirect approaches, in *The Juxtaglomerular Apparatus*, edited by AEG Persoon, U Boberg, Amsterdam, Elsevier, 1988, pp 79–87
5. Schnermann J, Briggs J: Function of the juxtaglomerular apparatus: Local control on glomerular hemodynamics, in *The Kidney*, edited by DW Seldin, G Giebish, New York, Raven Press, 1985, pp 669–697
6. Persson AEG, Salomonsson M, Westerlund P, Greger R, Schlatter E, Gonzalez E: Macula densa cell function. *Kidney Int* 39:S39–S44, 1991
7. Lapointe J-Y, Bell PD, Hurst AM, Cardinal J: Basolateral ionic permeabilities of macula densa cells. *Am J Physiol* 260:F856–F860, 1991
8. Lapointe J-Y, Bell PD, Cardinal J: Direct evidence for apical Na^+:$2Cl^-$:K^+ cotransport in macula densa cells. *Am J Physiol* 258: F1466–F1469, 1990
9. Bell PD, Lapointe J-Y, Cardinal J: Direct measurement of basolateral membrane potentials from cells of the macula densa. *Am J Physiol* 257:F463–F468, 1989
10. Schlatter E, Salomonsson M, Persson AEG, Greger R: Macula densa cells sense luminal NaCl concentration via furosemide sensitive $Na^+2Cl^-K^-$ cotransport. *Pflügers Arch* 414:286–290, 1989
11. Schlatter E: Effect of various diuretics on membrane voltage of macula densa cells. Whole-cell patch clamp experiments. *Pflügers Arch* 423:74–77, 1993
12. Hurst AM, Lapointe J-Y, Laamarti A, Bell PD: General properties and potential regulators of the apical K channel in macula densa cells. *J Gen Physiol* 103:1055–1070, 1994
13. Borensztein P, Leviel F, Froissart M, Houillier P, Poggioli J, Marty E, Bichara M, Paillard M: Mechanisms of H^+/HCO_3^- transport in the medullary thick ascending limb of rat kidney. *Kidney Int* 40:S43–S46, 1991
14. Boron WH: Intracellular pH regulation in epithelial cells. *Ann Rev Physiol* 48:377–388, 1986
15. Chantrelle B, Cogan MG, Rector FCJ: Evidence for coupled sodium/hydrogen exchange in the rat superficial proximal convoluted tubule. *Pflügers Arch* 395:186–189, 1982
16. Clark JD, Limbird LE: Na^+-H^+ exchanger subtypes: a predictive review. *Am J Physiol* 261:C945–C953, 1991
17. Froissart M, Borensztein P, Houillier P, Leviel F, Poggioli J, Marty E, Bichara M, Paillard M: Plasma membrane Na^+-H^+ antiporter and H^+-ATPase in the medullary thick ascending limb of rat kidney. *Am J Physiol* 262:C963–C970, 1992
18. Good DW: Sodium-dependent bicarbonate absorption by cortical thick ascending limb of rat kidney. *Am J Physiol* 248:F821–F829, 1985
19. Ives HE, Yee VJ, Warnock DG: Asymmetric distribution of the Na^+-H^+ antiporter in the renal proximal tubule epithelial cell. *J Biol Chem* 258:9710–9716, 1983
20. Kikeri D, Azar S, Sun A, Zeidel ML, Hebert SC: Na^+-H^+ antiporter and Na^+-$(HCO_3^-)_n$ symporter regulate intracellular pH in mouse medullary thick limbs of Henle. *Am J Physiol* 258:F445–F456, 1990

21. PREISIG PA, IVES HE, CRAGOE EJ JR, ALPERN RJ, RECTOR FC JR: Role of the Na^+/H^+ antiporter in rat proximal tubule bicarbonate absorption. *J Clin Invest* 80:970–978, 1987
22. SUN AM, KIKERI D, STEVEN CH: Vasopressin regulates apical and basolateral Na^+-H^+ antiporters in mouse medullary thick ascending limbs. *Am J Physiol* 262:F241–F247, 1992
23. BELL PD, NAVAR LG: Relationship between tubuloglomerular feedback responses and perfusate hypotonicity. *Kidney Int* 22:234–239, 1982
24. SCHNERMANN J, BRIGGS J, SCHUBERT G: In situ studies of the distal convoluted tubule in the rat. Evidence for NaCl secretion. *Am J Physiol* 243:F160–F166, 1982
25. ROUCH AJ, CHEN L, KUDO H, BELL PD, FOWLER BC, CORBITT BD, SCHAFER JA: Intracellular Ca and PKC activation do not inhibit Na and water transport in rat CCD. *Am J Physiol* 265:F569–F577, 1993
26. CARMINES PK, FOWLER, BC, BELL PD: Segmental distinct effects of depolarization on intracellular [Ca] in renal arterioles. *Am J Physiol* 265:F677–F685, 1993
27. ALPERN RJ: Mechanism of basolateral membrane $H^+/OH^-/HCO_3^-$ transport in the rat proximal convoluted tubule. *J Gen Physiol* 86:613–636, 1985
28. CHAILLET JR, BORON WF: Intracellular calibration of a pH-sensitive dye in isolated perfused salamander proximal tubules. *J Gen Physiol* 86:765–794, 1985
29. LAPOINTE J-Y, LAAMARTI A, HURST AM, FOWLER BC, BELL PD: Activation of Na:2Cl:K contransport by luminal chloride in macula densa cells. *Kidney Int* 47:752–757, 1995
30. HAGGERTY JG, AGARWAL N, REILLY RF, ADELBERG EA, SALYMAN CW: Pharmacologically different Na/H antiporters on the apical and basolateral surfaces of cultured porcine kidney cells (LLC-PK). *Proc Natl Acad Sci USA* 85:6797–6801, 1988
31. KNICKELBEIN RG, ARONSON PS, DOBBINS JW: Characterization of Na-H exchangers on villus cells in rabbit ileum. *Am J Physiol* 259: G802–G806, 1990
32. TSE CM, MA AL, YANG VW, WATSON AJM, LEVINE S, MONTROSE MH, POTTER J, SARDET C, POUYSSEGUR J, DONOWITZ M: Molecular cloning and expression of a cDNA encoding the rabbit ileal villus cell basolateral membrane Na/H exchanger. *EMBO J* 10:1957–1967, 1991
33. ORLOWSKI J, KANDASAMY A, SHULL GE: Molecular cloning of putative members of the Na/H exchanger gene family. *J Biol Chem* 267:9331–9339, 1992
34. TSE C-M, BRANT SR, WALKER MS, POUYSSEGUR J, DONOWITZ M: Cloning and Sequencing of a rabbit cDNA encoding an intestinal and kidney-specific Na/H exchanger isoform (NHE-3). *J Biol Chem* 267: 9340–9346, 1992
35. ORLOWSKI J: Heterologous expression and functional properties of amiloride high affinity (NHE-1) and low affinity (NHE-3) isoforms of the rat Na/H exchanger. *J Biol Chem* 268:16369–16377, 1993
36. BIDET M, TAUC M, MEROT J, VANDEWALLE A, POUJEOL P: Na-H exchnger in proximal cells isolated from rabbit kidney. I. Functional characteristics. *Am J Physiol* 253:F935–F944, 1987

TROISIÈME ARTICLE

Activation of Na :2Cl :K cotransport by luminal chloride in macula densa cells

Lapointe J.Y., Laamarti M.A., Hurst A.M, Fowler B.C., and P.D. Bell

Kidney International, Vol. 47 (1995), pp. 752–757

Activation of Na:2Cl:K cotransport by luminal chloride in macula densa cells

JEAN-YVES LAPOINTE, ANOUAR LAAMARTI, ANNETTE M. HURST, BETH C. FOWLER, and P. DARWIN BELL

Groupe de recherche en transport membranaire, Université de Montréal, Montréal, Québec, Canada, and Nephrology Research and Training Center and Departments of Medicine and Physiology University of Alabama at Birmingham, Birmingham, Alabama, USA

Activation of Na:2Cl:K cotransport by luminal chloride in macula densa cells. Changes in macula densa intracellular pH (pH_i) were used to monitor the direction of flux mediated by the apical Na:2Cl:K cotransporter. At the macula densa, a decrease in luminal [Cl] ($[Cl]_l$) from 60 to 1 mM produced cellular alkalinization secondary to a cascade of events involving a decrease in apical Na:2Cl:K cotransport, a fall in intracellular [Na] ($[Na]_i$) and a stimulation of Na:H exchange. This is supported by the fact that 97% of the change in macula densa pH_i with reduction in $[Cl]_l$ was bumetanide-sensitive whereas 92% of this pH change was amiloride-sensitive. We found that, in the presence of 20 mM Na and 5 mM K, a $[Cl]_l$ of 14.3 ± 2.4 mM ($N = 7$) produced equilibrium of the apical cotransporter since the pH_i obtained under this condition was identical to the pH_i found after reducing the net ionic flux to zero with bumetanide. Using this value together with the expected stoichiometry for the bumetanide-sensitive cotransporter, it was estimated that the intracellular [Cl] ($[Cl]_i$) at equilibrium (or in the presence of bumetanide) could be as low as 5 mM. Also, using a Hill number of 2 which is consistent with the present data, the affinity for $[Cl]_l$ was found to be 32.5 mM. Under physiological luminal conditions prevailing at the end of the thick ascending limb (~3.5 mM K, and ~25 to 30 mM NaCl), macula densa cells are probably operating close to equilibrium while maintaining a small net reabsorption of Na/K and Cl. Since macula densa cells appear capable of reducing $[Cl]_i$ to very low levels, a reabsorptive flux should continue to occur until $[NaCl]_l$ is reduced to 18 mM.

Recent electrophysiological data from macula densa cells have established the presence of a furosemide-sensitive apical Na:2Cl:K cotransporter which is thought to act as a sensor by which macula densa cells may detect changes in luminal [NaCl] ($[NaCl]_l$) [1–4]. Inhibition of the cotransporter with furosemide or bumetanide produces a large effect on membrane potential presumably through alterations in intracellular [Cl] ($[Cl]_i$) in the presence of a Cl-conductive basolateral membrane [2, 4]. Our previous finding that furosemide depolarized macula densa cells in the presence of 25 mM $[NaCl]_l$ while it seemed to hyperpolarize cells in the presence of 150 mM $[NaCl]_l$ [1, 3], was interpreted as evidence that the Na:2Cl:K cotransporter secreted NaCl into the lumen at low $[NaCl]_l$ and reversed to reabsorb NaCl at some intermediate $[NaCl]_l$ between 25 and 150 mM. Since $[NaCl]_l$ measured in the early distal fluid is ~40 to 70 mM [5, 6], it was tempting to speculate that macula densa cells might be at or near the equilibrium point of the Na:2Cl:K cotransporter under normal conditions.

The purpose of the present study was to further evaluate NaCl transport in macula densa cells with emphasis on estimating the equilibrium point of the cotransporter under physiological conditions. It was therefore necessary to develop a method to monitor flux through the apical cotransporter that was not dependent upon the use of microelectrodes in order to avoid any possible alterations in transmembrane ionic gradients that may occur upon cell impalement. Our method is based on measurements of intracellular pH (pH_i) with the fluorescent probe 2',7'-bis-2-carboxyethyl-5(and -6)carboxyfluorescein (BCECF). As shown in the accompanying paper [7], the presence of an amiloride-sensitive Na:H exchanger at the apical membrane of macula densa cells has been demonstrated. We noticed that luminal administration of furosemide or bumetanide in the presence of 25 mM $[NaCl]_l$ alkalinized macula densa cells, suggesting that inhibition of apical Na:2Cl:K cotransport induced a reduction in intracellular [Na] ($[Na]_i$) which in turn activated the Na:H exchanger. Further experiments have supported the fact that, at constant $[Na]_i$, measurements of macula densa pH_i might serve as an index of the Na:2Cl:K transport activity. Comparing the effect of different $[Cl]_l$'s to the effect of bumetanide on macula densa pH_i, we were able to determine the $[Cl]_i$ at which the Na:2Cl:K cotransporter was at equilibrium. Results suggest that the apical Na:2Cl:K cotransporter is normally reabsorbing NaCl but is operating quite close to its equilibrium under physiological conditions.

Methods

Perfusion

The techniques used in these studies were similar to those described in previous papers from our laboratories [1–3]. Briefly, cortical thick ascending limbs (CTAL) with attached glomeruli were dissected from the midcortical region of kidneys from New Zealand white female rabbits. The CTAL was transferred to a thermoregulated Lucite chamber mounted on an inverted Zeiss microscope and cannulated with concentric pipettes as originally described by Burg et al [8]. The distal end of the tubule was left open to the bath and a holding pipette was placed on top of the glomerulus in order to stabilize and position the preparation.

Received for publication July 8, 1994
and in revised form October 10, 1994
Accepted for publication October 10, 1994

The tubule was bathed at 39°C in a solution containing (in mM): 137 NaCl, 5 K-gluconate, 1 $MgSO_4$, 1.35 $CaCl_2$, 1.2 Na_2HPO_4, 0.3 NaH_2PO_4, 5 glucose, 10 mannitol, 10 N-2-hydroxyethylpiperazine-N'-2-ethane-sulfonic acid (Hepes) and 7.2 Tris-(hydroxymethyl)-aminomethane. Since [NaCl]'s were close to 140 mM, this solution was designated as the 140/140 solution (that is, Na over Cl concentrations). The luminal perfusate had the same composition except that the [NaCl] was reduced by replacing Na with N-methyl-D-glucamine and Cl by cyclamate. Unless otherwise stated, the final [Na] was always 20 mM and the [Cl] was adjusted to 1, 5, 10, 20, 30, 60 and 140 mM. Perfusate solutions were respectively called 20/1, 20/5, 20/10, etc. For all solutions, pH was adjusted to 7.4 after bubbling with 100% O_2 and the osmolality was maintained at 300 mOsm/kg. In some experiments either 1 mM amiloride, 5 μM bumetanide or 10 μM nigericin (all three compounds from Sigma Chemical Co., St. Louis, MO, USA) were added to the luminal or basolateral solutions from concentrated stock solutions using ethanol as solvent. The solvent concentration in the final solution never exceeded 0.2%.

Fluorescence

Upon cannulation of the CTAL, tubules were perfused and bathed in the 140/140 solution. The glomerulus was positioned and held at the bottom of the chamber using a glass pipette in such a way that the macula densa plaque could be directly view with a 40× objective (Nikon Fluor-40). The tubule was exposed to excitation light (500 or 450 nm) from a dual excitation spectrofluorimeter (model CM-III; Spex Industries, Edisson, NJ, USA) while monitoring counts (at 535 nm) through a window positioned directly over the macula densa plaque. Over the course of the experiment, the position of the macula densa plaque within the photometer window was carefully verified. Experiments were discarded if displacement of the macula densa was noted or if there was a rapid fall in cps of both excitation wavelengths. Once background counts were obtained, 5 μM of the acetoxy-methyl form of 2',7'-bis-2-carboxyethyl-5(and -6) carboxyfluorescein (BCECF-AM) was added to the luminal perfusate and maintained in the lumen until counts for both excitations wavelengths had increased by at least one order of magnitude. BCECF-AM was removed from the lumen and $[Na]_i$ was reduced to 20 mM (20/140 solution). A stabilization period of five minutes was allowed to elapse before starting experiments.

Calibration was performed in a separate series of tubules using the nigericin method [9]. During the calibration procedure, luminal and basolateral solutions were identical and contained in mM: 120 KCl, 1 $MgCl_2$, 2 NaH_2PO_4, 25 NaCl, 0.005 nigericin and a mixture of Tris and Hepes (25 mM total) giving pH(s) of 6.6, 7.2, 7.4 and 7.8.

Statistics

Results are given as ± SE and N is number of tubules. Statistical analysis was performed using the Student's t-test for paired data and significance was set at $P < 0.05$.

Results

Effect of $[Cl]_i$ on pH_i

Figure 1 presents the average response of pH_i to changes in $[Cl]_i$ from 140 to 1 mM in the presence of 20 mM $[Na]_i$ and 5 mM $[K]_i$ ($N = 8$). In the presence of the 20/140 solution in the lumen, pH_i averaged 7.00 ± 0.11 and increased to 7.50 ± 0.19 with the 20/1 solution. Cl-induced alkalinization of 0.5 pH unit occurred exclusively between 60 and 1 mM $[Cl]_i$.

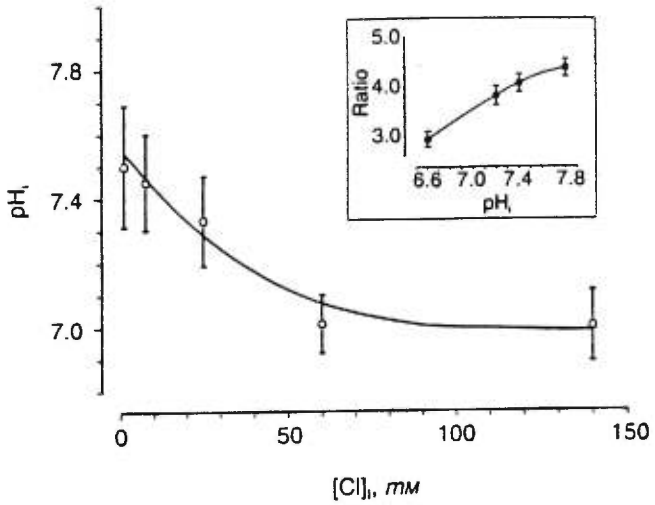

Fig. 1. *Effect of changes in $[Cl]_i$ on pH_i.* Luminal concentrations of Na and K were 20 and 5 mM, respectively, and were constant. Each average was calculated using 7 to 8 independent experiments, where at least 4 different $[Cl]_i$ were tested. The line is a free hand regression fitted to the data. The insert shows a calibration curve averaged from 4 independent determinations using the nigericin method.

Mechanism of action

In the next series of seven paired experiments, we compared the effects of decreasing $[Cl]_i$ from a high concentration (either 140 or 60 mM) to 1 mM in the presence or absence of 5 μM luminal bumetanide. In the absence of bumetanide, a reduction in $[Cl]_i$ to 1 mM alkalinized macula densa cells by 0.56 ± 0.07 pH units. Addition of bumetanide to the 20/140 solution produced an increase in pH_i from 7.07 ± 0.13 to 7.54 ± 0.21 and, in the presence of bumetanide, reduction in $[Cl]_i$ to 1 mM did not significantly change pH_i (+0.02 ± .03 pH unit, $N = 7$; Fig. 2A). Since Cl-induced cell alkalinization was almost completely (96.9%) blocked by bumetanide, we concluded that the effect of $[Cl]_i$ on macula densa cell pH reflects transport through the bumetanide-sensitive Na:2Cl:K cotransporter, and therefore pH_i measurements can be used to monitor apical cotransporter activity.

If the effects of reductions in $[Cl]_i$ on pH_i occur through a reduction in $[Na]_i$ and Na:H exchange, then this effect should be sensitive to amiloride. A series of four paired experiments were performed to determine if Cl-dependent alkalinization could be attenuated by addition of 1 mM amiloride to the luminal and basolateral solution. In the absence of amiloride, reducing $[Cl]_i$ from 140 (20/140 solution) to 5 mM (20/5 solution) alkalinized macula densa cells by 0.47 ± 0.05 pH unit (from 6.81 ± 0.08 to 7.28 ± 0.03, $P < 0.05$, $N = 4$). In the presence of amiloride and 20 mM Na, a similar reduction in $[Cl]_i$ did not significantly change pH_i (from 6.84 ± 0.08 to 6.88 ± 0.07, NS, $N = 4$). Therefore, 91.6% of the Cl-induced cell alkalinization was amiloride-sensitive (Fig. 2B). These results support the hypothesis that changes in $[Cl]_i$ alter $[Na]_i$ through the apical Na:2Cl:K cotransporter, which

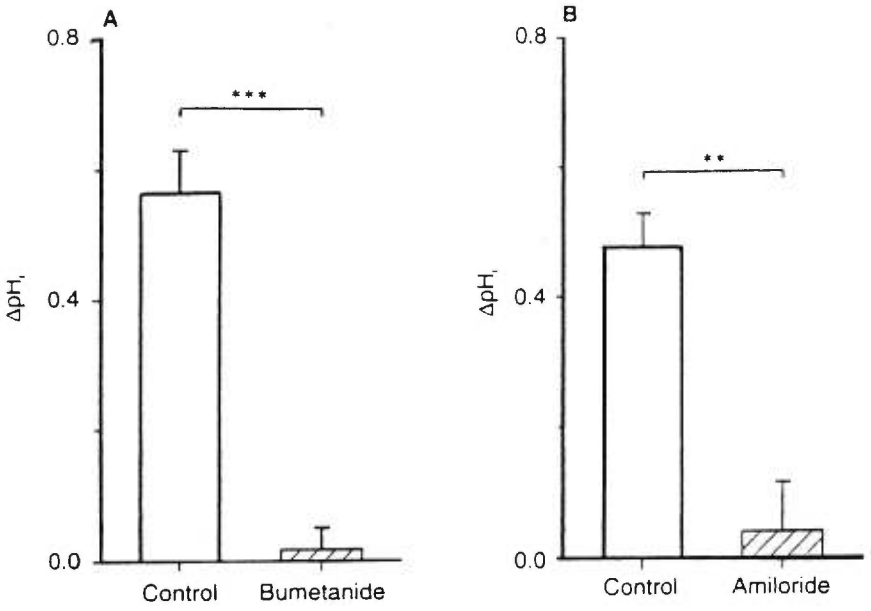

Fig. 2. *Effect of bumetanide and amiloride on the change in pH_i induced by reduction of $[Cl]_i$ from either 60 or 140 mM to 1 mM.* **A.** Significant inhibition ($P < 0.001$; $N = 7$) of the effect of changes in $[Cl]_i$ on pH_i by addition of 5 μM bumetanide in the lumen. **B.** Significant inhibition ($P < 0.005$; $N = 4$) of the effect of changes in $[Cl]_i$ on pH_i by addition of 1 mM amiloride to lumen and bath.

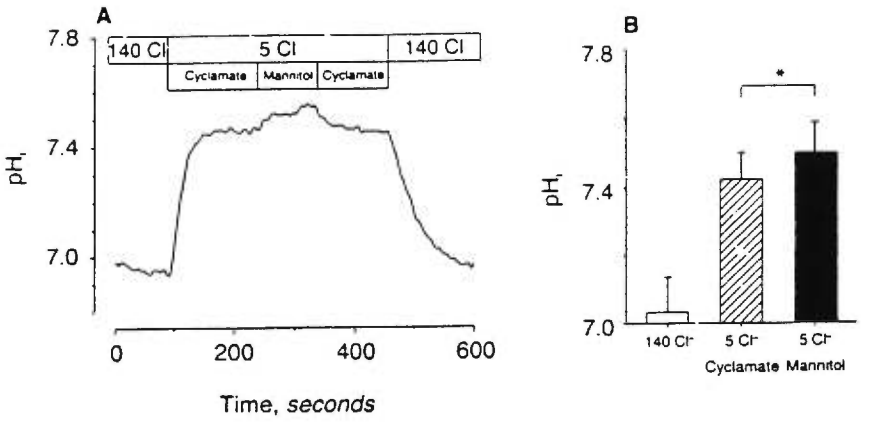

Fig. 3. *Efficiency of cyclamate as a replacement anion for Cl.* **A.** A typical recording of pH_i when $[Cl]_i$ was reduced from 140 to 5 mM (Cl was replaced by cyclamate) and when 135 mM cyclamate (together with the non-transported cation N-methyl-D-glucamine) was replaced by mannitol. **B.** The averaged effect of replacing $[Cl]_i$ with cyclamate compared to the effect of replacing N-methyl-D-glucamine/cyclamate by mannitol ($N = 4$). The effect of mannitol was significantly different from the effect of cyclamate ($P < 0.05$; $N = 4$).

in turn produces changes in pH_i through the activity of an amiloride-sensitive Na:H exchanger.

Evaluation of cyclamate as the replacement anion for Cl

Additional experiments were performed to verify that cyclamate was not transported through the apical Na:2Cl:K cotransporter and therefore was an adequate substitute for $[Cl]_i$. In a series of four experiments, pH_i was measured while $[Cl]_i$ was reduced from 140 mM (20/140 solution) to 5 mM (20/5 solution). N-methyl-D-glucamine and cyclamate in the 20/5 solution was then replaced with mannitol, which reduced cyclamate concentration from 135 mM to 15 mM and N-methyl-D-glucamine concentration from 120 mM to zero. Figure 3 shows a typical recording together with the average change in pH_i measured during Cl replacement with cyclamate compared to replacement of N-methyl-D-glucamine/cyclamate with mannitol. Reduction of $[Cl]_i$ alkalinized macula densa cells by 0.39 ± 0.06 pH unit (from 7.03 ± 0.10 to 7.42 ± 0.08, $P < 0.01$, $N = 4$), whereas replacement of N-methyl-D-glucamine/cyclamate with mannitol further alkalinized these cells by only 0.08 ± 0.02 pH unit ($P < 0.05$, $N = 4$). Considering the possible effects of reducing the ionic strength with mannitol (**Discussion**), we conclude that cyclamate was an adequate Cl substitute which was not transported to any significant extent by the apical Na:2Cl:K cotransporter.

Determination of the equilibrium $[Cl]_i$ for the Na:2Cl:K apical cotransporter

Since the effects of $[Cl]_i$ on pH_i were completely bumetanide-sensitive, it was possible to evaluate the $[Cl]_i$ at which the Na:2Cl:K transporter was at equilibrium by determining the $[Cl]_i$ which produced the pH_i obtained whenever bumetanide was added to the luminal solution. For these experiments, different $[Cl]_i$ were tested before and after the addition of bumetanide. Figure 4 illustrates a typical experiment where reductions in $[Cl]_i$ alkalinized macula densa cells while addition of bumetanide increased pH_i and rendered the pH of macula densa cells insensitive to changes in $[Cl]_i$. Equilibrium $[Cl]_i$ in the presence of 20 mM $[Na]_i$ and 5 mM $[K]_i$, was obtained from the intersection of the two curves (with and without bumetanide) and averaged 14.3 ± 2.4 mM in seven experiments of the type shown in Figure 4.

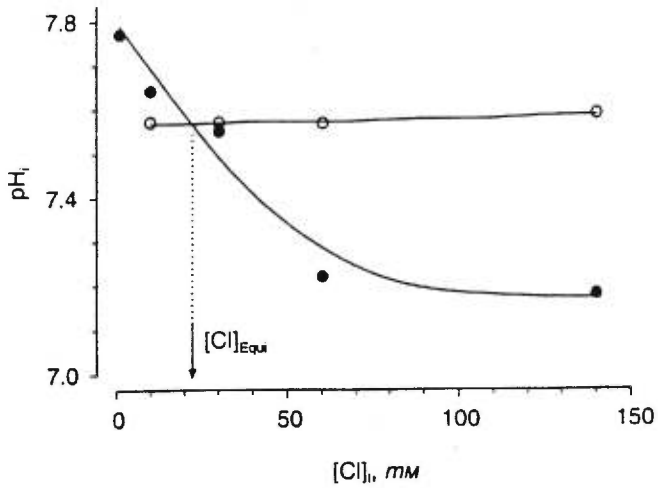

Fig. 4. *Determination of the equilibrium $[Cl]_i$ ($[Cl]_{Equ}$) by comparing the effect of changes in $[Cl]_i$ first in the absence (●) and then in the presence (○) of bumetanide 5 μM for a representative experiment.* The lines used for interpolation were free regressions.

Discussion

Transport properties of macula densa cells represent a fundamental factor in understanding the mechanism used by these cells to detect changes in the luminal fluid composition and elicit tubuloglomerular feedback signals. Recent studies have demonstrated that macula densa cells possess a Na:2Cl:K cotransporter [2, 4], a Na:H antiporter [7] and a K channel [4, 10] on the apical membrane together with a Cl conductance at the basolateral membrane [2, 4]. This transport scheme is similar to that described for the CTAL [11]; however, because of a rather low density of basolateral Na-K-ATPase [12] in macula densa cells, it was expected that macula densa cells may have a limited transport capacity in comparison with CTAL. The observation that luminal furosemide produced a small hyperpolarization of macula densa cells when added to a 150 mM $[NaCl]_i$ solution [1] while it depolarized macula densa cells in the presence of 25 mM NaCl [3] suggested that the apical cotransporter was reabsorbing NaCl in the first case but secreting it in the second case. This indicated that the direction of ionic flux through the apical cotransporter might reverse at some intermediate $[NaCl]_i$ between 25 mM and 150 mM, possibly in the range from 25 to 50 mM where macula densa cells are the most sensitive to changes in luminal fluid composition [13]. The possibility that macula densa cells operate close to the equilibrium of the Na:2Cl:K cotransporter was attractive as it would be an efficient and sensitive way to detect changes in $[NaCl]_i$. The energy requirement for NaCl transport by macula densa cells would then be minimal and alterations in $[NaCl]_i$ could effect both transport rate and the direction of NaCl transport.

To test this hypothesis, it was necessary to determine a set of luminal Na, K and Cl concentrations that would result in equilibration of the apical Na:2Cl:K cotransporter. In past studies, activity of the neutral apical cotransporter was indirectly observed through the secondary effect that Na:2Cl:K cotransport had on intracellular [Cl] and therefore on membrane potential [3]. Electrophysiological measurements with conventional microelectrodes are very difficult to perform on macula densa cells, and a substantial variation in baseline basolateral membrane potentials was observed from impalement to impalement. This prompted us to look for a less invasive method to monitor the activity of the Na:2Cl:K cotransporter. We found that pH_i measurements with BCECF constitute a convenient and sensitive method to measure this activity. Experiments reported in Figures 2 and 4 clearly demonstrate that $[Cl]_i$ can affect pH_i through a single apical transport mechanism: the bumetanide-sensitive Na:2Cl:K cotransporter. The absence of an effect of Cl on macula densa pH_i in the presence of bumetanide indicates that there is no significant apical Cl/base exchange activity at least under our experimental conditions (nominally bicarbonate -free solutions). In addition, we found that the effect of $[Cl]_i$ on pH_i was almost completely inhibited by amiloride. The completeness of the amiloride inhibition shown in Figure 2B was probably due to the fact that luminal Na which normally competes with amiloride for binding on the exchanger [14] was only 20 mM in these experiments.

The simplest explanation for the effect of $[Cl]_i$ on pH_i is that an elevation in $[Cl]_i$ results in an increase in transport rate of the Na:2Cl:K cotransporter. This in turn produces an increase in macula densa $[Na]_i$ which triggers a cellular acidification through the Na:H exchanger. For example, in the presence of 20 mM Na and a low $[Cl]_i$, $[Na]_i$ is probably less than 20 mM and the Na:H exchanger allows for Na entry and H extrusion. This assertion is supported by the fact that pH_i decreased with Na:H exchanger inhibition by amiloride under these conditions (pH_i ~7.5 with the 20/5 solution but ~6.9 if amiloride was added). At constant $[Na]_i$, an elevation in $[Cl]_i$ would enhance transport and increase $[Na]_i$, resulting in a reduced Na gradient across the apical membrane and diminished H extrusion (pH_i decreased from 7.5 to 7.0 upon Cl addition; Fig. 1).

One important assumption in the interpretation of these results is that cyclamate, which was used to replace Cl, was not transported by the Na:2Cl:K cotransporter. As reported by O'Grady, Palfrey and Field [15], one of the two sites on the cotransporter for Cl appears to have a limited selectivity and may accept some large anions. The results in Figure 4 demonstrate that replacement of cyclamate (and N-methyl-D-glucamine) with mannitol produced a very small change in pH_i compared to the change in pH_i produced by replacement of Cl with cyclamate. At this point, it is not known if this small change in pH_i with mannitol replacement was due to removal of cyclamate or N-methyl-D-glucamine or some other effect such as a decrease in the ionic strength of the luminal solution. This latter possibility might involve an unmasking of fixed negative surface charges and a decrease in the local concentration of Cl present near the apical membrane. If pH_i obtained with mannitol represents the maximal effect of removing 135 mM Cl from the luminal solution, then Cl replacement with cyclamate would be quite efficient producing a change in pH_i that was 83.9% of that obtained with mannitol replacement.

The control experiments presented above show that pH_i measurements can be used to detect the activity of the apical Na:2Cl:K cotransporter. If, over the range of $[Cl]_i$'s used in these studies, no saturation occurs in the relationship between ionic flux through the cotransporter and $[Na]_i$ as well as between Na:H exchanger activity and $[Na]_i$, then pH_i can be directly related to the cotransport rate ($J_{Na:2Cl:K}$) and described by the following equation:

$$pH_i = pH_{BUM} - A * J_{Na:2Cl:K} \quad (1)$$

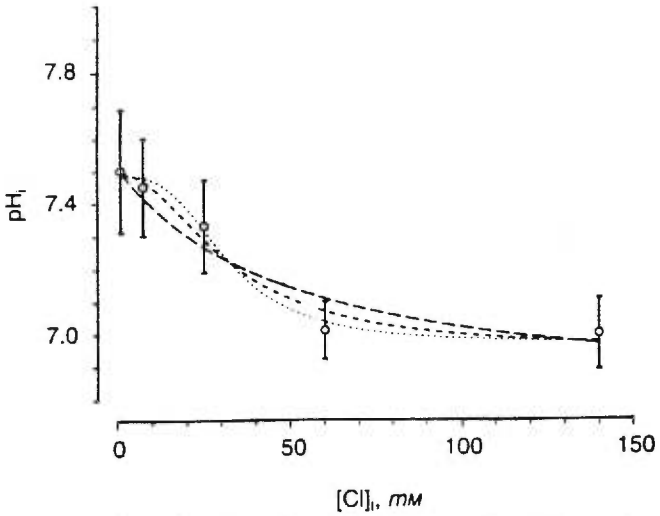

Fig. 5. *The data to Fig. 1 were fitted with Eq. 3 using different Hill's numbers ("n").* With a Hill's number of 2, the apparent affinity of the apical Na:2Cl:K cotransporter for $[Cl]_i$ is 32.5 mM. (– –) n = 1; (---) n = 2; (· · · ·) n = 3.

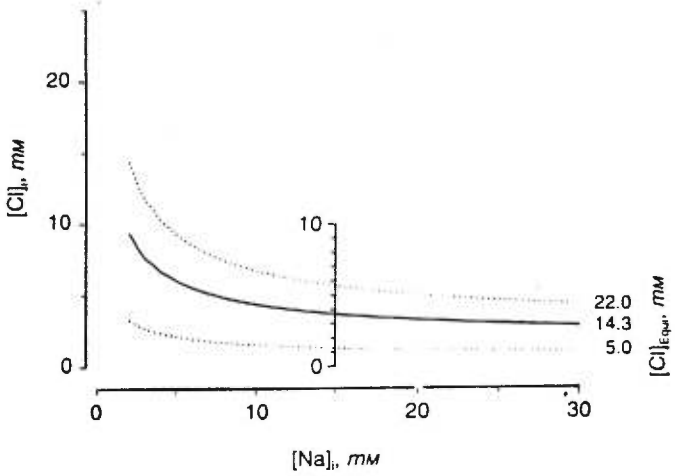

Fig. 6. *Prediction of the $[Cl]_i$ based on the equilibrium concentration of luminal Cl (14.3 mM), the stoichiometry of the Na:2Cl:K cotransporter, the $[Na]_i$ and the assumption that $[K]_i$ equals 120 − $[Na]_i$, mM.* The range of $[Cl]_i$ corresponding to the 95% confidence interval is also illustrated.

where pH_{BUM} is the pH_i obtained after cotransporter inhibition and "A" is a proportionality constant. Dividing the net flux through the cotransporter between an efflux (E) and a $[Cl]_i$-dependent influx (using a maximal influx "I", a Cl affinity of "K_M" and a Hill number "n"), Eq. 1 becomes:

$$pH_i = pH_{BUM} - A * \left[\frac{I * [Cl]_i^n}{K_M^n + [Cl]_i^n} - E \right] \quad (2)$$

If changes in efflux following perturbations in $[Cl]_i$ can be neglected as a first approximation, Eq. 2 can be rearranged to give:

$$pH_i = C - A * \left[\frac{I * [Cl]_i^n}{K_M^n + [Cl]_i^n} \right] \quad (3)$$

where "C" is a constant. Figure 5 presents the best fits of Figure 1 data using Eq. 3 and different Hill numbers. Clearly, a Hill number of 2 or more is required to adequately fit the data, especially between 60 and 140 mM where pH_i was found to be almost constant. Using a Hill number of 2 which is consistent with the present data and the known stoichiometry of bumetanide-sensitive transporters in other tissues, the affinity for luminal Cl was found to be 32.5 mM. The K_M of the cotransporter for Cl is quite similar to values reported for a variety of other tissues (K_M = 15 to 50 mM) [15, 16]. The Na:2Cl:K transporter from CTAL has a K_M for Cl of 50 mM [11], while the K_M value for the transporter recently cloned from shark rectal gland is 110 mM [17].

The effects of bumetanide on pH_i can also be used to determine the equilibrium $[Cl]_i$ in the presence of 20 mM Na and 5 mM K. The method used simply consists of finding the $[Cl]_i$ that mimics the effect of blocking the apical cotransporter with bumetanide. Equilibrium values were found between 5 and 22 mM and averaged 14.3 ± 2.4 mM (N = 7); this determination has several implications. First, these low equilibrium values for $[Na]_i$ and $[Cl]_i$ indicate that the cellular $[Cl]_i$ can reach very low values in the presence of a loop diuretic (furosemide or bumetanide) or when the transporter is at equilibrium. By definition, when the apical cotransporter is at equilibrium, there is no change in the electrochemical potential of the transported ions during the transport process. Using the stoichiometry of 1 Na, 2Cl and 1 K for the bumetanide-sensitive cotransporter, the following relationship must be observed at equilibrium.

$$RT \ln[Na]_l + RT \ln[K]_l + 2RT \ln[Cl]_l = RT \ln[Na]_i + RT \ln[K]_i + 2RT \ln[Cl]_i \quad (4)$$

or

$$[Na]_l \times [K]_l \times [Cl]_l^2 = [Na]_i \times [K]_i \times [Cl]_i^2 \quad (5)$$

Using the known luminal concentrations and the following relationship as a rough estimate of $[K]_i$ as a function of $[Na]_i$,

$$[K]_i(mM) = 120 - [Na]_i\,(mM) \quad (6)$$

one can estimate $[Cl]_i$ as a function of $[Na]_i$. Figure 6 provides this estimate together with the 95% confidence interval using the SE of the average equilibrium $[Cl]_i$. One can see that calculated $[Cl]_i$ is not very dependent on $[Na]_i$ within the physiological range and is extremely low when the apical cotransporter is at equilibrium (between 1 and 6 mM; Fig. 6). While this value is in agreement with earlier fluorescent studies of Salomonson et al using the fluorescent probe SPQ [18], it is significantly lower than more recent determinations of $[Cl]_i$ by the same group [19], where $[Cl]_i$ was found to be 28.6 ± 10 mM in the presence of furosemide. Such a high $[Cl]_i$ is in clear contradiction with Eqs. 5 and 6 and our observation that the bumetanide-sensitive flux through the Na:2Cl:K cotransporter is equilibrated at a $[Cl]_i$ of 14.3 mM. As acknowledged by the authors, this discrepancy probably come from an overestimation of $[Cl]_i$ using SPQ since the value reported for CTAL [19] is also much higher than the corresponding value measured with ion-selective microelectrode [20]. It is interesting to note that for CTAL, microelectrodes measurements of $[Cl]_i$ also show that $[Cl]_i$ decreases to very low values (< 9 mM) upon inhibition of the apical Na:2Cl:K transporter with furosemide [20].

The second implication of the estimated equilibrium condition of Na:2Cl:K cotransport concerns the physiological operating point of the apical Na:2Cl:K cotransporter. In general, early distal tubular fluid [NaCl] reported for the rat ranges between 40 and 70 mM [5, 6], while [K] is between 3 and 4 mM [21, 22]. It is recognized that the composition of early distal fluid samples represent an overestimation of actual [NaCl] at the macula densa cells, since there is NaCl secretion between macula densa and superficial loops of the distal tubule. More accurate estimations of the macula densa $[NaCl]_i$ have been obtained in micropuncture experiments on Wistar rats, taking advantage of the presence of superficial glomeruli (24.6 mM Cl and 35.8 mM Na [6]) or using a stop/pulse flow method with a conductivity microprobe (27 mM NaCl [5]). Even if several combinations of $[Na]_i$, $[K]_i$ and $[Cl]_i$ can equilibrate the Na:2Cl:K cotransporter in macula densa cells, the intracellular ionic concentrations obtained at equilibrium are expected to be independent of the various combinations of the three luminal ions that are producing the equilibrium. Consequently, the right hand side of Eq. 5 always equals to ($20 \times 5 \times 14.3^2$ mM^4) whenever equilibrium is reached and can be used to find different equilibrium luminal concentrations. For example, in the presence of 3.5 mM K and equal Na and Cl concentrations, one finds an equilibrium $[NaCl]_i$ of 18 mM. As the expected $[NaCl]_i$ at the macula densa level is about 10 mM higher than this value (25 to 30 mM), macula densa cells are predicted to reabsorb NaCl under physiological conditions. In terms of $[Cl]_i$, the apical cotransporter is operating between the equilibrium concentration and its K_M for Cl. In addition, the estimated equilibrium $[NaCl]_i$ correspond closely to the concentration required for initiating tubuloglomerular feedback signals in micropuncture experiments [13].

In conclusion, it is possible to determine the Na:2Cl:K equilibrium $[Cl]_i$ by the fluorescence method presented in this paper when a specific blocker of the transport system is available and when $[Cl]_i$ affects pH_i mostly through cotransport. This procedure provides an estimate of equilibrium $[Cl]_i$ that does not depend upon the calibration procedure and is independent of the actual values of pH_i obtained in this study. In the case of macula densa cells, the apical Na:2Cl:K transporter was predicted to reverse at a $[NaCl]_i$ of 18 mM which corresponds to the minimum [NaCl] required to elicit tubuloglomerular feedback signals. When the apical Na:2Cl:K transporter was inhibited or in equilibrium, $[Cl]_i$ was capable of reaching values as low as 5 mM. Under physiological conditions, the macula densa apical Na:2Cl:K cotransporter is exposed to $[Cl]_i$'s between the equilibrium concentration and the apparent K_M for this ion; a domain of $[Cl]_i$ where the Na:2Cl:K transport rate is relatively low but very sensitive to a rise in $[Cl]_i$.

Acknowledgments

This work was supported by the Kidney Foundation of Canada (J.Y.L.) and a National Institutes of Health Grant AM-32032 (P.D.B.). A.M.H. was a recipient of a post-doctoral fellowship from the Science and Engineering Research Council-NATO, UK and B.C.F. was supported by a National Institutes of Health Training Grant DK-07545. We thank Marcelle Duplain for technical support and Martha Yeager for secretarial assistance.

Reprint requests to Dr J-Y Lapointe, Groupe de recherche, en transport membranaire, Université de Montréal, P.O. box 6128-A, Montréal, Québec, Canada, H3C 3J7.

References

1. Bell PD, Lapointe JY, Cardinal J: Direct measurement of basolateral membrane potentials from cells of the macula densa. *Am J Physiol* (Renal Fluid Electrol Physiol 26):F463–F468, 1989
2. Lapointe JY, Bell PD, Hurst AM, Cardinal J: Basolateral ionic permeabilities of macula densa cells. *Am J Physiol* 260 (Renal Fluid Electrol Physiol 29):F856–F860, 1991
3. Lapointe JY, Bell PD, Cardinal J: Direct evidence for apical Na^+:$2Cl^-$:K^+ co-transport in macula densa cells. *Am J Physiol* 258 (Renal Fluid Electrol Physiol 27):F1466–F1469, 1990
4. Schlatter E, Salomonson M, Persson AEG, Greger R: Macula densa cells sense luminal NaCl concentration via furosemide sensitive $Na^+2Cl^-K^+$ cotransport. *Pflügers Arch* 414:286–290, 1989
5. Gutsche H-U, Muller-Suur R, Hegel U, Hierholzer K: Electrical conductivity of tubular fluid of the rat nephron. *Pflügers Arch* 383:113–121, 1980
6. Schnermann J, Briggs J, Schubert G: *In situ* studies of the distal convoluted tubule in the rat. I. Evidence for NaCl secretion. *Am J Physiol* 243 (Renal Fluid Electrol Physiol 12):F160–F166, 1982
7. Fowler BC, Chang YS, Laamarti A, Higdon M, Lapointe JY, Bell PD: Evidence for apical sodium proton exchange in macula densa cells. *Kidney Int* 47:746–751, 1995
8. Burg MB, Grantham J, Abramov MA, Orloff J: Preparation and study of fragments of single rabbit nephrons. *Am J Physiol* 210:1293–1298, 1966
9. Thomas JA, Buchsbaum RN, Fimniak A, Racker S: Intracellular pH measurements in Ehrlich ascites tumor cells utilizing spectroscopic probes generated in situ. *Biochem J* 18:2210–2218, 1979
10. Hurst AM, Lapointe JY, Laamarti A, Bell PD: Basic properties and potential regulators of the apical K^+ channel in macula densa cells. *J Gen Physiol* 103:1055–1070, 1994
11. Greger R: Ion transport mechanism in thick ascending limb of Henle's loop of mammalian nephron. *Physiol Rev* 65:760–797, 1985
12. Schnermann J, Marver D: ATPase activity in macula densa cells of the rabbit kidney. *Pflügers Arch* 407:82–86, 1986
13. Schnermann J, Briggs JP: Function of the juxtaglomerular apparatus: Local control of glomerular hemodynamics and renin secretion, in *The Kidney,* edited by DW Seldin, G Giebish, New York, Raven Press, 1992, pp. 1249–1289
14. Benos DJ: Amiloride: Chemistry, kinetics and structure-activity relationship, in *Na/H Exchange,* edited by S Grinstein, Baton Rouge, CRC Press, 1988, p 127
15. O'Grady SM, Palfrey HC, Field M: Characteristics and functions of Na-K-Cl cotransport in epithelial tissue. *Am J Physiol* 253 (Cell Physiol 22):C177–C192, 1987
16. Molony DA, Reeves WB, Andreoli TE: Na:2Cl:K-cotransport and the thick ascending limb. *Kidney Int* 36:418–426, 1989
17. Xu JC, Lytle C, Zhu TT, Payne JA, Benz E Jr, Forbrush B III: Molecular cloning and functional expression of the bumetanide sensitive Na-K-Cl cotransporter. *Proc Natl Acad Sci USA* 91:2201–2205, 1994
18. Salomonsson M, Gonzalez E, Westerlund P, Persson AEG: The effect of furosemide on the chloride concentration in the macula densa and in cortical thick ascending limb cells. *Acta Physiol Scand* 139:387–388, 1990
19. Salomonsson M, Gonzalez E, Kornfeld M, Persson AEG: The cytosolic chloride concentration in macula densa and cortical thick ascending limb cells. *Acta Physiol Scand* 147:305–313, 1993
20. Greger R, Oberleithner H, Schlatter E, Cassola AC, Weidtke C: Chloride activity in cells of isolated perfused cortical thick ascending limb of rabbit kidney. *Pflügers Arch* 399:29–34, 1983
21. Marsh DJ, Ullrich KJ, Rumrich G: Micropuncture analysis of the behavior of potassium ions in rat renal cortical tubules. *Pflügers Arch* 277:107–119, 1963
22. Morgan T, Barliner RW: A study of continuous microperfusion of water and electrolyte movement in the loop of Henle and distal tubule of the rat. *Nephron* 6:388–405, 1969

QUATRIÈME ARTICLE

Determination of NH_4^+/NH_3 fluxes across the apical membrane of macula densa cells : a quantitative analysis

Laamarti M.A., and Lapointe J.Y.

Determination of NH_4^+/NH_3 fluxes across apical membrane of macula densa cells: a quantitative analysis

M. ANUAR LAAMARTI AND JEAN-YVES LAPOINTE
Groupe de Recherche en Transport Membranaire, Université de Montréal, Montréal, Quebec, Canada H3C 3J7

Laamarti, M. Anuar, and Jean-Yves Lapointe. Determination of NH_4^+/NH_3 fluxes across apical membrane of macula densa cells: a quantitative analysis. *Am. J. Physiol.* 273 (*Renal Physiol.* 42): F817–F824, 1997.—Luminal addition of 20 mM NH_4^+ produced a rapid acidification of rabbit macula densa (MD) cells from 7.50 ± 0.06 to 6.91 ± 0.05 at an initial rate of 0.071 ± 0.008 pH unit/s. In the luminal presence of 5 μM bumetanide, 5 mM Ba^{2+} or both, the acidification rate was reduced by 57%, 35% and 93% of control levels. In contrast, intracellular pH (pH_i) recovery after removing luminal NH_4^+ was unaffected by bumetanide and Ba^{2+} but was sensitive to 1 mM luminal amiloride (71% inhibition). The bumetanide-sensitive acidification rate represents most certainly the NH_4^+ flux mediated by the apical Na^+:K^+ (NH_4^+):$2Cl^-$ cotransporter, but the Ba^{2+}-sensitive portion does not seem to be associated with the apical K^+ channels previously characterized by us. The effects of NH_4^+ entry across the apical membrane were simulated using a simple model involving five adjustable parameters: apical and basolateral permeabilities for NH_4^+ and NH_3 and a parameter describing a pH-regulating mechanism. The model shows that the apical membrane of MD cells is much more permeable to NH_3 than it is to NH_4^+ and, under control conditions, the apical NH_4^+ flux appears surprisingly high (11–20 mM/s) and challenges the notion that MD cells present a low intensity of ionic transport.

ammonium permeability; sodium-potassium-chloride cotransporter; potassium channels; bumetanide; verapamil

THE MACULA DENSA (MD) is a plaque of epithelial cells located at the distal end of the thick ascending limb (TAL) that is thought to function as a sensor device detecting increases in luminal NaCl concentrations and initiating the signals involved in the control of renin secretion and in the initiation of the tubuloglomerular feedback (24). Because of their small number (~30 cells/plaque), MD cells could not be directly studied using conventional methods, and their transport properties remained largely unknown until 1985, when it was demonstrated that MD cells could be visualized during microperfusion experiments of isolated TAL dissected with their attached glomerulus (15). Their transport properties could then be studied using fluorescent probes (7, 19, 20, 21), conventional electrophysiology (4, 17, 18, 23), and patch-clamp techniques (9, 22). The transport model that emerged from these studies consists of Na^+:K^+:$2Cl^-$ cotransporters, Na^+/H^+ exchangers, and K^+ channels on the apical membrane and a major Cl^- conductance, a K^+ conductance, Na^+/Ca^{2+} exchangers, and Na^+-K^+-adenosinetriphosphatases (Na^+-K^+-ATPases) on the basolateral membrane. Even though the proposed model for MD cells is qualitatively similar to the cortical TAL (CTAL) model, differences were reported on the basis of the properties of the apical K^+ channels observed at the single channel level (9) and on the Na^+:K^+:$2Cl^-$ isoform detected in MD cells (10). Also, CTAL cells were presumed to be much more active than MD cells in terms of absolute transport rates, as the density of basolateral Na^+-K^+-ATPase was estimated to be 40 times smaller in MD cells vs. CTAL cells (reported per unit of cell volume) (Ref. 25; see also Refs. 3 and 11). So far, the level of membrane or transepithelial transport mediated by MD cells has never been measured. More information on MD cells properties, including membrane transport properties, is required to understand the way these cells play their crucial role in the kidney.

Recently, we have presented a method to detect the direction of ionic flux mediated by the apical Na^+:K^+:$2Cl^-$ cotransporter using intracellular pH (pH_i) measurements (19). The method gave interesting results but was quite indirect as pH_i was shown to be linked to the apical Na^+:K^+:$2Cl^-$ flux through the modulation of intracellular Na^+ concentration ($[Na^+]_i$) and the activity of the Na^+/H^+ exchanger. In the present study, we apply to MD cells a method previously used for medullary TAL (MTAL) that is based on the fact that NH_4^+ can substitute for K^+ in several membrane transporters and channels including the Na^+:K^+:$2Cl^-$ cotransporter (14) and directly affect pH_i by dissociating into NH_3 + H^+. It will be shown that luminal addition of NH_4^+ produces a rapid cellular acidification that can be almost completely inhibited by bumetanide and Ba^{2+}. A simple model is presented for the quantitative interpretation of these results. The rate of NH_4^+ entry across the apical membrane was found to be surprisingly high, which suggests that, even if MD cells have a low density of basolateral Na^+-K^+-ATPase, their apical membrane presents a large ionic permeability.

MATERIALS AND METHODS

Microperfusion. Microperfusion of rabbit CTALs dissected with their attached glomeruli was performed as described in previous reports from this laboratory (4, 17, 18, 19). The distal end of the tubule was left open to the bath, and a holding pipette was placed over the glomerulus to position the preparation in such a way that the MD plaque could be clearly visualized using a ×40 objective. Tubules were bathed with a bicarbonate-free solution containing (in mM) 146 NaCl, 5 potassium gluconate, 1 $MgCl_2$, 1 $CaCl_2$, 5 glucose, 10 *N*-2-hydroxyethylpiperazine-*N*′-2-ethanesulfonic acid (HEPES), and 7.2 tris(hydroxymethyl)aminomethane (Tris). Luminal solutions were identical to the bathing solution with the exception that the luminal NaCl concentration was maintained at 25 mM by isosmotically replacing Na^+ with *N*-methyl-D-glucamine (NMDG) and Cl^- with cyclamate. Addition of luminal NH_4^+ (20 mM) and or Ba^{2+} (5 mM) was

accomplished by replacement of NMDG-cyclamate at constant luminal [Na^+] and [Cl^-]. In some experiments, 5 μM bumetanide, 1 mM amiloride, 1 μM ionomycin, or 0.1 mM verapamil (all compounds from Sigma Chemical, St. Louis, MO) was added to the perfusion solution from concentrated solutions in ethanol (final ethanol concentration in perfusates was <0.2%). All solutions were adjusted to a pH of 7.4, and all experiments were performed at 39°C.

Fluorescence measurements. pH_i was measured using the fluorescent probe 2',7'-bis(carboxyethyl)-5(6)-carboxyfluorescein (BCECF) as previously described (7, 19). In brief, after a CTAL was cannulated and perfused on the stage of an inverted microscope, background fluorescence was measured over a window positioned over the MD plaque, and 5 μM of the acetoxymethyl ester form of BCECF (BCECF-AM) was added to the luminal perfusate. Intracellular dye was excited alternately at 500 and 450 nm wavelengths (Spex model CM-III; Spex Industries, Edison, NJ), and fluorescence emission was monitored at 530 nm using a photomultiplier tube and a band-pass filter. BCECF-AM was not removed from the lumen until the fluorescence measured for both excitation wavelengths had increased by a least one order of magnitude with respect to background fluorescence.

BCECF fluorescence was calibrated using the high-K^+ nigericin technique (26). At different periods during our study, a total of seven tubules were perfused and bathed with identical solutions containing (in mM) 120 KCl, 1 $MgCl_2$, 2 NaH_2PO_4, 25 NaCl, 0.006 nigericin, and a mixture of Tris and HEPES (25 mM total) giving pH values of 6.4, 6.8, 7.2, 7.6, and 8.0. Calibration curves were obtained, and one can see that the fluorescence ratios converge to the same value in acidic conditions (6.4–6.8), whereas all the ratios were distributed within ± 7% of the mean at a pH_i of 7.6. As a complete calibration could not be performed in each experiment, one or two calibration points (including pH_i = 7.6) were obtained at the end of each experiment, and the calibration curve which best satisfied these points was used to scale the measured fluorescence ratios.

Buffering capacity. The buffering capacity of the cell (β_i) was determined from the following equation using the measured change in pH_i when 10 mM of trimethylamine (TMA) was removed from the luminal solution.

$$\beta_i = \Delta H/\Delta pH$$

where ΔH is the concentration of proton released when TMA is removed from the luminal solution as calculated from pH_i and a pK_a of 9.83. This measurement was performed by adjusting the luminal and basolateral solution pH to three different values (6.4, 7.4, and 8.0) to estimate β_i at a variety of pH_i.

Acidification rates and flux units. Initial rates of pH_i change (dpH_i/dt) were calculated from a fit (FigP, version 6.0; Biosoft, Milltown, NJ) of the recorded pH_i to an exponential relaxation curve for the initial 20–30 s following a change in luminal solution. On a few occasions where changes in pH_i were clearly not exponential during this period, a linear regression was fitted to the initial change in pH_i. Acidification rates can be transformed into proton production rates in units of millimolar per second by simply multiplying dpH_i/dt by β_i. Similarly, ionic fluxes can be expressed in the same convenient units (mM/s), which directly indicates the rate at which an intracellular concentration would change following a given transmembrane flux. Care should be taken, however, in comparing ionic fluxes among different cell types, as cellular volume may vary quite significantly from one cell type to another.

Statistics. Statistical significance of a difference between two average results was tested using Student's *t*-test for paired sample. $P < 0.05$ was considered significant.

RESULTS

Buffering capacity. Intrinsic buffering power was obtained as described above using 10 mM TMA. As displayed in Fig. 1, one can see that β_i increases very significantly from 16 to 141 mM/pH unit as pH_i decreases from 8.1 to 6.7. This can be directly appreciated in the *inset* of Fig. 1; with a pK_a of 9.83 for TMA, the quantity of proton released upon removal of TMA is slightly larger (by ~10%) at pH_i 6.4 than at pH_i 7.8; however, the acidification induced by TMA removal was much smaller at pH_i 6.4 than at 7.8. For each experiment, the conversion between dpH_i/dt and proton production-rate was calculated using interpolated β_i estimates as depicted in Fig. 1.

Effects of luminal ammonium addition on pH_i. In the absence of ammonium, the steady-state pH_i was 7.50 ± 0.06 (n = 8) when the CTAL lumen was perfused with a low NaCl concentration (25 mM). Addition of 20 mM NH_4^+ to the luminal perfusate caused occasionally a small increase of pH_i [average of +0.02 ± 0.009 pH unit, not significant (NS)], which was followed by a rapid cell acidification (Fig. 2*A*) at an initial rate given in Table 1. A final pH_i of 6.91 ± 0.05 was usually reached within 30 s. Removal of luminal NH_4^+ caused an additional but transient acidification by an average of 0.058 ± 0.015 pH unit (n = 8) followed by a cellular alkalinization at a rate corresponding to about one-third of the absolute value of the initial NH_4^+-induced acidification (see Table 1) and a stable pH_i of 7.53 ± 0.06 was reached within 90 s.

Effects of NH_4 in presence of bumetanide and Ba^{2+}. To determine whether apical Na^+:K^+:2Cl^- cotransporters are involved in NH_4^+ transport, the effect of adding 20 mM NH_4^+ to the lumen was evaluated in the presence of

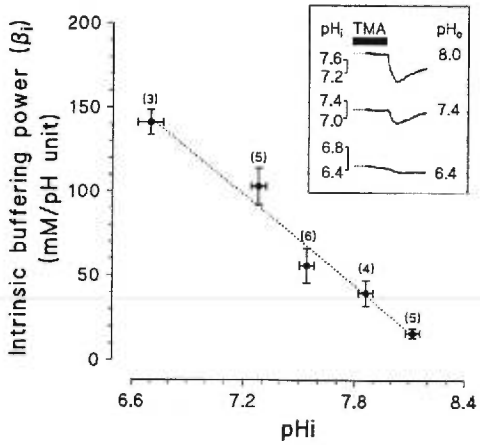

Fig. 1. Buffering capacity of macula densa (MD) cells. MD cells intracellular pH (pH_i) was varied by use of different extracellular pH (from 6.4 to 8.0), and buffering capacity was determined by measuring the change in pH_i immediately following removal of 10 mM trimethylamine (TMA) from the luminal solution. Data points are means ± SE, and for each, the number shown in parentheses is the number of MD plaques studied.

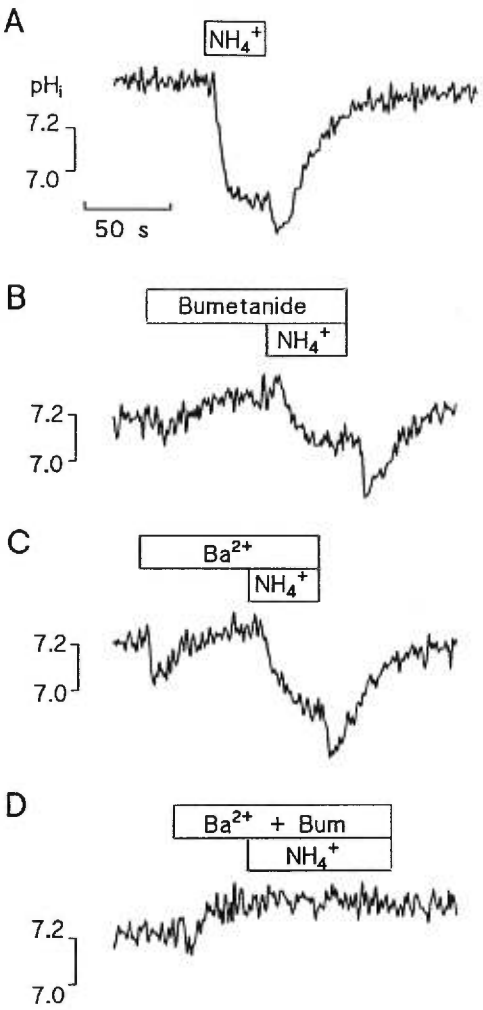

Fig. 2. Effects of adding 20 mM luminal NH_4^+ on MD pH_i. The experiment was done for the same MD plaque in control conditions (*A*) or in presence of 5 μM bumetanide (*B*), 5 mM Ba^{2+} (*C*), or both (*D*).

5 μM bumetanide. A typical tracing of the effect of bumetanide is shown in Fig. 2*B*. As summarized in Table 1, bumetanide produced a very significant effect on NH_4^+-induced acidification ($P < 0.002$, $n = 5$), which was reduced by 57%, in the presence of the inhibitor. Time control experiments were performed to check the reproducibility of the NH_4^+-induced acidification. In a series of four different experiments in which NH_4^+ was added and removed twice at 5- to 10-min intervals, the second NH_4^+-induced acidification was not significantly different from the initial acidification (the average change in the initial acidification rate was +5 ± 9%; $P = 0.50$, NS).

Thus apical Na^+:K^+:$2Cl^-$ cotransporters are likely to be involved in the NH_4^+ entry mechanism, but the incomplete effect of bumetanide suggests the presence of a second pathway. Since K^+ channels are present at the apical membrane of MD cells (9), and since Ba^{2+} is an effective inhibitor of several K^+ channels and was shown to significantly inhibit NH_4^+-induced acidification in rat MTAL cells (8, 12, 13, 27), the effect of 5 mM Ba^{2+} was tested on MD cells. In eight tubules, addition of 5 mM Ba^{2+} to the luminal medium reduced the NH_4^+-induced acidification by 35% compared with control values (Fig. 2*C*; Table 1). Interestingly, the effects of bumetanide and Ba^{2+} appeared additive, as the simultaneous presence of 5 μM bumetanide and 5 mM Ba^{2+} inhibited the NH_4^+-induced cell acidification nearly completely, reducing the initial acidification rate by 93% (Table 1; Fig. 2*D*).

The results presented above are similar to the results reported for MTAL (8, 12, 13, 27) and were interpreted in the past as evidence that NH_4^+ is indeed entering through apical Na^+:K^+:$2Cl^-$ cotransporters and Ba^{2+}-sensitive K^+ channels. On the other hand, it was shown for rat TAL that their apical K^+ channels do not conduct NH_4^+ (5, 6), and it was recently suggested that, in the case of suspensions of rat MTAL, NH_4^+ was able to replace the proton in a K^+/H^+ exchanger that was sensitive to Ba^{2+} and verapamil (1). As we have recently reported in a series of patch-clamp experiments that the apical K^+ channels of MD cells could be inhibited by a rise in intracellular Ca^{2+} induced by application of 1 μM ionomycin (9), we tested the effect of ionomycin on the Ba^{2+}-sensitive NH_4^+ transport through the apical membrane of MD cells. The results are shown in Fig. 3. In this series of experiments, bumetanide and Ba^{2+} reduced the NH_4^+-induced acidification rate to 10% of its control value ($n = 12$). Clearly, 1 μM ionomycin could not mimic the effect of Ba^{2+} on NH_4^+-induced acidification, as an acidification rate corresponding to 79% of the control acidification rate could be recorded (see Fig. 3 for an example), which suggests that the Ba^{2+}-sensitive NH_4^+ influx is not mediated by the K^+ channels that we previously observed in patch-clamp experiments (9). In the following series of experiments, the effect of 0.1 mM verapamil was tested in the presence of 5 μM bumetanide and in the presence of 5 mM Ba^{2+} to see its effect through the putative K^+/H^+ (NH_4^+) exchanger on each of the two components of the

Table 1. *Initial pH_i and acidification rate induced by luminal addition/removal of 20 mM NH_4^+*

	n	pH_i	dpH_i/dt, pH unit/s
Group 1			
Control	8	7.50 ± 0.06	−0.071 ± 0.008
Ba^{2+}	8	7.44 ± 0.08	−0.046 ± 0.004
Group 2			
Control	5	7.51 ± 0.06	−0.074 ± 0.009
Bum	5	7.52 ± 0.08	−0.032 ± 0.009
Bum + Ba^{2+}	5	7.53 ± 0.07	−0.005 ± 0.001
Group 3			
Control	7	6.77 ± 0.02	+0.024 ± 0.005
Bum + Ba^{2+}	7	6.81 ± 0.04	+0.025 ± 0.001
Amiloride	7	6.69 ± 0.02	+0.007 ± 0.02

Values are means ± SE; n = number of tubules for 3 different groups of tubules. The effect of 5 mM Ba^{2+} on the NH_4^+-induced acidification rate was tested in the first group, the effects of 5 μM bumetanide (Bum) and 5 μM bumetanide + 5 mM Ba^{2+} were tested in the second group, and the rate of intracellular pH (pH_i) recovery following NH_4^+ removal was measured in control conditions or in presence of 5 μM bumetanide + 5 mM Ba^{2+} or 1 mM amiloride in the third group.

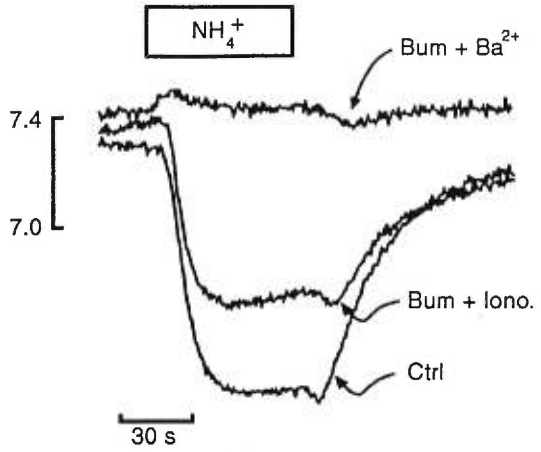

Fig. 3. Comparison between effect of ionomycin and effect of Ba^{2+} on NH_4^+-induced acidification. NH_4^+, 20 mM, was added to luminal perfusate in control conditions, in presence of 5 μM bumetanide + 1 μM ionomycin, or 5 μM bumetanide + 5 mM Ba^{2+}.

NH_4^+-induced acidification. In six experiments, the NH_4^+-induced acidification rate was shown to be 0.073 ± 0.010 pH unit/s in the presence of bumetanide and verapamil, a value not significantly different from the value of 0.090 ± 0.013 pH unit/s obtained in the presence of bumetanide alone ($P = 0.24$). In the presence of Ba^{2+}, verapamil also failed to significantly affect the acidification rate (0.076 ± 0.025 pH unit/s before and 0.070 ± 0.024 pH unit/s after the addition of verapamil, $P = 0.14$, $n = 5$).

pH_i recovery after NH_4^+ removal. To determine whether NH_4^+ could exit MD cells via the pathways involved in the entry process, the pH_i recovery during NH_4^+ washout was evaluated in the presence of bumetanide and Ba^{2+} (Table 1). Under control conditions, alkalinization rate during the recovery period was not changed by the presence of bumetanide and Ba^{2+} (Fig. 4*A*; Table 1). If amiloride was present in the lumen, then the alkalinization rate was reduced to 29% of the control value indicating a dominant role for the apical Na^+/H^+ exchanger in pH_i recovery following NH_4^+ removal (Fig. 4*B*; Table 1).

DISCUSSION

Comparison between NH_4^+-induced acidification in MD vs. TAL cells. The results presented above indicate that, qualitatively, MD cells behave like mouse (12, 13) and rat (1, 27) MTAL cells when their apical membrane is exposed to NH_4^+. In the cases where microperfusion was used, a dominant acidification was systematically recorded after luminal NH_4^+ addition, which could be blocked almost completely by furosemide and Ba^{2+} (12, 13, 27). For MTAL suspensions (1, 12, 13), similar acidifications were observed after bilateral NH_4^+ addition, but ouabain was needed in addition to Ba^{2+} and furosemide to block the acidification completely. Our average acidification rate under control conditions (0.071 pH unit/s) compares with published determinations in MTAL: 0.047 pH unit/s for microperfused mice MTAL (13), 0.053 pH unit/s for rat MTAL suspension (1), and 0.185 pH unit/s for microperfused rat MTAL (27).

Conversion of acidification rates into net proton production (J_H) requires an estimate of the buffering capacity for each cell type. We have found a steep dependence of β_i as a function of pH_i in MD cells that is obvious from the raw data (see *inset* of Fig. 1). The average β_i of MD cells at a pH_i of 7.5 is 70 mM/pH unit. In mouse MTAL cells, β_i was also shown to increase with cellular acidification and averages 29.7 mM/pH unit in the pH_i range of 7.0 to 7.6 (13). Higher β_i values were estimated for rat MTAL (85 mM/pH unit, unpublished data cited in Ref. 27) whereas in rabbit proximal tubules (16), β_i was estimated to 42.8 mM/pH unit (84.6 mM/pH unit in the presence of CO_2/HCO_3^-). In consequence, net proton production rates after adding luminal NH_4^+ ($dpH_i/dt \times \beta_i$) were 5.0 mM/s for MD cells in control conditions, 1.4 mM/s for mice MTAL (13), and 15.7 mM/s for rat MTAL (27), as estimated from their unpublished value for β_i. One can see that the net proton production rate may vary considerably depending on the species and on the buffering capacity estimated in each case. Nevertheless, proton production rate in MD cells induced by NH_4^+ addition is clearly not 40 times smaller than the corresponding values for MTALs. This is in contrast with the low intensity of ionic transport expected for MD cells, given the fact that the MD Na^+-K^+-ATPase activity was estimated to be 1/40 of the TAL activity (expressed per unit of cell volume as is also the case of proton production rates; see Ref. 25; see also Ref. 3). However, the interesting parameters to estimate are the NH_4^+ and NH_3 fluxes (J_{NH4} and J_{NH3}), and the following model will help us in going from J_H to J_{NH4} and J_{NH3}.

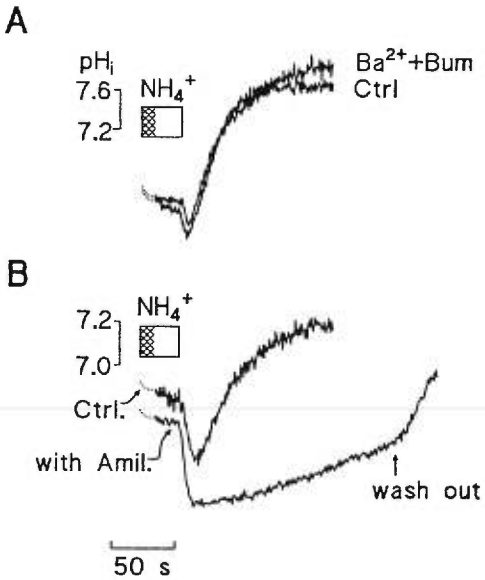

Fig. 4. pH_i recovery during luminal NH_4^+ wash out in MD cells. *A*: for a single MD plaque, there was an absence of any significant effect of 5 μM bumetanide + 5 mM Ba^{2+} in the lumen on the rate of pH change during the recovery period. *B*: effect of 1 mM luminal amiloride on the alkalinization rate following luminal NH_4^+ removal. At the vertical arrow, amiloride was removed from the perfusate.

Transport model for simulating NH_4^+/NH_3 fluxes in epithelial cells. It has been previously assumed that a powerful intracellular acidification following addition of NH_4^+ indicated the presence of an NH_4^+ permeability (P_{NH4}) much larger than the NH_3 permeability (P_{NH3}) (12, 27) and that the proton production rate ($dpH_i/dt \times \beta_i$) could be directly assimilated to the net flux of NH_4^+ (J_{NH4}) (13). However, as recognized by Watts and Good (27), with a pK_a of 9.0 for the NH_4^+ dissociation reaction and a pH_i of 7.4, only 1/40 ($\sim 10^{-1.6}$) of NH_4^+ ions entering the cell should dissociate to $NH_3 + H^+$. In the case of mouse MTAL, the proton production rate would then correspond to a J_{NH4} of 56 mM/s, a clearly unacceptable value that is inconsistent with the fact that pH_i and presumably intracellular NH_4^+ concentration require up to 30 s to reach a steady-state level. The model briefly presented here and in more detail in the APPENDIX will show that both of these assumptions ($P_{NH4} > P_{NH3}$ and J_{NH4} = proton production rate) are wrong in the case of MD cells and most likely in the case of MTAL cells as well.

We are considering a simple model that takes into account a pH_i regulation system together with NH_3 and NH_4^+ fluxes across apical and basolateral membrane. Permeabilities are defined as the coefficient (in s^{-1}) by which a *cis* concentration (mM) has to be multiplied to obtain a unidirectional flux (mM/s) in the *trans* direction. In the case of a simple diffusion of neutral substrate (as for NH_3, for example) permeability coefficients for influx are naturally set equal to the corresponding coefficient for efflux across a given membrane. In the case of NH_4^+, however, provisions are made to allow different permeability coefficients for influx and efflux in such a way that membrane potential and/or cotransported substrates have the possibility to generate asymmetrical fluxes producing intracellular NH_4^+ accumulation. The Na^+/H^+ exchanger that has been recently identified in the apical membrane of MD cells (7) was arbitrarily modeled in such a way that the proton efflux was made proportional to the value of $7.5 - pH_i$, which roughly mimics the general function of an Na^+/H^+ exchanger in the presence of a constant Na^+ gradient (2). In the absence of basolateral NH_3/NH_4^+, the five parameters to adjust are as follows: the apical and basolateral permeabilities for NH_3 (P^a_{NH3} and P^{bl}_{NH3}, respectively), the apical NH_4^+ permeability for influx (P^{ai}_{NH4}), the sum of basolateral and apical NH_4^+ permeability for efflux (P^e_{NH4}) and the pH_i sensitivity (S_H) of the pH_i-regulating mechanism [proton efflux being given as $S_H \times (7.5 - pH_i)$]. In this simple model, the dissociation of NH_4^+ was assumed to be sufficiently fast to continuously keep intracellular NH_4^+ close to the equilibrium with intracellular NH_3 and H^+. Finally, the measured buffering power was represented as a linear function of pH_i that corresponds to the measured values between a pH_i of 6.7 and 8.1 (Fig. 1) (see APPENDIX for further details on the simulation program).

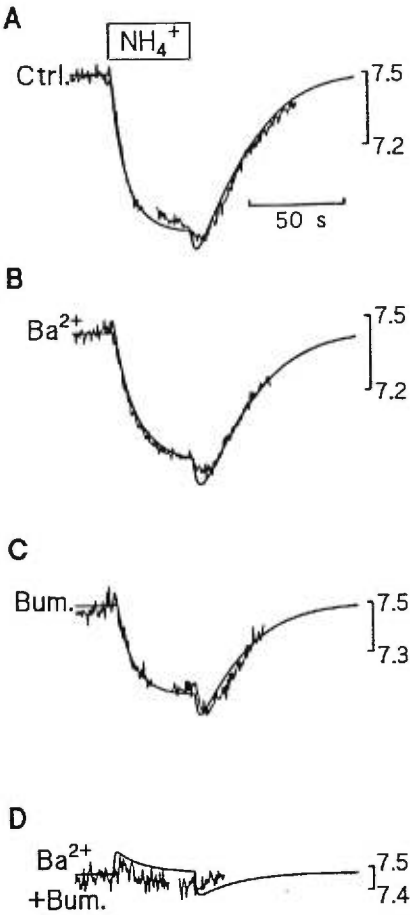

Fig. 5. Fits of the average pH_i time courses following luminal addition of 20 mM NH_4^+. Parameters in the transport model are given in Table 2 for the following four cases studied: control (*A*), in presence of 5 mM Ba^{2+} (*B*), in presence of 5 μM bumetanide (*C*), and in presence of both inhibitors simultaneously (*D*).

Analysis of NH_4^+-induced acidification in MD cells. First, average records were obtained from five experiments in which pH_i was measured following luminal NH_4^+ addition in control conditions or in the presence of different inhibitors. Acceptable fits could be obtained with a variety of P^a_{NH3} values ranging from 10 to 40 s^{-1}. Interestingly, in this range of P^a_{NH3}, good fits could be obtained with $P^a_{NH3} = P^{bl}_{NH3}$. For example, the fits shown in Fig. 5, *A–D*, were obtained with the parameters given in Table 2, in which P^a_{NH3} and P^{bl}_{NH3} were set equal

Table 2. *Parameters used for the different curves of Fig. 5*

	Fig. 5*A*	Fig. 5*B*	Fig. 5*C*	Fig. 5*D*
P^{ai}_{NH4}, s^{-1}	0.68	0.50	0.42	0.05
P^e_{NH4}, s^{-1}	0.25	0.18	0.28	0.10
P^a_{NH3}, s^{-1}	20	20	20	20
P^{bl}_{NH3}, s^{-1}	20	20	20	20
S_H, $mM \cdot s^{-1} \cdot pH\ unit^{-1}$	3.7	3.7	3.7	3.7

P^{ai}_{NH4} and P^e_{NH4}, apical membrane permeability coefficient for NH_4^+ influx and efflux, respectively; P^a_{NH3} and P^{bl}_{NH3}, apical and basolateral membrane permeability coefficient for NH_3, respectively; S_H, pH_i sensitivity of the pH_i regulatory mechanism.

to 20 s^{-1}. All the characteristics of the recorded pH_i values are correctly reproduced by the model, and none of the remaining parameters (P^{ai}_{NH4}, P^{e}_{NH4}, S_H) could be changed by more than 25% without sensibly affecting the quality of the fits. The simulation program used with the best set of parameters (with $P^{a}_{NH3} = P^{bl}_{NH3} = 20$ s^{-1}), which is given in Table 2, displays unexpected features. First, the large NH_4^+-induced acidification rate observed in control conditions can be closely reproduced with an apical NH_3 permeability 30 times larger than the apical NH_4^+ permeability for influx (this observation is valid for the whole range of acceptable P^{a}_{NH3} values). This relatively large ratio of NH_3 to NH_4^+ permeabilities contradicts previous estimations for MTAL where, with pH_i recordings quite similar to those presented here, P^{a}_{NH3} was assumed low or negligible with respect to P^{ai}_{NH4} (12, 13, 27). In rat MTAL, the apical NH_3 permeability was latter shown to exist in experiments where NH_4^+ pathways were blocked (8). Experimentally, this significant P^{a}_{NH3} in MD cells expresses itself by a small initial alkalinization upon NH_4^+ addition, which was, in some occasions, clearly observed (see Figs. 2*B* and 3), and by a larger acidification upon washing out luminal NH_4^+. A second feature readily explained by the model is the experimental observation that pH_i recovery after NH_4^+ removal is insensitive to bumetanide and Ba^{2+}. The model reveals that it takes only 4.5 s at the beginning of the washout period to bring the intracellular NH_4^+ concentration from 38 mM at the end of the luminal NH_4^+ application to 1 mM which causes the rapid acidification observed in the first few seconds following NH_4^+ removal. The relatively slower pH_i recovery following this initial acidification is the expression of a classic pH_i regulation system mainly depending on the Na^+/H^+ exchanger. A third feature of the best fit obtained is that the initial NH_4^+ influx is not 40 times larger than the proton production rate as predicted earlier (27) but only ≈2.1 times larger (J_{NH4} = 13 mM/s and $dpH_i/dt \times \beta_i$ = 6.3 mM/s). Even if J_{NH4} is not equal to the proton production rate, comparison of Table 1 and 2 shows that the J_{NH4} values calculated by the model are in proportion with the measured dpH_i/dt values in the different experimental conditions.

Absolute value of apical NH_4^+ influx. Beeuwkes and Rosen (3) have suggested a low or absent Na^+-K^+-ATPase activity in MD cells, and microenzymatic measurement of Na^+-K^+-ATPase activity revealed an enzyme activity per unit of cell volume of ~1/40th of that found in TAL (25). Low levels of Na^+-K^+-ATPase in the basal membrane of MD cells have also been demonstrated by using monoclonal antibodies against the enzyme (11). Thus those studies suggest that relative to TAL cells, MD cells cannot maintain a very significant transepithelial NaCl transport through, presumably, the activity of the apical Na^+:K^+:$2Cl^-$ cotransporter and a Ba^{2+}-sensitive pathway and a basolateral Na^+-K^+-ATPase. It is therefore surprising to find in the present study an NH_4^+-induced proton production rate of comparable amplitude vs. that found in TAL. If the MD apical permeability coefficient for NH_4^+ was in proportion to the low activity expected for the basolateral Na^+-K^+-ATPase (everything being normalized to the cell volume), then the NH_4^+-induced proton production rate (also per unit of cell volume) would be expected to be at least one order of magnitude lower for MD cells vs. TAL cells.

Transport pathways for luminal NH_4^+. One of the pathways used by NH_4^+ to induce bumetanide-sensitive cell acidification is very likely the Na^+:K^+(NH_4^+):$2Cl^-$ cotransport. We found that 5 μM bumetanide inhibits 57% of the initial rate of cell acidification observed with luminal addition of NH_4^+. This finding agrees with recent work which indicated that the active NH_4^+ transport in TAL proceeds via the substitution of NH_4^+ for K^+ in the apical membrane Na^+:K^+:$2Cl^-$ cotransporter (1, 8, 12–14, 27).

Our studies show that bumetanide did not completely prevent the intracellular acidification induced by luminal NH_4^+ and that the residual acidification (35–40% of control) observed with bumetanide was inhibited by luminal Ba^{2+}. On the basis of previous observations that a component of NH_4^+-induced cell acidification was Ba^{2+} sensitive, it was suggested that NH_4^+ entry in the TAL occurs via apical membrane K^+ channels (12, 13, 27). We have indeed directly observed a single class of K^+ channels in the apical membrane of MD cells using the patch-clamp technique (9). However, we have also shown that complete inhibition of these K^+ channels can be achieved by increasing intracellular [Ca^{2+}] with 1 μM ionomycin. As this maneuver does not prevent the Ba^{2+}-sensitive NH_4^+-induced cell acidification (Fig. 3), it is unlikely that NH_4^+ ions use the K^+ channels that we have previously observed (9). We have to recognize that a different class of K^+ channels that may have remained undetected in our patch-clamp experiments could be responsible for the Ba^{2+}-sensitive NH_4^+ influx observed in the present study. Luminal application of 5 mM Ba^{2+}, however, produces an instantaneous cell acidification (see Fig. 2*C*) that is unexpected from the blockade of K^+ channels and the ensuing depolarization. It was recently argued that for rat MTAL, the Ba^{2+}-sensitive portion of NH_4^+-induced acidification was not related to K^+ channels but rather to a verapamil-sensitive K^+/H^+(NH_4^+) antiport (1). This is not likely to be the case in MD cells as, first, 0.1 mM verapamil had no effect on NH_4^+-induced acidification, and second, contrary to what was happening in TAL cells, Ba^{2+} systematically produced an instantaneous acidification of MD cells, which discards any direct effect from a putative K^+/H^+ exchanger in MD cells. The nature of this NH_4^+ pathway could not be identified in the present studies; however, the transporter/channel involved should mediate H^+ efflux under control conditions, be Ba^{2+} sensitive, and transport NH_4^+ from the lumen to the cytosol upon luminal NH_4^+ addition.

In conclusion, MD cells behave just like MTAL cells when 20 mM NH_4^+ is presented in the luminal perfusate: a dominant cell acidification is observed with

bumetanide-sensitive and Ba^{2+}-sensitive components. Contrary to previous interpretations, these results can be quantitatively explained with an apical NH_3 permeability 30 times larger than the NH_4^+ apical permeability, if we allow for a significant basolateral NH_3 permeability and/or an apical NH_4^+ entry mechanism which has the capacity to accumulate NH_4^+ in the cell. The calculated NH_4^+ apical permeability is surprisingly high with respect to MTAL, given the fact that the basolateral pumping capacity was reported to be much lower.

APPENDIX

Transport model for simulating NH_3/NH_4^+ fluxes in epithelial cells. pH_i, $[NH_4^+]$, and $[NH_3]$ can be simulated on a personal computer as a function of time following luminal addition of 20 mM NH_4^+. Concentrations are given in units of mM, permeabilities in units of s^{-1}, and fluxes appear in units of mM/s as defined in MATERIAL AND METHODS. As briefly explained in the DISCUSSION, the following five parameters are used in this simple model: apical and basolateral permeability coefficients for NH_3 (P^a_{NH3}, P^{bl}_{NH3}), permeability coefficients for NH_4^+ entry across apical membrane (P^{ai}_{NH4}) and for NH_4^+ exit across both apical and basolateral membranes (P^e_{NH4}), and the sensitivity (S_H) of a pH_i regulatory mechanism which transports protons out of the cell according to the simple relation $J_H = S_H \times (7.5 - pH_i)$. For each time increment (0.1 s), unidirectional influx and efflux of NH_4^+ and NH_3, and resulting intracellular concentrations are calculated. Then, at a given pH_i, $[NH_4^+]$ is allowed to equilibrate with $[NH_3]$ and [H], keeping the total $[NH_4^+] + [NH_3]$ constant. This equilibration process releases or captures a given amount of protons which are added to the efflux of proton mediated by the pH_i-regulating mechanism. Finally, a new pH_i is calculated based on the proton net flux and the known buffer capacity of the cell.

Each of the five parameters play a specific role, as can be easily seen in the simulation. S_H, the sensitivity of the pH_i regulatory mechanism, has, of course, a crucial role to play in the amplitude of the acidification produced by apical NH_4^+ addition. While other parameters can also influence this amplitude, S_H is the only parameter affecting the slow alkalinization observed in the recovery period following removal of apical NH_4^+. P^a_{NH3} specifically influences the size of the initial pH_i changes upon apical NH_4^+ addition or removal. At a given S_H and P^a_{NH3}, P^{ai}_{NH4} affects the NH_4^+-induced acidification rate, and the ratio P^{ai}_{NH4}/P^e_{NH4} together with P^{bl}_{NH3} determine the final pH_i reached. This makes good sense as the pH_i level reached in the presence of apical NH_4^+ depends on a large intracellular proton production rate. This proton production rate is maintained elevated if the dissociation reaction $NH_4^+ = NH_3 + H^+$ is set slightly off equilibrium by a concentrating NH_4^+ uptake mechanism (large P^{ai}_{NH4}/P^e_{NH4}) or by a low $[NH_3]$ set by a large basolateral NH_3 permeability coefficient (P^{bl}_{NH3}). The model clearly shows that the large acidification rate seen after apical NH_4^+ addition is not indicative of a larger apical permeability for NH_4^+ than for NH_3. If one sets $P^{ai}_{NH4} = P^e_{NH4}$, and if the NH_3 efflux through the basolateral membrane is minimized ($P^{bl}_{NH3} = 0$), then one cannot generate a significant NH_4^+-induced cellular acidification no matter how large one sets the apical NH_4^+ permeability. The conditions that generate such an acidification rate are a reduction of $[NH_3]$ through basolateral exit and an accumulative mechanism for apical NH_4^+ entry, which can be secondary to cotransported solutes or to membrane electrical potential.

This work was supported by the Kidney Foundation of Canada awarded to J.-Y. Lapointe.

Address for reprint requests: J.-Y. Lapointe, Groupe de Recherche en Transport Membranaire, Université de Montréal, P.O. Box 6128 Succursalle (centre-ville), Montréal, Quebec, Canada H3C 3J7.

Received 11 October 1996; accepted in final form 16 July 1997.

REFERENCES

1. **Amlal, H., M. Paillard, and M. Bichara.** $NH4^+$ transport pathways in cells of medullary thick ascending limb of rat kidney: NH_4^+ conductance and $K^+/NH_4^+(H^+)$ antiport. *J. Biol. Chem.* 269: 21962–21971, 1994.
2. **Aronson, P. S.** Kinetic properties of the plasma membrane Na^+-H^+ exchanger. *Annu. Rev. Physiol.* 47: 545–560, 1985.
3. **Beeuwkes, III, R., and S. Rosen.** Renal Na^+-K^+-ATPase: localization and quantitation by means of its K^+-dependent phosphatase activity. In: *Current Topics in Membranes and Transport. Cellular Mechanisms of Renal Tubular ion Transport*, edited by E. L. Boulpaep. New York: Academic, 1980, vol. 13, p. 343–354.
4. **Bell, P. D., J.-Y. Lapointe, and J. Cardinal.** Direct measurement of basolateral membrane potentials from cells of the macula densa. *Am. J. Physiol.* 257 (*Renal Fluid Electrolyte Physiol.* 26): F463–F468, 1989.
5. **Bleich, M., E. Schlatter, and R. Greger.** The luminal K^+ channel of the thick ascending limb of Henle's loop. *Pflügers Arch.* 415: 449–460, 1990.
6. **Bleich, M., M. Köttgen, E. Schlatter, and R. Greger.** Effect of NH_4^+/NH_3 on cytosolic pH and the K^+ channels of freshly isolated cells from the thick ascending limb of Henle's loop. *Pflügers Arch.* 429: 345–354, 1995.
7. **Fowler, B. C., Y. S. Chang, A. Laamarti, M. Higdon, J.-Y. Lapointe, and P. D. Bell.** Evidence for apical sodium proton exchange in macula densa cells. *Kidney Int.* 47: 746–751, 1995.
8. **Good, D. W.** Ammonium transport by the thick ascending limb of Henle's loop. *Annu. Rev. Physiol.* 56: 623–647, 1994.
9. **Hurst, A. M., J.-Y. Lapointe, A. Laamarti, and P. D. Bell.** Basic properties and potential regulators of the apical K^+ channel in macula densa cells. *J. Gen. Physiol.* 103: 1055–1070, 1994.
10. **Kaplan, M. R., M. D. Plotkin, W. S. Lee, Z. C. Xu, J. Lytton, and S. C. Hebert.** Apical localization of the Na-K-Cl cotransporter, RBSC1, on rat thick ascending limbs. *Kidney Int.* 49: 40–47, 1996.
11. **Kashgarian, M., D. Biemesderfer, M. Caplan, and B. Forbush.** Monoclonal antibodies to Na-K-ATPase: immunocytochemical localization along nephron segments. *Kidney Int.* 28: 899–913, 1985.
12. **Kikeri, D. A., M. Sun, L. Zeidel, and S. C. Hebert.** Cell membranes impermeable to NH_3. *Nature* 339: 478–480, 1989.
13. **Kikeri, D. A., M. Sun, L. Zeidel, and S. C. Hebert.** Cellular NH_4^+/K^+ transport pathways in mouse medullary thick limb of Henle. *J. Gen. Physiol.* 99: 435–461, 1992.
14. **Kinne, R., E. Kinne-Saffran, H. Shutz, and B. Scholermann.** Ammonium transport in medullary thick ascending limb of rabbit kidney: Involvement of the Na^+:K^+:$2Cl^-$ cotransporter. *J. Membr. Biol.* 94: 279–284, 1986.
15. **Kirk, K. L., P. D. Bell, D. W. Barfuss, and M. Ribadeneira.** Direct visualization of the isolated and perfused macula densa. *Am. J. Physiol.* 248 (*Renal Fluid Electrolyte Physiol.* 17): F890–F894, 1985.
16. **Krapf, R., R. J. Alpern, F. C. Rector, and C. A. Berry.** Basolateral membrane Na/base cotransport is dependent on CO_2/HCO_3 in the proximal convoluted tubule. *J. Gen. Physiol.* 90: 833–853, 1987.
17. **Lapointe, J. Y., P. D. Bell, and J. Cardinal.** Direct evidence for apical Na^+:K^+:$2Cl^-$ cotransport in macula densa cells. *Am. J. Physiol.* 258 (*Renal Fluid Electrolyte Physiol.* 27): F1466–F1469, 1990.
18. **Lapointe, J. Y., P. D. Bell, A. M. Hurst, and J. Cardinal.** Basolateral ionic permeabilities of macula densa cells. *Am. J. Physiol.* 260 (*Renal Fluid Electrolyte Physiol.* 29): F856–F860, 1991.

19. **Lapointe, J. Y., A. Laamarti, A. M. Hurst, B. C. Fowler, and P. D. Bell.** Activation of Na:2Cl:K cotransport by luminal chloride. *Kidney Int.* 47: 752–757, 1995.
20. **Salomonsson, M., E. Gonzalez, M. Kornfeld, and A. E. G. Persson.** The cytosolic chloride concentration in macula densa and cortical thick ascending limb cells. *Acta Physiol. Scand.* 147: 305–313, 1993.
21. **Salomonsson, M., E. Gonzalez, L. Sjöli, and A. E. G. Persson.** Simultaneous measurement of cytosolic free Ca^{2+} in macula densa cells and in cortical thick ascending limb cells using fluorescence digital imaging microscopy. *Acta Physiol. Scand.* 138: 425–426, 1990.
22. **Schlatter, E.** Effect of various diuretics on membrane voltage of macula densa cells. Whole-cell patch clamp experiments. *Pflügers Arch.* 423: 74–77, 1993.
23. **Schlatter, E., M. Salomonsson, A. E. G. Persson, and R. Greger.** Macula densa cells sense luminal NaCl concentration via furosemide sensitive Na^+:K^+:$2Cl^-$ cotransport. *Pflügers Arch.* 414: 286–290, 1989.
24. **Schnermann, J., and J. Briggs.** Function of the juxtaglomerular apparatus: local control on glomerular hemodynamics. In: *The Kidney*, edited by D. W. Seldin and G. Giebish. New York: Raven, 1992, p. 1249–1289.
25. **Schnermann, J., and D. Marver.** ATPase activity in macula densa cells of the rabbit kidney. *Pflügers Arch.* 407: 82–86, 1986.
26. **Thomas, J. A., R. N. Buchsbaum, A. Fimniak, and S. Racker.** Intracellular pH measurements in Ehrlich ascites tumor cells utilizing spectroscopic probes generated in situ. *Biochem. J.* 18: 2210–2218, 1979.
27. **Watts, B. A., and D. W. Good.** Effects of ammonium on intracellular pH in rat medullary thick ascending limb: mechanisms of apical membrane NH_4^+ transport. *J. Gen. Physiol.* 103: 917–36, 1994.

CINQUIÈME ARTICLE

Transport and regulatory properties of the apical Na^+ :K^+ :$2Cl^-$ cotransporter of the macula densa cells

Laamarti M.A., P.D. Bell and Lapointe J.Y.

(En révision)

Transport and regulatory properties of the apical $Na^+:K^+:2Cl^-$ cotransporter of macula densa cells

M. ANUAR LAAMARTI, DARWIN BELL[†] & JEAN-YVES LAPOINTE

Groupe de recherche en transport membranaire, Université de Montréal, Montréal, Québec, Canada, H3C 3J7 and, [†]Department of Medicine and Physiology, University of Alabama at Birmingham, Birmingham, Alabama, 35294.

Corresponding address: Dr. J-Y Lapointe
Groupe de recherche en transport membranaire
Université de Montréal
P.O. box 6128 Succursalle « centre-ville »
Montréal, Quebec, Canada, H3C 3J7
Tel:514-343-7046 / Fax: 514-343-7146
E-mail: lapoinj@ere.umontreal.ca

Abbreviated title: **Transport and regulation of $Na^+:K^+:2Cl^-$**

ABSTRACT

NH_4^+/NH_3 fluxes were used to probe apical Na^+:K:2Cl transport activity of macula densa cells from rabbit kidney. In the presence of 25 mM NaCl and 5 mM Ba^{2+}, addition of 20 mM NH_4^+ to the lumen produced a profound intracellular acidification and ~80% of the initial acidification rate was bumetanide sensitive. The NH_4^+-induced acidification rate was dependent on luminal Cl^- and Na^+ with apparent affinities of 17 ± 4 mM (Hill number 1.45) and 1.0 ± 0.3 mM, respectively. In the presence of saturating luminal [NaCl], blockade of basolateral Cl^- efflux with 10 μM nitro-phenylpropyl-amino-benzoic acid (NPPB) reduced the NH_4^+-induced acidification rate by 51 ± 6 % ($p > 0.01$, n=5). Under similar conditions, dbcAMP + forskolin increased the NH_4^+-induced acidification rate by 27% while it produced no detectable effect at low luminal NaCl concentration. Most of the observed dbcAMP + forskolin effect was probably due to the stimulation of the basolateral Cl^- conductance since, in the presence of basolateral NPPB, this activation was changed to a 17.1% and 16.6% inhibition of the NH_4^+-induced acidification rate observed at high or low luminal [NaCl], respectively. We conclude that the Na:K:2Cl cotransporter found in MD cells displays, with respect to thick ascending limbs, a relatively high affinity for luminal Na^+ and luminal Cl^- and can be specifically inhibited by increases in intracellular Cl^- and cAMP

concentrations. This can either indicate the presence of different isoforms (22) or different regulatory states of the same transporter.

Index terms: Na-K-2Cl, cAMP, forskolin, PKA, bumetanide, kinetics.

INTRODUCTION

Macula densa cells (MD) are thought to function as sensor devices detecting increases in luminal NaCl concentration ($[NaCl]_L$) and initiating signals controlling renin secretion and tubulo-glomerular feedback (TGF). Since both renin secretion and TGF are bumetanide (or furosemide) sensitive (17,45), the apical Na:K:2Cl cotransporter found in MD cells (26,39) is very likely to be responsible for detecting changes in $[NaCl]_L$. After many years of investigation, the exact nature of the signal(s) transmitted to smooth muscle and granular cells remains elusive although a number of factors capable of modulating signal transmission have been identified (41). These include angiotensin II (18), adenosine (9,40), arachidonic acid metabolites (3,8,49), cAMP (2), Ca^{2+} (3) and nitric oxide (44). Some of these factors are probably involved in the adjustment of TGF amplitude and sensitivity which are expected in different physiological conditions (5) but the mechanism of action and even the cell type affected remain uncertain.

In terms of the MD cells, nothing is known about the effect of any of the factors mentioned above on the different transport pathways already identified in these cells (4,7,19,25-27,39). A central mechanism in the function of MD cells is the apical Na:K:2Cl cotransporter which, under the ionic

conditions prevailing ($[NaCl]_L$ = 20-60 mM) at the end of the thick ascending limbs (TAL), mediates NaCl reabsorption and is exquisitely sensitive to changes in $[NaCl]_L$ (28). Following the cloning of the thiazide-sensitive Na-Cl cotransporter (10) and the cloning of the secretory form of the Na:K:2Cl cotransporter (46), specific isoforms of the Na:K:2Cl cotransporters for kidney and intestine (NKCC2 or rBSC1) were identified in rabbit (34), rat (11), mouse (20) and human (35). Mouse NKCC2 and rat rBSC1 are ~97% identical and are localised to the apical membrane of medullary and cortical TAL (22,30). In the case of MD cells, anti-rBSC1 antibody failed to detect a significant signal in rat MD cells but, after denaturation with SDS and 2-mercaptoethanol, a weak signal could be found (22). Using an antisense probe for the apical form of the Na:K:2Cl cotransporter, mRNA was found in both TAL and MD cells from rat and rabbit kidney (31). More specifically, the B isoform of the NKCC2 cotransporter was detected in rat MD-containing tubule segments using polymerase chain reaction with isoform-specific primers (47).

In this paper, we use the fact that, in the presence of Ba^{2+}, more than 80% of the luminal NH_4^+-induced acidification rate is bumetanide sensitive. As discussed earlier (25), this indicates that NH_4^+ is taken up by the Na:K:2Cl cotransporter and dissociates within the cell to $H^+ + NH_3$. This provides a sensitive method to measure the NH_4^+ influx rate, obtain apparent affinity

constants for luminal Na^+ and Cl^- and identify some of the intracellular factors capable of modulating the activity of MD apical Na:K:2Cl cotransporter.

MATERIAL AND METHOD

Microperfusion and fluorescence measurements Microperfusion of rabbit cTAL's dissected with their attached glomeruli was performed exactly as described in a recent paper from this laboratory (25). Tubules were bathed with a bicarbonate-free solution containing (in mM) : 146 NaCl, 5 K-gluconate, 1 $MgCl_2$, 1 $CaCl_2$, 5 glucose, 10 N-2-hydroxyethylpiperazine-N'-2-ethane-sulfonic-acid (Hepes) and 7.2 Tris-(hydroxymethyl)-aminomethane. Luminal solutions were identical to the bathing solution with the exception that the $[NaCl]_L$ was maintained at 25 mM by isosmotically replacing Na^+ with N-methyl-D-glucamine and Cl^- with cyclamate. Addition of luminal NH_4^+ (20 mM) and/or Ba^{2+} (5 mM) was accomplished by isosmotic replacement of NMDG-cyclamate with either ammonium acetate or barium acetate at constant luminal $[Na^+]$ and $[Cl^-]$. All solutions were adjusted to a pH of 7.4 and all experiments were performed at 39°C.

Intracellular pH was measured using the fluorescent probe 2',7'-bis(2-carboxyethyl)-5(6)-carboxyfluorescein (BCECF) as previously described (6,23,26). Intracellular dye was alternately excited at 500 and 450 nm wavelengths (Spex model CM-III; Spex Industries, Edisson, NJ, USA), and fluorescence emission was monitored at 530 nm using a photomultiplier tube

and a pass-band filter. BCECF-AM was perfused through the lumen and loading was continued until the fluorescence measured for both excitation wavelengths had increased by a least one order of magnitude with respect to background fluorescence. Calibration curves for BCECF fluorescence were obtained using the high $[K^+]$-nigericin technique (42) as described previously (25). Since a complete calibration curve could not be performed in each experiment, we obtained one or two calibration points (including pH_i ~7.2-7.4) at the end of each experiment and used previously obtained calibration curves to convert fluorescence ratios to pH measurements.

Determination of apical NH_4^+ transport rates Initial acidification rates were obtained from fitting exponential or linear equations to the recorded pH time-courses after replacing 20 mM of luminal NMDG/Cl with 20 mM NH_4Cl. It was quantitatively shown that the resulting acidification rate multiplied by the MD cell buffering power was proportional to the apical NH_4^+ influx rate (25). The buffering power was previously measured for MD cells and was found to double when the cell acidified from 7.5 to 6.7 (25). Under the experimental conditions of the present studies, no systematic changes in the initial pHi (before adding luminal NH_4^+) was found in any experimental group. For example, even if an abrupt increase in luminal Cl^- concentration was observed to acidify MD cells as previously reported (28), the pHi obtained

after luminal NH_4^+ addition (2-3 min) and washout (5-7 min) in the presence of a different luminal Cl^- concentration was not statistically different from the initial pHi. This allows us to use NH_4^+-induced acidification rate without having to add a correction factor based on the average buffering power previously measured for a different series of experiments.

Statistics Data are presented as mean ± SE and "n" is the number of MD plaques studied. In some experiments, data were fitted to theoretical equations using a commercial software and the uncertainty of fitted parameters is the standard error of the fit (FigP 6.0, Biosoft, Milltown, New-Jersey). Statistical significance of the difference between two means was assessed using Student's t-test for paired samples. $P<0.05$ was considered significant.

RESULTS

NH_4^+-induced acidification As previously shown, NH_4^+ is mainly transported across the apical membrane of MD cells through a bumetanide-sensitive pathway and a Ba^{2+}-sensitive pathway in an additive manner (57% and 35% of the initial NH_4^+-induced acidification rate was sensitive to bumetanide and Ba^{2+} respectively, ref. 25). In the present series of experiments where 5 mM Ba^{2+} was constantly present in the lumen, we confirmed that NH_4^+-induced acidification was largely mediated by the Na:K:2Cl cotransporter: 89 ± 14 % of the maximal acidification rate observed was Cl^- dependent (n=6) and 84 ± 7 % was Na^+ dependent (n=6) (see below). This is illustrated in Fig 1 where we compare, in the same experiment, the NH_4^+-induced acidification obtained in the presence of 25 mM $[NaCl]_L$ with that obtained in the absence of functional Na:K:2Cl cotransport (0 mM Na^+ + 5 μM bumetanide) In these experiments, 1 mM amiloride was also present in the lumen to block the apical Na^+:H^+ exchanger (7).

Cl^- and Na^+ affinity In the presence of 25 mM luminal Na^+ concentration ($[Na^+]_L$), NH_4^+-induced acidification rate was measured with luminal Cl^- concentration ($[Cl^-]_L$) varying from 1 to 100 mM. At high $[Cl^-]_L$ (i.e. 100 mM), the initial dpH_i/dt averaged 0.095 ± .019 pH units s^{-1} (n=6). Individual

measurements were normalised using the value measured at 100 mM $[Cl^-]_L$ and averaged data at each $[Cl^-]_L$ was fitted (see Fig 2) using the following expression:

$$\frac{dpH_i}{dt} = C + \frac{V_{MAX} \times [Cl]_L^{\,h}}{K_M^{Cl\ h} + [Cl]_L^{\,h}}$$

where "h" is the Hill number, K_M^{Cl} is the luminal Cl^- apparent affinity constant, "C" is the remaining dpH_i/dt at zero luminal Cl^- and V_{MAX} +C is the maximal dpH_i/dt at infinite $[Cl^-]_L$. The Cl^- affinity constant was found to be 17 ± 4 mM and the Hill number was significantly larger than 1 (1.45 ± .45) which is consistent with the expected stoichiometry of the cotransporter.

In obtaining the apparent cotransporter affinity for luminal Na^+, care must be taken to avoid systematic pH_i variations due to the activity of the recently described luminal Na^+:H^+ exchanger (7). Thus, these experiments were performed in the presence of 1 mM luminal amiloride while $[Na^+]_L$ was varied from 0 to 60 mM. The final $[Na^+]_L$ for solutions nominally containing 0, 0.5, 1 and 2 mM Na^+ were measured using flame photometry (IL943, Instrumentation Laboratory S.P.A., Milan, Italia) and found to be 0.47, 0.98,

1.47 and 2.67 mM respectively. Based on preliminary experiments, the acidification rates obtained with 0.47 and 0.98 mM Na^+ were very weak and we choose to add 5 μM bumetanide to these solutions in order to obtain a better estimation of the baseline acidification rate (i.e. bumetanide-insensitive). The data were normalized using the measured acidification rate obtained at 60 mM $[Na^+]_L$ and 25 mM $[Cl^-]_L$ which averaged 0.046 ±.006 pH units s^{-1} (n=6). After normalization, the data (see Fig 3) could be fitted to a modified Michaelis-Menten equation like the one given in Eq. 1 in the case of Cl^-. The Na^+ apparent affinity constant was 1.0 ± 0.3 mM (n=6).

Effects of intracellular Cl^- concentration Under normal conditions, the apical Na:K:2Cl cotransporter mediates NaCl entry in MD cells (28) and maintains intracellular Cl^- above its electrochemical equilibrium. This provides the driving force for Cl^- exit across the basolateral membrane Cl^- conductance (27). Intracellular Cl^- could interfere with the apical cotransporter activity by either reducing the chemical gradient for Cl^- entry across the apical membrane or by changing the phosphorylation state of the cotransporter (16). The level of intracellular Cl^- was modulated by blocking the basolateral Cl^- conductance with 10 μM nitro-phenylpropyl-amino-benzoic acid (NPPB) (39). In the presence of saturating $[Na^+]_L$ and $[Cl^-]_L$ (25 mM Na^+ and 60 mM Cl^-), basolateral addition of NPPB reduced the NH_4^+-induced acidification rate from

0.075 ±.010 to 0.035 ±.004 ($p<.01$, n=5), an average inhibition of 51 ±6%. In the presence of low $[Na^+]_L$ and $[Cl^-]_L$ (1 mM Na^+ and 5 mM Cl^-), basolateral NPPB did not significantly affect NH_4^+-induced acidification (0.023 ±.003 to 0.017 ±.002, n.s., n=5). Interestingly, under these conditions, the apical cotransporter is expected to mediate a minimal NaCl net influx (28) and, consequently, basolateral NPPB application is not expected to produce any significant increase in intracellular Cl^- concentration.

Effects of cAMP TGF was previously shown to be partially inhibited by cAMP (2). In a variety of tissues, maneuvers that increase intracellular cAMP levels and PKA activity were found to stimulate (15,16,32) or inhibit the Na:K:2Cl cotransporter (14,29,32,36). The effects of 0.1 mM luminal dibutyryl cAMP (dbcAMP) and 1 μM forskolin on NH_4^+-induced acidification rate are shown in Fig 5. In the presence of 25 mM $[Na^+]_L$ and 60 mM $[Cl^-]_L$, NH_4^+-induced acidification rate was 0.079 ±.010 pH units s^{-1} and increased to 0.100 ±.010 pH units s^{-1} in the presence of dbcAMP and forskolin (a significant stimulation by 26.6%, $p<0.05$, n=11). This effect appeared to require a high apical Na:K:2Cl cotransport rate since, in the presence of 1 mM $[Na^+]_L$ and 5 mM $[Cl^-]_L$, dbcAMP and forskolin did not stimulate NH_4^+-induced acidification rate (0.033 ±.008 vs 0.032 ±.008, n=11).

As previously shown, intracellular Cl^- concentration affects the apical cotransporter phosphorylation state and activity (16). This raises the question of whether dbcAMP modulates the apical Na:K:2Cl cotransporter in a direct or indirect manner. Indeed, the basolateral Cl^- conductance (27) may also be affected by cAMP which, in turn, would provide a secondary stimulation of the apical cotransporter. For example, in TAL, the basolateral Cl^- channel was reported to be activated by a rise in intracellular cAMP (13,33). This would tend to decrease intracellular Cl^- concentration, a situation that was shown to stimulate the apical cotransporter. Therefore the effects of luminal dbcAMP and forskolin were further measured in the presence of 10 μM basolateral NPPB. Under these conditions and in the presence of saturating $[Na^+]_L$ and $[Cl^-]_L$ (25 and 60 mM respectively), the NH_4^+-induced acidification rate averaged 0.035 pH units s^{-1} and was reduced to 0.029 ±.004 pH units s^{-1} in the presence of dbcAMP and forskolin ($p<0.05$, n=5, see Fig 6). This significant inhibition by 17.1% was paralleled by a reduction of 16.6% when the effects of dbcAMP and forskolin were tested in the presence of low $[Na^+]_L$ and $[Cl^-]_L$ (1 mM Na^+ and 5 mM Cl^-). Under these conditions, the NH_4^+-induced acidification rate was reduced from 0.017 ±.002 to 0.014 ±.003 pH units s^{-1} ($p<0.002$, n=5).

DISCUSSION

Utilization of the NH_4^+/ NH_3 technique was proven useful in obtaining an estimate for NaCl transport rate mediated by MD cells and in the detection of new transport mechanisms (1, 25). In the present study, it was shown that this method is also sensitive enough to detect small variations in transport rates, and to provide data on both kinetic parameters and regulatory mechanisms for the Na:K:2Cl cotransporter.

Kinetic parameters The apparent affinity of the cotransporter for luminal Cl^- was found to be 17 mM in the presence of 25 mM $[Na^+]_L$, 5 mM luminal K^+ and 20 mM luminal NH_4^+. We had previously obtained an initial estimation for Cl^- affinity of 32.5 mM using a less direct method (28) which was primarily used to determine the direction of Na:K:2Cl flux. In that previous study, Na:K:2Cl activity was estimated based on intracellular Na^+ induced changes in pH_i occuring through the activity of the apical Na^+:H^+ exchanger. To obtain an affinity for luminal Cl^-, in that study, the assumptions were: i) stimulation of the cotransporter would produce a proportional increase in intracellular Na^+ concentration ($[Na^+]_i$), ii) the apical Na^+:H^+ exchanger is sensitive to changes in $[Na^+]_i$ over a wide range, and iii) changes in the steady-state level of pH_i is proportional to Na^+:H^+ exchanger activity. It is likely that,

at least, some of these conditions would not be fully satisfied thereby introducing a degre of uncertainty regarding the estimation of Cl^- cotransporter affinity. The method used in the present study is more direct since it is based on the initial acidification rate (instead of steady-state pH_i levels) directly resulting from NH_4^+ influx. The complete time-course of NH_4^+-induced acidification and recovery was analyzed in a previous study (25) where it was shown that the initial acidification rate times the buffering power was proportional to the absolute value of apical NH_4^+ influx. In the present studies, baseline pH_i for a given series of experiments (for example: the effect of changes in $[Na^+]_L$ in the presence of amiloride) were similar so that buffering power can be assumed to be constant and need not to be considered here.

An apparent affinity constant for $[Cl^-]_L$ of 17 mM appears to be significantly lower than the value of 50 mM reported for the rabbit cTAL cotransporter (13) and the value of 67 mM for mouse TAL in culture (21) (note that a much smaller value of 15.3 mM was obtained from vesicles obtained from TAL cells, see ref. 24). For a variety of different epithelial tissues possessing the Na:K:2Cl cotransporter, apparent Cl^- affinities ranging from 20 to 75 mM have been reported (32). Thus MD cells express a cotransporter with a relatively high Cl^- affinity.

The apparent affinity constant of the MD apical cotransporter for $[Na^+]_L$ was found to be 1 mM which is slightly lower than the 2 to 3 mM Na^+ affinity constant reported for the cTAL cotransporter (13). In the case of mouse mTAL cells in culture, a Na^+ affinity constant of 7 mM was reported (21). In other epithelial tissues, Na^+ affinity constants vary between 0.42 mM for LLC-PK_1 cells to 15 mM for human fibroblasts (32). Therefore the MD cells cotransporter displays a high affinity for Na^+ which is also the case for the cotransporter of TAL cells.

The affinity for luminal K^+ was not determined in the present study because 20 mM NH_4^+ was present and should effectively compete for the cotransporter site with the 5 mM luminal K^+. If NH_4^+ affinity for the MD cotransporter is similar to the one reported for mTAL ($K_{½}$=0.5 mM NH_4^+, ref. 23), 20 mM is well above the Km value and should completely displace K^+ from its site on the cotransporter.

Regulation of cotransporter activity As expected from previous experiments on the Na:K:2Cl cotransporter (15,16), intracellular Cl^- was shown to play an important role in modulation of apical cotransporter activity. In agreement with these observations, increasing intracellular $[Cl^-]$ by blocking basolateral Cl^- channels with NPPB inhibited NH_4^+-induced acidification rate

by 51%. These results do not discriminate between an inhibition due to a diminished Cl^- chemical gradient across the apical membrane or through a change in the phosphorylation state of the cotransporter as directly shown in dog tracheal cells (16). Nevertheless, MD intracellular Cl^- does appear to be an important regulator of the apical cotransporter. Any manoeuvre that affects basolateral electrogenic Cl^- efflux (blockade of apical K^+ channels, inhibition of basolateral Na/K-ATPase, inhibition/stimulation of basolateral Cl^- channels, hormonal regulation etc.) should alter cotransporter activity through changes in intracellular $[Cl^-]$.

Interestingly, stimulation by cAMP of the NH_4^+-induced acidification rate was clearly shown to include an effect of cAMP on basolateral Cl^- channels. Indeed, a stimulation of cotransporter activity by 26.6% with cAMP was reversed to an inhibition by 17.1% when basolateral Cl^- channels were inhibited by NPPB. Therefore, the specific effect of cAMP on the apical Na:K:2Cl cotransporter is, most likely, an inhibition which can be detected both at saturating and non-saturating $[Na^+]_L$ and $[Cl^-]_L$. The similarity of the level of inhibition at low and high apical $[Na^+]_L$ and $[Cl^-]_L$ suggests that the effect of cAMP occurs exclusively on the cotransporter V_{max}. However, the % inhibition is likely to be much higher at low $[Na^+]_L$ and $[Cl^-]_L$, if one corrects for the bumetanide-insensitive component which would suggest that cAMP has

also increased Na^+ and/or Cl^- Km. In other cell types, regulation in Na:K:2Cl cotransport activity is often, but not always (6), accompanied by a parallel change in the number of bumetanide binding sites suggesting an effect through addition or removal of transporter units in the membrane (14,15). Also, cAMP has been shown to both stimulate and inhibit the Na:K:2Cl cotransporter depending on the cell type studied (14,15). In the case of the TAL, vasopressin stimulates cAMP production but the amplitude of its stimulatory effects on transepithelial NaCl fluxes (J_{NaCl}) are both species dependent and heterogeneous (cortical vs. medullary) (37). Similar to what we have found in MD cells, cAMP was shown to stimulates the basolateral Cl^- conductance in TAL (12,33,38). In a mouse mTAL cell line, the basolateral cAMP-dependent Cl^- channel has recently been identified as rdClC-Ka a member of the ClC family (48). In addition, cAMP was also shown to stimulate the TAL apical Na:K:2Cl cotransporter independently of its effect on the basolateral Cl^- conductance (i.e. the presence of basolateral Cl^- channel blockers) (43). Thus, the specific effect of cAMP on MD apical Na:K:2Cl cotransporter appears to be different from the effects reported in the case of TAL.

In conclusion, we have shown that the NH_4^+/NH_3 method which has been successfully used for monitoring apical ionic flux through at least two types of pathways (25) can also be used to determine affinity constants and

identify regulatory mechanisms of the apical Na:K:2Cl cotransporter activity. With respect to Na:K:2Cl cotransporters of other tissues, including TAL, the MD cell cotransporter has a relatively high affinity for luminal Na^+ and Cl^-. In addition, intracellular Cl^- is a potent regulator of cotransporter activity in MD cells and cAMP directly inhibits the cotransporter activity independently of its effect on basolateral Cl^- channels. These new properties of the MD Na:K:2Cl cotransporter will be helpful in understanding the role of MD cells in TGF and the alteration in sensitivity and amplitude of feedback responses in different experimental or physiological conditions.

Acknowledgments

This work was supported by the Kidney Foundation of Canada (J.Y.L.) and by National Institute of Health (P.D.B., #NIDDK 32032).

REFERENCES

1. Amlal, H., M. Paillard, M. Bichara. NH_4^+ transport pathways in cells of medullary thick ascending limb of rat kidney. NH_4^+ conductance and $K^+/NH_4^+(H^+)$ antiport. *J. Biol. Chem.* 269(35):21962-71, 1994.

2. Bell P.D. Cyclic AMP-calcium interaction in the transmission of tubuloglomerular feedback signals. *Kidney Int.* 28(5):728-32, 1985.

3. Bell P.D., M. Franco, L.G. Navar. Calcium as a mediator of tubuloglomerular feedback. *Annu. Rev. Physiol.* 49:275-93, 1987.

4. Bell P.D., J.Y. Lapointe, J. Cardinal. Direct measurement of basolateral membrane potentials from cells of the macula densa. *Am. J. Physiol.* 257(3 Pt 2):F463-8, 1989.

5. Braam B., K.D. Mitchell, H.A. Koomans, L.G. Navar. Relevance of the tubuloglomerular feedback mechanism in pathophysiology. *J. Am. Soc. Nephrol.* 4(6):1257-74, 1993.

6. D'Andrea, L., C. Lytle, J.B. Matthews, P. Hofman, B. Forbush III, J.L. Madara. Na:K:2Cl cotransporter (NKCC) of intestinal epithelial cells. *J. Biol. Chem.* 271: 28969-28976, 1996.

7. Fowler, B.C., Y.S. Chang, M.A. Laamarti, M. Higdon, J.Y. Lapointe, P.D. Bell. Evidence for apical sodium proton exchange in macula densa cells. *Kidney Int.* 47: 746-751,1995.

8. Franco, M., P.D. Bell, L.G. Navar. Evaluantion of prostaglandins as mediators of tubuloglomerular feedback. *Am. J. Physiol.* 254 (Renal Fluid Electrolyte Physiol. 23): F642-F649, 1988.

9. Franco,M., P.D. Bell, L.G. Navar. Effects of adenosine A1 analog on tubuloglomerular feedback mechanism. *Am. J. Physiol.* 257:F231-F236, 1989.

10. Gamba, G., S.N. Saltzberg, M. Lombardi, A. Miyanoshita, J. Lytton, M.A. Hediger, B.M. Brenner, S.C. Hebert. Primary structure and functional expression of a cDNA encoding the thiazide-sensitive, electroneutral sodium-chloride cotransporter. *Proc. Natl. Acad. Sci.* USA 90(7):2749-53, 1993.

11. Gamba G., A. Miyanoshita, M. Lombardi, J. Lytton, W.S. Lee, M.A. Hediger. Molecular cloning, primary structure, and characterization of two members of the mammalian electroneutral sodium-(potassium)-chloride cotransporter family expressed in kidney. *J. Biol. Chem.* 269(26):17713-22, 1994.

12. Guinamard R., A. Chraibi., J. Teulon. A small-conductance Cl- channel in the mouse thick ascending limb that is activated by ATP and protein kinase *Am. J. of Physiol.* 485 (Pt 1):97-112, 1995.

13. Greger R. Ion transport mechanisms in thick ascending limb of Henle's loop of mammalian nephron. *Physiol. Rev.* 65(3):760-97, 1985.

14. Haas, M. Properties and diversity of (Na-K-Cl) cotransporters. *Annu. Rev. Physiol.* 51: 443-457, 1989.

15. Haas, M. The Na-K-Cl cotransporters. *Am. J. Physiol.* 267 (Cell Physiol. 36): C869-C885, 1994.

16. Haas, M., D. McBrayer, C. Lytle. $[Cl^-]_i$-dependent phosphorylation of the Na-K-Cl cotransport protein of dog tracheal epithelial cells. *J. Biol. Chem.* 270: 28955-28961, 1995.

17. He, X.-R., S.G. Greenberg, J.P. Briggs, J. Schnermann. Effects of furosemide and verapamil on the NaCl dependency of macula densa-mediated renin secretion. *Hypertension* 26:137-142, 1995.

18. Huang W.C., P.D. Bell, D. Harvey, K.D. Mitchell, L.G. Navar. Angiotensin influences on tubuloglomerular feedback mechanism in hypertensive rats. *Kidney Int.* 34(5):631-7, 1988.

19. Hurst, A.M., J.Y. Lapointe, M.A. Laamarti, P.D. Bell. Basic properties and potential regulators of the apical K^+ channel in macula densa cells. *J. Gen. Physiol.* 103(6):1055-70, 1994.

20. Igarashi, P., G.B. Vanden Heuvel, J.A. Payne, B. Forbush 3rd. Cloning, embryonic expression, and alternative splicing of a murine kidney-specific Na-K-Cl cotransporter. *Am. J. Physiol.* 269(3 Pt 2):F405-18, 1995.

21. Kaji, DM. Na+/K+/2Cl- cotransport in medullary thick ascending limb cells: kinetics and bumetanide binding. *Biochim. Biophys. Acta.* 1152(2):289-99, 1993.

22. Kaplan, M.R., M.D. Plotkin, W.S. Lee, Z.C. Xu, J. Lytton, S.C. Hebert. Apical localization of the Na-K-Cl cotransporter, rBSC1, on rat thick ascending limbs. *Kidney Int.* 49(1):40-7, 1996.

23. Kikeri, D., A. Sun, M.L. Zeidel, S.C. Hebert. Cellular NH_4^+/K^+ transport pathways in mouse medullary thick limb of Henle. Regulation by intracellular pH. *J.Gen. Physiol.* 99(3):435-61, 1992.

24. Koenig, B., S. Ricapito, R. Kinne. Chloride transport in the thick ascending limb of Henle's loop: potassium dependence and stoichiometry of the NaCl cotransport system in plasma membrane vesicles. *Pflügers Arch.* 399(3):173-9, 1983.

25. Laamarti, A.M., J.Y. Lapointe. Determination of NH_4^+/NH_3 fluxes across the apical membrane of macula densa cells : a quantitative analysis. *Am. J. Physiol.* (in press)

26. Lapointe, J.Y., P.D. Bell, J. Cardinal. Direct evidence for apical Na^+:2Cl^- :K^+ cotransport in macula densa cells. *Am. J. Physiol.* 258(5 Pt 2): F1466-1469, 1990.

27. Lapointe, J.Y., P.D. Bell, A.M. Hurst, J. Cardinal. Basolateral ionic permeabilities of macula densa cells. *Am. J. Physiol.* 260(6 Pt 2):F856-60, 1991.

28. Lapointe, JY., M.A. Laamarti, A.M. Hurst, B.C. Fowler, P.D. Bell. Activation of Na:2Cl:K cotransport by luminal chloride in macula densa cells. *Kidney Int.* 47(3):752-7, 1995.

29. Leung, S., M.E. O'Donnell, A. Martinez, H.C. Palfrey. Regulation by nerve growth factor and protein phosphorylation of Na:K:2Cl cotransport and cell volume in PC12 cells. *J. Biol. Chem.* 269:10581-9, 1994.

30. Lytle, C., J.C. Xu, D. Biemesderfer, B. Forbush 3rd. Distribution and diversity of Na-K-Cl cotransport proteins: a study with monoclonal antibodies. *Am. J. Physiol.* 269(6 Pt 1):C1496-505, 1995.

31. Obermuller, N., S. Kunchaparty, D.H. Ellison, S. Bachmann. Expression of the Na-K-2Cl cotransporter by macula densa and thick ascending limb cells of rat and rabbit nephron. *J. of Clin. Invest.* 98(3):635-40, 1996.

32. O'Grady, S.M., H.C. Palfrey, M. Field. Characteristics and functions of Na-K-Cl cotransport in epithelial tissues. *Am. J. Physiol.* 253, (Cell Physiol. 22): C177-C192, 1987.

33. Paulais, M., J. Teulon. cAMP-activated chloride channel in the basolateral membrane of the thick ascending limb of the mouse kidney. *J. Membr. Biol.* 113(3):253-60, 1990.

34. Payne, J.A., B. Forbush 3rd. Alternatively spliced isoforms of the putative renal Na-K-Cl cotransporter are differentially distributed within the rabbit kidney. *Proc. Natl. Acad. Sci.* USA 91(10):4544-8, 1994.

35. Payne, JA., J.C. Xu, M. Haas, C.Y. Lytle, D. Ward, B. Forbush 3rd. Primary structure, functional expression, and chromosomal localization of the bumetanide-sensitive Na-K-Cl cotransporter in human colon. *J. Biol. Chem.* 270(30):17977-85, 1995.

36. Raat, N.J.H., A. Hartog, C.H. Van Os, R.J.M. Bindels. Regulation of Na^+-K^+-$2Cl^-$ cotransport activity in rabbit proximal tubule in primary culture. *Am. J. Physiol.* 267, (Renal Fluid Electrolyte Physiol. 36): F63-F69, 1994.

37. Reeves, W.B., T.A. Andreoli. Sodium chloride transport in the loop of Henle. In: The Kidney: Physiology and Pathophysiology. chap. 54, pp1975-2001, ed. D.W. Seldin & G. Giebish, Raven Press, New York, 1992.

38. Schlatter, E., R. Greger. cAMP increases the basolateral Cl^-conductance in the isolated perfused medullary thick ascending limb of Henle's loop of the mouse. . *Pflügers Arch.*. 405: 367-376, 1985.

39. Schlatter, E., M. Salomonsson, A.E. Persson, R. Greger. Macula densa cells sense luminal NaCl concentration via furosemide sensitive Na+2Cl-K+ cotransport. . *Pflügers Arch.*. 414(3):286-90, 1989.

40. Schnermann, J. Effect of adenosine analogues on tubuloglomerular feedback responses. *Am. J. Physiol.* 255: F33-F42, 1988.

41. Schnermann, J., J.P. Briggs. The juxtaglomerular apparatus. In: The Kidney: Physiology and Pathophysiology. chap. 35, pp1249-1289, ed. D.W. Seldin & G. Giebish, Raven Press, New York, 1992.

42. Thomas, JA., R.N. Buchsbaum, A. Fimniak, and S. Racker. Intracellular pH measurements in Ehrlich ascites tumor cells utilizing spectroscopic probes generated in situ. *Biochem. J.* 18: 2210-2218, 1979.

43. Vuillemin, T., J. Teulon, M. Geniteau-Legendre, B. Baudoin, S. Estrade, R. Cassingena, P. Ronco, A. Vandewalle. Regulation by calcitonin of Na(+)-K(+)-Cl(-) cotransport in a rabbit thick ascending limb cell line. *Am. J. of Physiol.*263 (3 Pt 1):C563-72, 1992.

44. Wilcox, C.S., W.J. Welch, F. Murad, S.S. Gross, G. Taylor, R. Levi, H.H.H.W. Schmidt. Nitric oxide synthase in macula densa regulates glomerular capillary pressure. *Proc. Natl. Acad. Sci.* USA. 89(24):11993-7, 1992.

45. Wright, F.S., J.P. Briggs. Feedback control of glomerular blood flow, pressure, and filtration rate. *Physiol. Rev.* 59(4):958-1006, 1979.

46. Xu, J.C., C. Lytle, T.T. Zhu, J.A. Payne, E. Benz Jr., B. Forbush 3rd. Molecular cloning and functional expression of the bumetanide-sensitive Na-K-Cl cotransporter. *Proc. Natl. Acad. Sci.* USA. 91(6):2201-5, 1994.

47. Yang ,T, Y.G. Huang, I. Singh, J. Schnermann, J.P. Briggs. Localization of bumetanide- and thiazide-sensitive Na-K-Cl cotransporters along the rat nephron. *Am. J. of Physiol.*271(4 Pt 2):F931-9, 1996.

48. Zimniak, L., C.J. Winters, W.B. Reeves, T.A. Andreoli. Cl-channels in basolateral renal medullary vesicles XI. rbClC-Ka cDNA encodes basolateral MTAL Cl-channels. *Am. J. of Physiol.* 270(6 Pt 2):F1066-72, 1996.

49. Zou, A.P., J.D. Imig, P.R. Ortiz de Montellano, Z. Sui, J.R. Falck, R.J. Roman. Effect of P-450 omega-hydroxylase metabolites of arachidonic acid on tubuloglomerular feedback. Am. J. Physiol. 266(6 Pt 2):F934-41, 1994.

FIGURE LEGENDS

Figure 1 Example of the NH_4^+-induced acidification in the presence of Ba^{2+}. In the presence of 25 mM NaCl in the lumen (and 1 mM amiloride), addition of 20 mM NH_4^+ produced a cell acidification at an initial rate of 0.031 pH units.s^{-1}. In contrast, with of 5 μM bumetanide (0 mM Na^+, 25 mM Cl^-), NH_4^+ induced acidification was reduced to 0.007 pH unit.s^{-1}. The dotted line represent exponential fits used to extrapolate initial acidification rate.

Figure 2 Activation of the Na^+K^+:$2Cl^-$ apical cotransporter by luminal Cl^- in the presence of 25 mM Na^+, 5 mM K^+ and 20 mM NH_4^+. Cl^- affinity constant was calculated to be 17 ± 4 mM and Cl^- -independent acidification rate represents 18.5 ± 6.4 % of the maximal rate.

Figure 3 Activation of the Na^+:K^+:$2Cl^-$ apical cotransporter by luminal Na^+ in the presence of 25 mM Cl^-, 5 mM K^+, 20 mM NH_4^+ and 1 mM amiloride. Na^+ affinity constant was calculated to be 1.0 ± 0.3 mM and Na^+-independent acidification rate represents 22.5 ± 6.0 % of the maximal rate.

Figure 4 Effect of basolateral Cl^- channel inhibition by 10 μM NPPB on apical Na^+:K^+:2Cl^- cotransporter activity. Estimation of the cotransporter activity was performed in the presence of either saturating Na^+ and Cl^- luminal concentration (25 mM Na^+ and 60 mM Cl^-) or non-saturating conditions (1mM Na^+ and 5 mM Cl^-).

Figure 5 Effect of 0.1 mM dbcAMP + 1 μM forskolin on the apical Na^+:K^+:2Cl^- cotransporter activity. Estimation of the cotransporter activity was performed in the presence of either saturating Na^+ and Cl^- luminal concentration (25 mM Na^+ and 60 mM Cl^-) or non-saturating conditions (1mM Na^+ and 5 mM Cl^-). dbcAMP + forskolin stimulated significantly ($p<0.05$, $n=11$) the apical cotransporter in the presence of saturating Na^+/Cl^- conditions but failed to produce any significant effect at low Na^+/Cl^- concentrations.

Figure 6 Effect of 0.1 mM dbcAMP + 1 μM forskolin on the apical Na^+:K^+:2Cl^- cotransporter mediated NH_4^+ acidification rate in the presence of 10 μM basolateral NPPB to block Cl^- channels. With saturating or low luminal Na^+/Cl^- concentrations, dbcAMP + forskolin succeeded in significantly inhibiting the apical cotransporter by 17.1 % ($p<0.05$, $n=5$) and by 16.6 % ($p<0.002$, $n=5$), respectively.

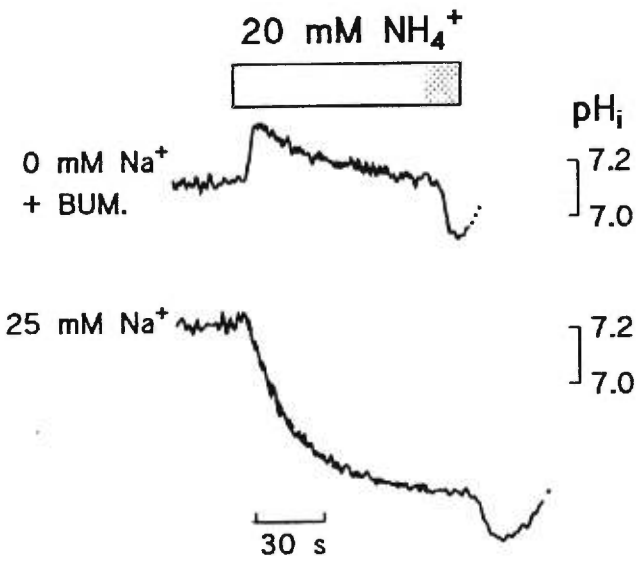
20 mM NH_4^+
pH_i
0 mM Na^+
+ BUM.
7.2
7.0
25 mM Na^+
7.2
7.0
30 s

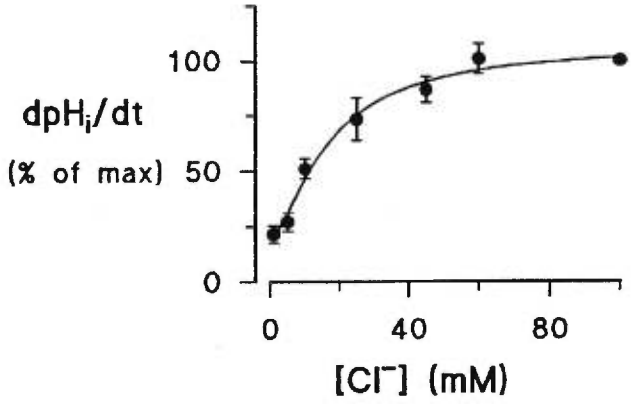
100
dpH$_i$/dt
(% of max) 50
0
0
40
80
[Cl$^-$] (mM)

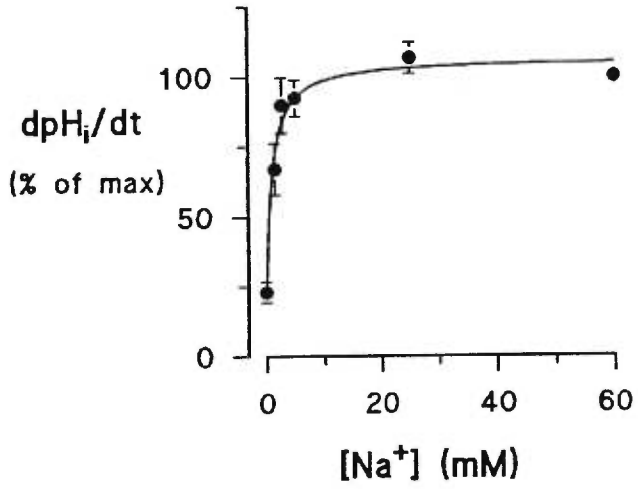
dpH$_i$/dt
(% of max)
100
50
0
0
20
40
60
[Na$^+$] (mM)

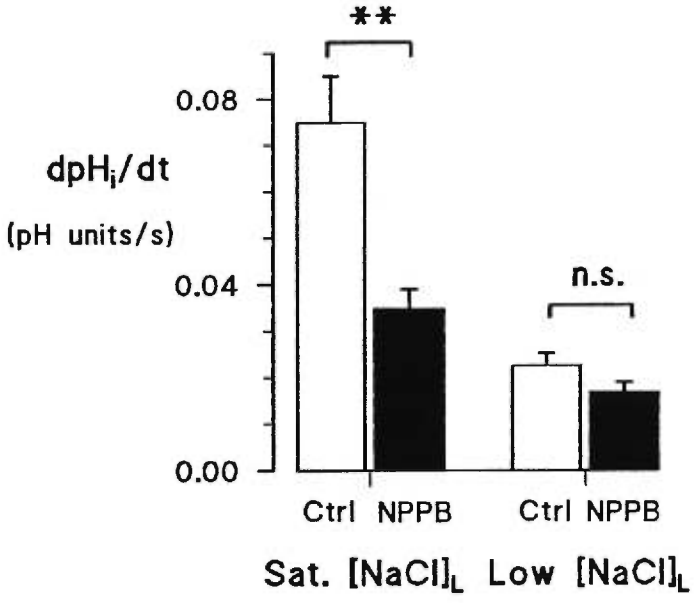
**
0.08
dpH$_i$/dt
(pH units/s)
0.04
n.s.
0.00
Ctrl NPPB
Ctrl NPPB
Sat. [NaCl]$_L$ Low [NaCl]$_L$

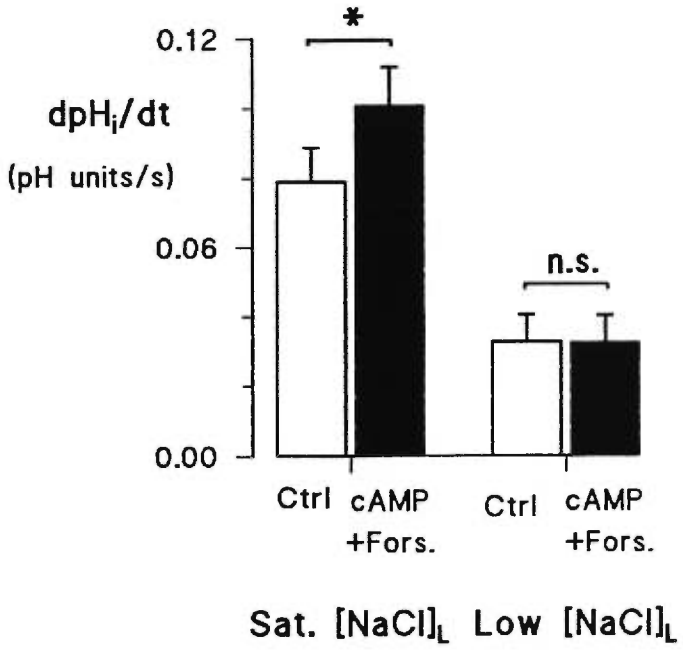
*
0.12
dpH$_i$/dt
(pH units/s)
0.06
n.s.
0.00
Ctrl
cAMP
+Fors.
Ctrl
cAMP
+Fors.
Sat. [NaCl]$_L$
Low [NaCl]$_L$

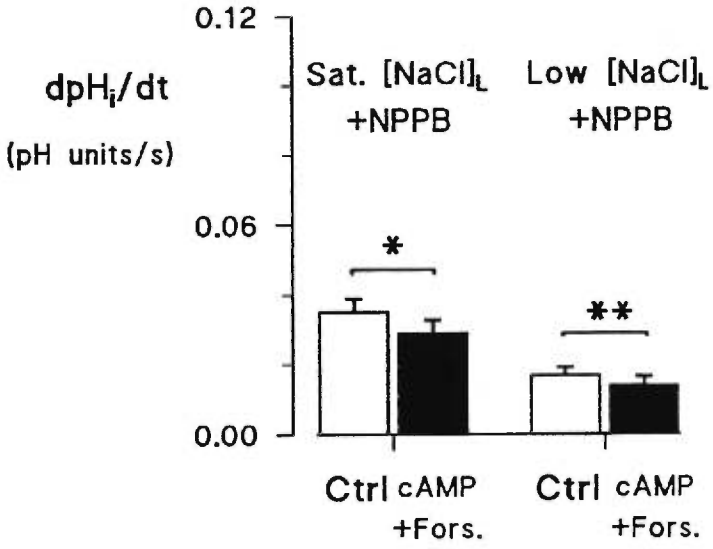
0.12
0.06
0.00
dpH$_i$/dt
(pH units/s)
Sat. [NaCl]$_L$
+NPPB
Low [NaCl]$_L$
+NPPB
*
**
Ctrl
cAMP
+Fors.
Ctrl
cAMP
+Fors.

C. DISCUSSION

DISCUSSION

La transmission du signal de la RTG implique la détection d'un changement dans la composition du liquide tubulaire par les cellules de la MD et le transfert d'un signal, probablement à travers des cellules mésangiales, vers les cellules musculaires lisses de l'AA. D'après ce schéma on comprend que les cellules de la MD jouent un rôle central dans le mécanisme de la RTG en se chargeant du rôle de détection et d'initiateur du signal. Il y a présentement un assez large consensus sur le fait que l'entrée de NaCl dans les cellules de la MD par le cotransporteur $Na^+:K^+:2Cl^-$ est l'étape initiale du signal de la RTG. Cependant, il n'existe à ce jour aucune preuve solide à ce sujet puisqu'en microponction in vivo, qu'elle soit ortho- ou rétrograde, toute solution luminale affecte également les cellules de la MD et les cellules de l'anse de Henle. Une meilleure définition quantitative des propriétés propres à ces deux types cellulaires permettra éventuellement d'attribuer avec plus de certitude un effet donné à un type cellulaire particulier. Une meilleure connaissance des perméabilités membranaires des cellules de la MD serait d'un grand secours pour progresser dans la compréhension de la RTG. Dans le présent travail nous avons présenté les résultats obtenus sur trois transporteurs (canal K^+, échangeur $Na^+:H^+$ et cotransporteur $Na^+:K^+:2Cl^-$), deux d'entre eux sont nouvellement identifiés dans la membrane apicale. Ces résultats sur la MD permettent de

comparer les caractéristiques de ces transporteurs avec les propriétés reportées pour ces même transporteurs dans la TAL, de spéculer sur leur implication dans le transport transépithélial et de discuter leur rôle possible dans la transmission du signal de la RTG. Dans notre discussion nous allons aborder dans un premier temps la comparaison de ces transporteurs entre la MD et la TAL et, dans un deuxième temps, nous allons spéculer sur la séquence d'événements susceptibles de suivre une augmentation de $[NaCl]_l$ grâce à notre nouvelle connaissance des propriétés des cellules de la MD.

I. COMPARAISON DES MÉCANISMES DE TRANSPORT IONIQUE DE LA MD ET L'ANSE LARGE ASCENDANTE

1. Canal K^+

L'anse large ascendante, relativement peu perméable à l'eau, est le siège d'une intense réabsorption de solutés. La séparation de l'eau et des solutés qui en résulte, a pour conséquence la diminution de la pression osmotique du fluide intratubulaire et l'augmentation de celle-ci dans le fluide péri-tubulaire, surtout médullaire. Au niveau de la membrane apicale les canaux K^+ sont responsables du recyclage du K^+ (46). Ce recyclage assure un approvisionnement continu en K^+ de la lumière tubulaire, essentiel pour un bon

fonctionnement du cotransporteur apical Na^+ :K^+ :2Cl^- et par conséquent de la réabsorption active de NaCl dans la TAL, et crée un potentiel positif dans la lumière favorisant ainsi la réabsorption par la voie paracellulaire. L'inhibition du recyclage de K^+ par perfusion de la lumière avec du barium entraîne d'ailleurs une inhibition du transport net de Na^+ (46). Il apparaît donc que dans la TAL, la conductance K^+ joue un rôle essentiel dans le transport transépithélial. Au niveau de la MD, la concentration de K^+ se trouve déjà fixée par la TAL, et on pense que les canaux K^+ apicaux sont plutôt impliqués dans le contrôle du potentiel membranaire et de ses effets sur l'efflux de Cl^- à travers le canal Cl^- basolatéral (13,83).

Dans les cellules de la MD, nous avons présenté les résultats d'un seul type de canal K^+, celui de 41 pS. Toutefois, un autre canal de faible conductance a été souvent observé (observations non publiées). Dans les cellules de la TAL, trois types de canaux K^+ ont été identifiés dans la membrane apicale : un canal à faible conductance (30 pS) chez le lapin et le rat, un canal à conductance intermédiaire (60-70 pS) uniquement chez le rat et un canal à forte conductance (100-200 pS) dans les cellules en culture de mTAL de lapin (17,47,166). Plusieurs propriétés biophysiques du canal K^+ des cellules de la MD, telles que l'indépendance de la probabilité d'ouverture vis-à-vis le voltage, la forte probabilité d'ouverture et la sensibilité au pH, sont similaire à celles du canal K^+ à faible conductance de la membrane apicale des

apicale des cellules de la TAL. Wang et Giebisch (167) et McNicholas et coll. (95) ont montré que le canal K_{ATP} des cellules principales du tubule collecteur peut être inhibé de façon réversible par le MgATP, alors qu'il est peu affecté par l'ATP. En se basant sur ces résultats, le Dr S. Hebert (53a) a critiqué nos résultats sur l'insensibilité du canal K^+ à l'ATP puisque nous avions utilisé du NaATP au lieu du MgATP. Nous avons fort apprécié ses commentaires, et très récemment nous avons testé le MgATP sur l'activité du canal K^+. Les expériences préliminaires ont montré que, comme le NaATP le MgATP n'a aucun effet sur le canal K^+ des cellules de la MD. Toutefois, il n'est pas impossible que ce canal K^+ soit le ROMK, d'autant plus que, la présence du ROMK aurait été détectée dans les cellules de la MD (S. Hebert, communication personelle).

Le canal K^+ des cellules de la MD et le canal K^+ de 70 pS de la membrane apicale des cellules de la TAL se comportent de la même façon vis-à-vis du Ca^{2+} intracellulaire (une inhibition à $[Ca^{2+}]$ élevée) (56). Cet effet du Ca^{2+} peut être médié par la PKC puisque la PKC inhibe le canal de 70 pS de la membrane apicale des cellules de la TAL (169). En outre, ce canal K^+ de 70 pS peut aussi être inhibé par l'acide arachidonique (168). Cet effet est médié par le 20-HETE, le métabolite majeur de la voie du cytochrome P450 dans la TAL (27). De même, la perfusion de la TAL avec le 20-HETE restore la RTG après bloquage du métabolisme endogène du cytochrome P450 (180). Il serait donc

intéressant dans le futur, de rechercher l'effet du 20-HETE sur l'activité du canal K^+ de la membrane apicale des cellules de la MD et l'implication de ce dernier dans la RTG.

2. Échangeur Na^+:H^+

Les mesures de pH intracellulaire avec la sonde fluorescente BCECF ont prouvé l'existence d'un échangeur Na^+:H^+ dans la membrane apicale des cellules de la MD. L'échangeur Na^+:H^+ a été identifié dans les membranes apicale et basolatérale de différents types de cellules épithéliales. L'échangeur Na^+:H^+ basolatéral a été identifié comme l'isoforme NHE-1, une isoforme sensible à l'amiloride et impliqué dans la régulation du pH_i et du volume cellulaire (22). On croit que l'isoforme NHE-3 présente exclusivement dans le rein et l'intestin est responsable de l'échange Na^+:H^+ apical. Elle est relativement résistante à l'amiloride et elle intervient dans la réabsorption de NaCl et de $NaHCO_3$ (22,111,101,15). Dans les cellules de la MD, l'échangeur Na^+:H^+ s'est avéré plutôt résistant à l'amiloride puisqu'une forte concentration de cette drogue (1mM) ne réduit que de 36% l'alcalinisation due à 150 mM de Na^+ dans la lumière. Dans la mTAL, 0.5 mM d'amiloride inhibe, en présence d'une concentration symétrique de 140 mM de NaCl, 80 à 90% de l'activité de l'échangeur Na^+:H^+ apical et basolatéral. Cette sensibilité vis-à-vis de

l'amiloride montre que l'échangeur $Na^+:H^+$ apical de la MD est probablement différent de l'échangeur de la mTAL.

3. Cotransporteur $Na^+:K^+:2Cl^-$

Le transport de Na^+ et de Cl^- par la TAL correspond à 25 % de la réabsorption rénale de NaCl et contribue à l'hypertonicité interstitielle de la médullaire qui est un élément du mécanisme de concentration des urines. Chez la MD, le transport de NaCl est probablement le facteur détecté pour la génération de la RTG qui contrôle le taux de filtration glomérulaire (GFR). Le transport transépithélial de Na^+ et de Cl^- est assuré par le cotransporteur $Na^+:K^+:2Cl^-$ qui opère en conjonction avec la pompe à Na^+, le canal K^+ et le canal Cl^- (132). Récemment, la protéine correspondante au cotransporteur $Na^+:K^+:2Cl^-$ (rBSC1 ou NKCC2) a été clonée chez le lapin (118), le rat (35), la souris (57) et l'homme (119). Chez le rat, la souris et le lapin, l'isoforme NKCC2 est localisée dans la membrane apicale de mTAL et cTAL (69,89,114). Dans le cas de la MD, l'utilisation de l'anticorps anti-NKCC2 n'a pas permis de déceler de signal significatif dans ces cellules (69). Plus récemment, le même groupe, cependant, a montré qu'un prétraitement du tissue rénal aux micro-ondes (cité dans114) ou au SDS (70) démasque l'immunoréactivité du NKCC2 au niveau de la membrane apicale des cellules

de la MD. Un autre groupe a montré chez le rat un taux d'expression similaire de ARNm du NKCC2 dans la TAL et la MD; chez le lapin l'expression est significativement plus intense dans la MD comparativement à la TAL (114).

La méthode de détermination de flux ioniques en utilisant le NH_4^+ fonctionne bien pour les cellules de la MD et tout particulièrement pour le cotransporteur Na^+:K^+:$2Cl^-$ qui représente 65% du flux apical total tandis qu'en présence de 5 mM de barium c'est 93% du flux qui passe par le cotransporteur. Cette technique donne un Km_{Cl} de 17 mM (81), qui est 3 fois plus petit que celui mesuré par Greger (45) dans la cTAL de lapin, et du même ordre de grandeur que celui mesuré dans les vésicules membranaires de la mTAL de lapin par Koenig et coll. (78). Une autre étude réalisée sur des vésicules membranaires préparées à partir de la médulla externe de lapin (25) a montré que l'accumulation maximale de Rb^+ se produit à des concentrations de Cl^- de moins de 50 mM, ce qui est en accord avec les résultats de Koenig et coll. (78). Pour ce qui est de l'affinité du cotransporteur pour le Na^+, nous avons mesuré un Km_{Na} de 1mM (81), valeur qui est plus faible que celle mesurée dans la cTAL (2-3 mM) (46) et dans les cellules de la mTAL en culture (7 mM) (68). D'une manière générale le cotransporteur Na^+ :K^+ :$2Cl^-$ des cellules de la MD présente une affinité élevée pour le Na^+ et le Cl^- comparativement à celles de la TAL. Cette différence de Km peut être due tout simplement à des techniques différentes, alors qu'il s'agit d'un même transporteur (BSC1) comme l'ont

indiqué les études de biologie moléculaire (114,179). Il peut aussi s'agir de deux isoformes de la même protéine (118,179).

Nous avons observé que l'AMPc augmente le taux d'acidification par le NH_4^+. Cette activation du cotransporteur par l'AMPc peut résulter soit d'un effet direct à travers la PKA, soit d'un effet indirect à travers l'activation de canal Cl^- basolatéral (50). On pense que cette deuxième possibilité est la plus plausible pour les cellules de la MD, car le bloquage du canal Cl^- inhibe complètement la réponse à l'AMPc. Dans la TAL, il est bien établi que l'hormone antidiurétique (ADH) stimule le transport de NaCl. Schlatter et Greger (131) ont proposé un effet direct de l'AMPc sur le canal Cl^- basolatéral. A l'appui de leur proposition, Schlatter et Greger démontraient que l'AMPc et l'ADH provoquaient une baisse de la résistance fractionnelle de la membrane basolatérale des cellules de la mTAL de souris, et ceci même lorsque $[Cl^-]_i$ est rendue faible par un bloquage de l'entrée de Cl^- à l'aide de furosémide (131). De même, Paulais et Teulon (117), en utilisant la technique de patch clamp, ont observé que la préincubation de segments de cTAL de souris avec la forskoline ou des analogues d'AMPc augmentent le nombre de canaux Cl^- dans les patch de membrane basolatérale.

II. ESTIMATION DES CONCENTRATIONS IONIQUES INTRACELLULAIRES

A l'aide des mesures de pH_i, nous avons montré, d'une part, qu'il est possible de déterminer l'activité du cotransporteur $Na^+ :K^+ :2Cl^-$, et d'autre part, nous avons mis en évidence l'échangeur $Na^+ :H^+$ apical. Puisque ces deux transporteurs constituent les principales voies de transport apical de NaCl dans les cellules de la MD, tout changement de $[NaCl]_l$ se traduira par un changement de leur activité et par conséquent des concentrations ioniques intracellulaires. Nous pouvons donc estimer ces changements en nous plaçant dans différentes situations, par exemple dans les conditions où le cotransporteur ou l'échangeur sont en équilibre.

Dans le premier cas, en comparant à $[Na^+]$ constante les pH_i atteint à différentes $[Cl^-]_l$ aux pH_i obtenus lorsque le cotransporteur est bloqué, nous avons démontré qu'en présence de 20 mM de Na^+ et de 5 mM de K^+ dans la lumière tubulaire, le cotransporteur s'équilibrait à 14 mM $[Cl^-]_l$ (84). En présence de furosémide, Schlatter (133) a trouvé à l'aide d'expériences de patch clamp en configuration "whole cell" un potentiel intracellulaire de -82 mV. Dans ces conditions où le cotransporteur est inhibé on présume que $[Cl^-]_i$ doit tomber à l'équilibre, alors Vm de -82 mV doit être près du potentiel

d'équilibre de K^+ et de celui de Cl^-. On estime ainsi $[K^+]_i$ autour de 80 mM et $[Cl^-]_i$ de 7 mM. On estime aussi $[Na^+]_i$ égale à 6 mM.

En présence de 20 mM de Na^+ et 140 mM de Cl^- dans la lumière, le pH_i est relativement acide, 6.81, et l'addition de 1 mM d'amiloride ne change pas le pH_i, qui reste au même niveau (6.84). Le fait que l'échangeur $Na^+:H^+$ ne réussisse pas à faire sortir les protons malgré un gradient de H^+ favorable (pH_e 7.40, pH_i 6.84) suggère que celui-ci est en équilibre. Pour atteindre cet équilibre le Na^+ intracellulaire doit monter à une valeur autour de 70 mM afin de contrebalancer le gradient de protons.

En absence d'un cotransporteur fonctionnel (furosémide) lorsque la $[NaCl]_l$ est de 25 mM, l'échangeur $Na^+:H^+$ réussit à faire sortir les protons comme en témoigne l'acidification par 1 mM d'amiloride [fig. 5 (32)] Dans cette situation où le gradient de proton est absent (pH_e 7.40 et pH_i 7.40), la $[Na^+]_i$ doit être inférieure à 25 mM.

Il apparaît donc clair que le signal de la RTG détecté par les cellules de la MD provoque un grand changement du contenu ionique intracellulaire. Nous avons vu que, à faible $[NaCl]_l$ ou lorsque le cotransporteur est inhibé, $[Cl^-]$ et $[Na^+]$ intracellulaires sont faibles : 7 mM et 6 mM, respectivement. Le pH_i est relativement élevé (7.4) alors que le Ca^{2+} intracellulaire est maintenu bas par l'échangeur $Na^+:Ca^{2+}$ basolatéral. Lorsque $[NaCl]_l$ augmente, le cotransporteur s'active, $[Na^+]$ et $[Cl^-]$ intracellulaires augmentent et peuvent atteindre des

valeurs assez élevées. L'augmentation de $[Na^+]_i$ réduit l'activité de l'échangeur $Na^+:Ca^{2+}$ et favorise l'augmentation du Ca^{2+} cytosolique.

III. AMPLITUDE DU TRANSPORT IONIQUE CHEZ LES CELLULES DE LA MACULA DENSA

Contrairement à la plupart des cellules animales, l'addition de NH_4^+ dans la lumière produisait dans les cellules de la MD une acidification cellulaire similaire à celle observée dans la mTAL (73,74,170). Dépendamment du pouvoir tampon, le taux de production de protons après addition de NH_4^+ varie d'une espèce à l'autre: il est de 5 $mM.s^{-1}$ dans les cellules de la MD chez le lapin, 1.4 $mM.s^{-1}$ dans la mTAL de souris (74) et 15.7 $mM.s^{-1}$ dans la mTAL de rat (170). A cause de la faible densité de la $Na^+:K^+$-ATPase dans la membrane basolatérale des cellules de la MD (143,71,5), on s'attendait à ce que ces cellules aient une capacité de transport limitée par rapport à celles de la TAL. Or, il est bien évident d'après les valeurs mentionnées ci-dessus que le taux de production de protons dans les cellules de la MD est loin d'être 40 fois plus faible que celui dans la TAL.

La $Na^+:K^+$-ATPase a été mesurée par unité de volume cellulaire, or le cytoplasme des cellules de la MD est très petit comparativement à celui des

cellules de la TAL (4). Il y a donc vraisemblablement une sous-estimation de la densité de l'enzyme dans la MD. Récemment, Obermuller et coll. (114) ont démontré chez le lapin que l'intensité d'expression d'ARNm du cotransporteur dans la MD est plus élevée que dans la TAL. Cette expression élevée peut refléter une synthèse élevée du cotransporteur dans la MD par rapport à la TAL et peut être reliée à une activité de transport élevée.

IV. INTERPRÉTATION DES FLUX DE NH_4^+ ET NH_3

L'acidification produite par le NH_4^+ a été interprétée dans le cas de la TAL par une imperméabilité de la membrane apicale au NH_3 (73). Cependant, la perméabilité au NH_3 de la membrane apicale de la mTAL de rat est similaire à la perméabilité au NH_3 mesurée pour d'autres cellules telles que les MDCK (36a) et les erythrocytes humain (77a). Ainsi, il a été suggéré que la caractéristique de la membrane apicale qui permet de la distinguer des autres membranes cellulaires et qui justifie la prédominance de l'entrée de NH_4^+ sur l'entrée de NH_3, est la présence de transporteurs favorisant l'entrée rapide de NH_4^+ et non pas l'absence de perméabilité au NH_3. Il est donc clair que l'entrée de NH_4^+ à travers la membrane apicale est associée à une acidification. Cependant, le mécanisme de cette acidification n'est pas clairement défini. Tel qu'il a été mentionné par Watt et Good, à pH_i 7.4, seulement 1/40 de NH_4^+ se

dissocie pour libérer un H^+ dans la cellule ; vu le pouvoir tampon qui est de 70 mM/unité de pH (80), il en résulterait une faible acidification. Ainsi, l'entrée de NH_4^+ ne peut à elle seule expliquer la grande acidification observée. D'autres mécanismes, en plus de l'entrée de NH_4^+, sont donc impliqués dans cette acidification. Le modèle que nous avons présenté montre que cette acidification provient du fait que la réaction de dissociation intracellulaire est maintenue légèrement hors de l'équilibre, soit parce que le NH_3 intracellulaire est maintenu inférieur au NH_3 luminal suite à une fuite continuelle à travers la membrane basolatérale, soit parce que le NH_4^+ intracellulaire est maintenu au dessus de sa concentration luminale par le fait que le NH_4^+ profite du gradient d'autres ions cotransportés ou utilise le potentiel intracellulaire négatif.

Ce modèle prédit une rapide alcalinisation initiale au moment de présenter le NH_4^+ dans la lumière, phénomène qui a été régulièrement observé même si dans certains cas cet effet se perd dans le bruit de la mesure. Nous avons trouvé que le transport de NH_4^+ n'est pas égal, mais 2 à 3 fois supérieures au taux de production de protons. De plus, loin de prétendre que la membrane apicale est imperméable au NH_3, l'ajustement des courbes expérimentales avec les prédictions du modèle nécessite une perméabilité apicale au NH_3 30 fois plus grande que la perméabilité apicale à l'entrée de NH_4^+ (80).

V. VOIES DE TRANSPORT DU NH_4^+

Une des voies utilisées par le NH_4^+ pour induire une acidification intracellulaire est vraisemblablement le cotransport $Na^+ :K^+(NH_4^+) :2Cl^-$. Nous avons trouvé que le bumétanide réduit de 57 % la vitesse initiale d'acidification due à l'addition de NH_4^+. Ceci est en accord avec des travaux récents qui ont montré que le transport actif de NH_4^+ dans la TAL s'effectue via la substitution du K^+ par le NH_4^+ dans le cotransporteur apical $Na^+ :K^+ :2Cl^-$ (42). Premièrement, Kinne et coll. (75) ont démontré que dans les vésicules de membrane apicale préparée à partir de TAL de lapin, le NH_4^+ entrait en compétition vis-à-vis du même site de liaison au niveau du cotransporteur $Na^+ :K^+ :2Cl^-$, et qu'en absence de K^+, le transport de Na^+ est maintenu en présence d'un gradient de NH_4^+. Deuxièmement, Good (41,40) a montré que dans la mTAL de rat, la réabsorption de NH_4^+ peut être inhibée par de fortes $[K^+]_l$, ce qui indique que le K^+ et le NH_4^+ sont en compétition pour un même transporteur. Finalement, dans la mTAL de souris, le furosémide inhibe partiellement l'acidification intracellulaire provoquée par l'addition de NH_4^+ (73). Le NH_4^+ peut aussi entrer dans les cellules de la MD par une autre voie sensible au barium. Dans la mTAL de souris cette voie était attribuée au canal K^+ (apical et/ou basolatéral). Toutefois, des études récentes de patch clamp sur la TAL de rat (16,17) ont montré que le canal K^+ est imperméable au NH_4^+.

Lorsque nous avons bloqué le canal K^+ apical des cellules de la MD en augmentant le calcium intracellulaire à l'aide de 1 μM d'ionomycine nous n'avons pas enregistré d'inhibition de l'acidification suite à l'addition de NH_4^+, ce qui écarte toute possibilité de transport de NH_4^+ par le canal K^+ que nous avons observé en patch clamp. Éventuellement, le NH_4^+ pourrait être transporté par une autre classe de canaux K^+. Cependant, l'acidification produite par le barium n'est pas en faveur de l'intervention de canaux K^+. Récemment, dans la mTAL de rat, cette voie de transport de NH_4^+ sensible au barium était attribuée à l'échangeur K^+:H^+(NH_4^+), sensible au vérapamil (1). Ceci n'est pas le cas dans les cellules de la MD, car d'une part le vérapamil n'a eu aucun effet sur l'acidification au NH_4^+, et d'autre part l'acidification induite par le barium écarte tout effet direct sur l'échangeur K^+:H^+ dans les cellules de la MD. La nature exacte de cette voie de transport de NH_4^+ sensible au barium n'a pu être déterminée dans ce travail. Toutefois, il est intéressant de souligner que ce transporteur est responsable de l'efflux de H^+ sensible au barium et qu'il transporte NH_4^+ vers le milieu intracellulaire.

VI. IMPLICATIONS PHYSIOLOGIQUES DES NOUVELLES DONNÉES PRÉSENTÉES DANS CETTE THÈSE

1) Canal K^+ : Ce n'était pas vraiment une surprise de voir un canal K^+ dans la membrane apicale des cellules de la MD puisque c'est aussi le cas pour la TAL et le tubule collecteur. La surprise a été de voir la forte densité de ces canaux. Alors que dans la très grande majorité des épithélia le potentiel membranaire est contrôlé par des canaux K^+ basolatéraux, ça pourrait être l'inverse chez les cellules MD. Cette hypothèse est d'ailleurs fortement supportée par le fait que la conductance potassique basolatérale est relativement faible (83). En étant responsable de l'établissement du potentiel membranaire négatif, les canaux potassiques apicaux que nous avons décrits contrôleraient un paramètre crucial dans la RTG: la concentration du Cl^- intracellulaire. En effet, la force motrice qui permet la sortie basolatérale du Cl^- contre son gradient chimique (~20 mM $[Cl^-]_i$ vs 150 mM $[Cl^-]_e$) est le potentiel membranaire négatif. Par exemple, une baisse de l'activité des canaux potassiques entraînerait une dépolarisation membranaire et une accumulation de Cl^- intracellulaire. On s'attendrait alors à une baisse de sensibilité au $[NaCl]_l$ lors du déclenchement de la RTG puisque le cotransporteur apical $Na^+:K^+:2Cl^-$ est moins actif en présence d'une $[Cl^+]_i$ élevée (81).

2) Échangeur $Na^+:H^+$: Le pH_i joue un rôle important non seulement dans la régulation des perméabilités membranaires mais aussi dans la signalisation intracellulaire. L'échangeur $Na^+:H^+$ est généralement considéré comme le principal régulateur du pH_i chez la plupart des cellules épithéliales. La présence de l'échangeur $Na^+:H^+$ dans la membrane apicale des cellules de la MD est particulièrement importante puisqu'il permet donc de relier directement le pH_i des cellules MD à la concentration luminale de Na^+ tel que nous l'avons démontré dans le troisième article. Donc la découverte de l'existence d'un échangeur $Na^+:H^+$ apical suffisament puissant pour faire changer le pH_i des cellules MD de 7.22 à faible $[Na^+]_l$ à 7.39 à fort $[Na^+]_l$ nous a permis d'identifier un des effets secondaires possiblement important lorsque la $[NaCl]_l$ augmente et déclenche la RTG.

3) Mesure de l'activité du cotransporteur $Na^+:K^+:2Cl^-$ grâce à l'utilisation du NH_4^+: Les deux articles réalisés avec cette méthode ont d'importantes retombées physiologiques. a) On remet en doute le vieux concept qui date de 1980 et selon lequel les cellules de la MD ont un faible taux de transport transépithélial. b) Par la méthode du NH_4^+/NH_3 on peut détecter le transport du $Na^+:(NH_4^+):2Cl^-$ qui est le signal initial de la RTG. c) Par la mesure des affinités, on explique que le signal détecté sera le $[Cl^-]_l$ puisque le Na^+ luminal devrait toujours être saturant. d) L'effet inhibiteur de l'AMPc sur le cotransporteur permet d'interpréter l'ancienne étude de microponction in vivo

(9a) qui avait démontrée une inhibition de la RTG par l'AMPc + forskoline. e) L'inhibition de l'activité du cotransporteur par une augmentation de $[Cl^-]_i$ permet de suggérer que toutes les manœuvres qui affectent l'efflux basolatéral du Cl^- devraient altérer l'activité du cotransporteur à travers le changement de $[Cl^-]_i$ et par conséquent influencer la RTG.

VII. RECONSTITUTION DES ÉVÉNEMENTS INITIAUX DE LA RÉTROACTION TUBULOGLOMÉRULAIRE

La réponse des cellules de la MD aux changements de $[NaCl]_l$ est complexe et implique divers processus cellulaires. En effet, lorsqu'on augmente $[NaCl]_l$ à 140 mM, on stimule le cotransporteur $Na^+:K^+:2Cl^-$ ainsi que l'échangeur $Na^+:H^+$ apical. Ces événements initiaux vont entraîner une première série de conséquences directes: une augmentation de $[Na^+]_i$, de $[Cl^-]_i$ et une augmentation du pH_i (Figure 5). Si les conséquences des changements du pH_i ne sont pas faciles à établir, il est clair que l'augmentation de $[Cl^-]_i$ va stimuler la sortie électrogénique de Cl^- à travers la membrane basolatérale et dépolariser les cellules MD. De plus, l'augmentation de $[Cl^-]_i$ va contribuer à inhiber partiellement le cotransporteur apical dans un mécanisme de rétroaction négative.

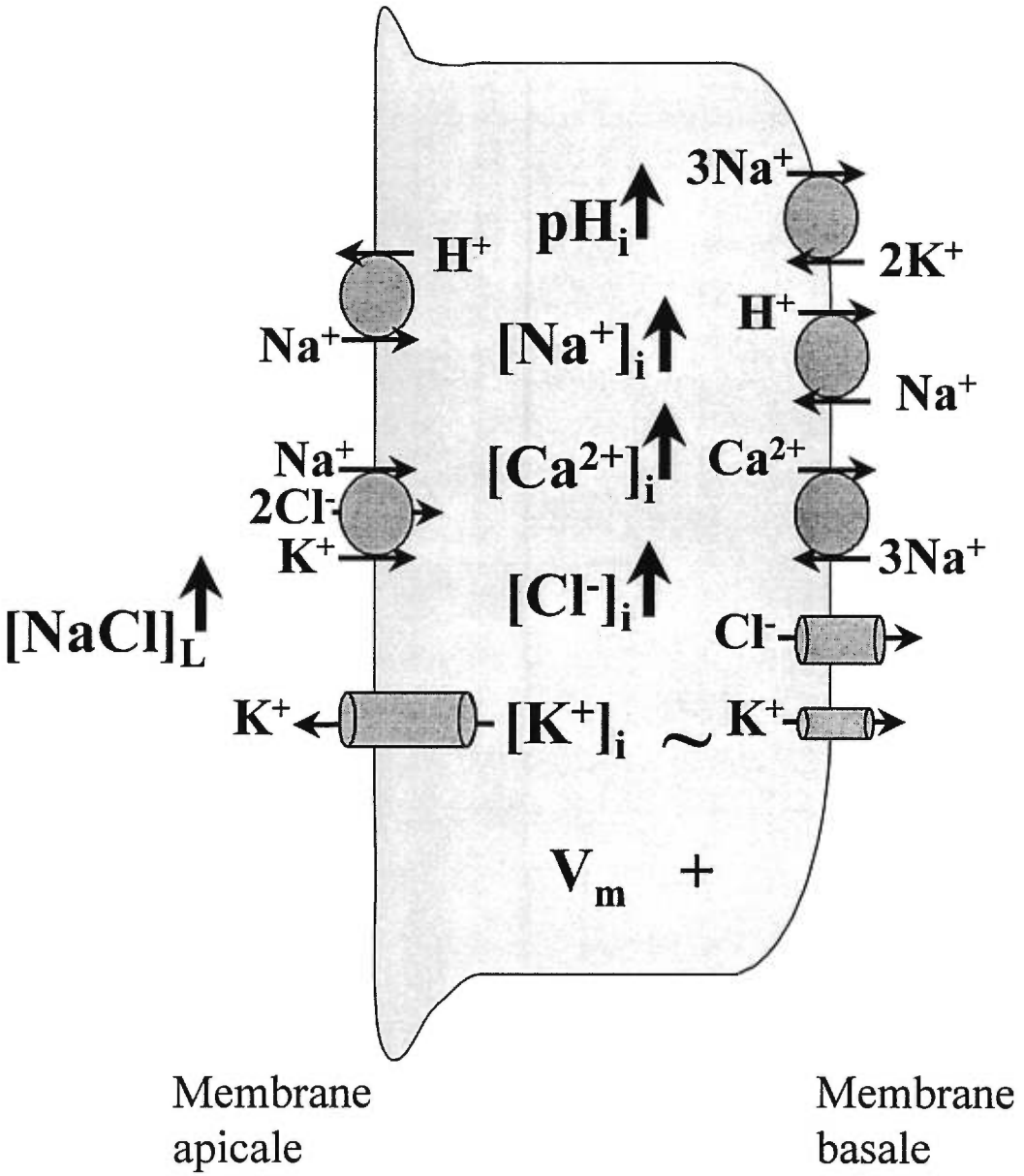

Figue 5. Effets intracellulaires de l'augmentation de $[NaCl]_L$

Un des effets les plus intéressants qu'une augmentation de $[Na^+]_i$ pourrait déclencher est une augmentation secondaire de $[Ca^{2+}]_i$. En effet, dans nos expériences de patch clamp, les effets du Na^+ extracellulaire étaient tout à fait compatibles avec la présence d'un échangeur Na^+:Ca^{2+}. Si cet échangeur est basolatéral, une augmentation de $[Na^+]_i$ diminuerait la grandeur du gradient de concentration pour le Na^+ à travers la membrane basolatérale et entraînerait une augmentation de $[Ca^{2+}]_i$. Le calcium intracellulaire étant un des messagers intracellulaires principaux, de nombreux effets sont attendus d'une augmentation de $[Ca^{2+}]_i$ (Figure 6):

- Le calcium intracellulaire peut activer la phospholipase A_2 (PLA_2) et augmenter le taux d'acide arachidonique. Celui-ci conduit à la formation de métabolites vasoactifs qui, en quittant les cellules de la MD par un moyen inconnu, vont agir sur l'AA. A date, le mécanisme d'action de ces métabolites reste encore un mystère.
- Le calcium intracellulaire peut aussi libérer l'ATP à partir des mitochondries. L'ATP peut être dégradé en adénosine ou sécrété directement dans l'interstitium. L'adénosine peut diffuser en dehors des cellules de la MD et exercer via les récepteurs de type A_1 un effet vasoconstricteur sur les cellules musculaires lisses de l'AA (171,172). L'ATP peut lui aussi diffuser (126,146) vers l'interstitium

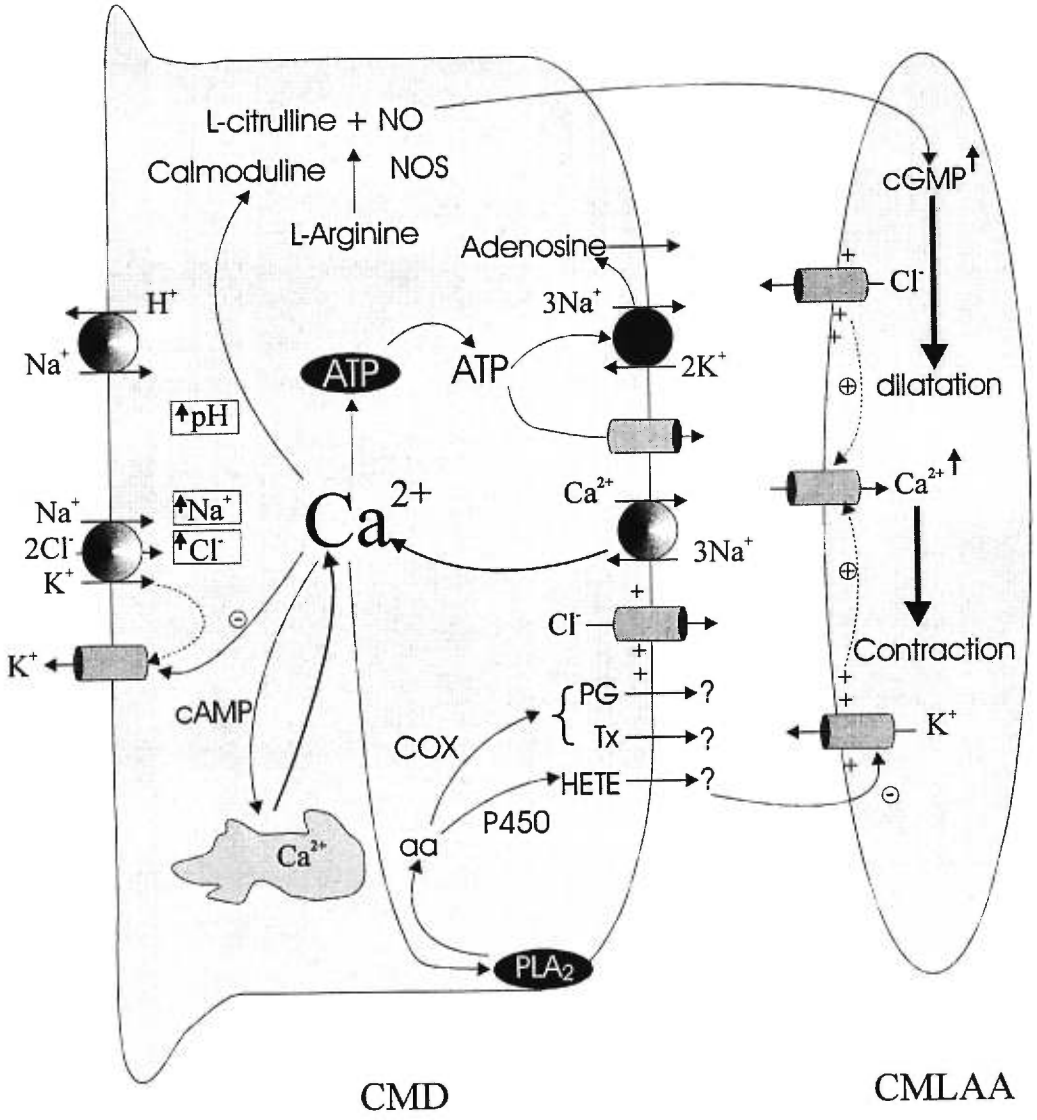

Figure 6. Les différentes voies possibles impliquées dans le signal de la rétroaction tubuloglomérulaire. CMD: cellule de la macula densa; CMLAA: cellule musculaire lisse de l'artériole afférente; COX: cyclooxygénase; PLA_2: phospholipase A_2; aa: acide arachidonique

et exercer via les récepteurs P_2 un effet vasocontricteur sur l'AA (58,59,60).

- Le calcium intracellulaire peut activer la NOS par l'entremise de la calmoduline. Le NO ainsi formée diffuse vers les cellules musculaires lisses de l'AA, où elle active la GC-s et augmente les taux intracellulaires de GMPc. Ce dernier par une série de phosphorylation-déphosphorylation relaxe le muscle lisse de l'AA.

La suite des événements qui relient une augmentation de $[Na^+]_i$, de $[Cl^-]_i$, et une alcalinisation des cellules de la MD d'une part, à la contraction des artérioles afférentes, d'autre part, reste encore à déterminer. On sait cependant que l'avant-dernière étape avant la contraction est une entrée de Ca^{2+} dans les cellules musculaires lisses de l'artériole afférente par l'intermédiaire de canaux calciques sensibles au potentiel et à la nifedipine (98). Le problème de la résolution des mécanismes de signalisation impliqués dans la RTG consiste à relier les événements initiaux dus à une augmentation de $[NaCl]_l$ aux mécanismes qui vont dépolariser les cellules musculaires lisses de l'artériole afférente. Il est fort possible que les cellules mésangiales extraglomérulaires soient impliquées dans la transmission du signal de la RTG. La présence au niveau des cellules mésangiales extraglomérulaires de canaux Cl^- activés par le Ca^{2+} (90) et la découverte de l'isoforme BSC2 du cotransporteur $Na^+ :K^+ :2Cl^-$

dans les cellules mésangiales extraglomérulaires et les cellules musculaires lisses de l'AA (70) commencent à donner de l'importance au Cl^- dans la transmission du signal de la RTG.

D. CONCLUSION GÉNÉRALE

Les résultats obtenus au cours des présents travaux ont enrichi considérablement notre connaissance des mécanismes de transport membranaire des cellules de la MD.

Nous avons démontré qu'il est possible d'exposer les cellules de la MD par microdissection et d'appliquer pour la première fois à ces cellules la technique de patch clamp. Avec celle-ci, nous ouvrons une voie d'étude nouvelle et prometteuse, qui pourrait avoir un impact très positif sur l'avancement de la compréhension de la RTG. En ce qui nous concerne, nous avons mis en évidence la présence dans la membrane apicale d'un canal K^+. Cette conductance K^+ est modulée par le Ca^{2+} et le pH mais est insensible à l'ATP. On ne sait cependant pas si elle est modulée par les niveaux physiologiques de Ca^{2+} cystosolique.

Nos études ont également mis en évidence la présence d'un échangeur Na^+ :H^+ sur la membrane apicale de la MD. Cet échangeur a la propriété d'être activé au cours de l'augmentation de $[NaCl]_l$ ou de $[Na^+]_l$, ce qui lui confère un rôle éventuel dans la RTG.

En ce qui concerne le cotransporteur Na^+ :K^+ :$2Cl^-$, nous avons démontré que celui-ci fonctionne près de son point d'équilibre et qu'il est capable de maintenir un flux (NH_4^+) de même grandeur que celui de la TAL. Nous devons donc reconsidérer l'hypothèse selon laquelle le taux de transport

des cellules de la MD est faible, compte tenu de la faible activité Na^+:K^+-ATPasique.

Nos travaux ont également identifié une modulation par l'AMPc de la conductance au Cl^- de la membrane basolatérale. En effet, nos résultats suggèrent que ce second messager active cette conductance. De même, l'AMPc s'est montré inhibiteur du cotransporteur Na^+ :K^+ :2Cl^-.

Contrairement à ce qu'il a été suggéré par les études antérieures, la membrane apicale est très perméable au NH_3. Par ailleurs, le flux de NH_4^+ n'est pas égal mais 2 à 3 fois supérieures au taux de production de H^+.

Enfin, le présent travail a permis d'identifier dans la membrane apicale un autre nouveau transporteur, capable d'exporter le H^+ et de faire entrer le NH_4^+ dans les cellules de MD.

E. PERSPECTIVES

Quoique les travaux menés jusqu'à présent aient identifié plusieurs types de transports, il reste beaucoup à apprendre sur leur rôle exact dans la transmission du signal de la RTG. Nous ne savons encore rien sur leur mécanisme de régulation, sur l'endroit où différents modulateurs de la RTG produisent leur effet, et sur ce qui se passe dans les cellules mésangiales extraglomérulaires. En fait, il existe jusqu'à nos jours un grand vide dans la compréhension du phénomène de transmission du signal de la RTG entre les effets immédiats du transport apical de NaCl et la dépolarisation des cellules musculaires lisses de l'AA. Trois approches peuvent s'avérer intéressantes pour combler cette lacune.

1. La technique de mesure de flux à l'aide de NH_4^+ pourrait permettre de compléter l'étude de la régulation du cotransporteur $Na^+:K^+:2Cl^-$, d'identifier le transporteur apical sensible au barium et de déterminer les mécanismes de transports basolatéraux incluant la $Na^+:K^+$-ATPase.

2. La technique de microperfusion, combinée à la mesure de changements de la concentration de Ca^{2+} dans les cellules musculaires lisses de l'AA, permettra d'étudier in vitro la transmission du signal de la RTG.

3. Une mise en culture des cellules de la MD permettra une caractérisation plus poussée de ces cellules. Finalement, une co-culture des cellules de la MD et

des cellules mésangiales extraglomérulaires devrait permettre de dévoiler le secret du mécanisme de transmission du signal de la RTG.

F. BIBLIOGRAPHIE

BIBLIOGRAPHIE

1. **Amlal H. Paillard M. Bichara M.** NH_4^+ transport pathways in cells of medullary thick ascending limb of rat kidney. NH_4^+ conductance and $K^+/NH_4^+(H^+)$ antiport. J. Biol. Chem. 269(35):21962-71, 1994 Sep 2.

2. **Bachmann S. Koeppen-Hagemann I. Kriz W.** Ultrastructural localization of Tamm-Horsfall glycoprotein (THP) in rat kidney as revealed by protein A-gold immunocytochemistry. Histochemistry. 83(6):531-8, 1985.

3. **Barajas, L., Salido, E.C., and Powers, K.V.,** Anatomical basis of the tubuloglomerular feedback mechanism: the juxtaglomerular apparatus. In: Persson AEG, Boberg U (eds) The juxtaglomerular apparatus. Elsevier Science Publishers New York pp7-26,1988.

4. **Barajas, L.** Cell-specific protein and gene expression in the juxtaglomerular apparatus. Clin.Exp. Pharmacol. Physiol. 24(7):520-526, 1997.

5. **Beeuwkes, R., III, and Rosen, S.** Renal Na-K-ATPase: Localization and quantitation by mean of its K -dependent phosphatase activity. In: Current Topics in Membranes and Transport, Vol. 13: Cellular Mechanisms of Renal Tubular ion Transport, edited by E. L. Boulpaep, Academic Press, New York, p. 344-354,1980.

6. **Bell PD. Navar LG. Ploth DW. McLean CB.** Tubuloglomerular feedback responses during perfusion with nonelectrolyte solutions in the rat. Kidney Int., 18(4):460-71, 1980 Oct.

7. **Bell PD. McLean CB. Navar LG.** Dissociation of tubuloglomerular feedback responses from distal tubular chloride concentration in the rat. Am. J. Physiol. 240(2):F111-9, 1981 Feb.

8. **Bell PD. Navar LG.** Cytoplasmic calcium in the mediation of macula densa tubulo-glomerular feedback responses. Science. 215(4533):670-3, 1982 Feb 5.

9. **Bell PD. Reddington M.** Intracellular calcium in the transmission of tubuloglomerular feedback signals. Am. J. Physiol. 245(3):F295-302, 1983 Sep.

9a. **Bell PD.** Cyclic AMP-calcium interaction in the transmission of tubuloglomerular feedback signals. Kidney Int. 28(5):728-32, 1985 Nov.

10. **Bell PD.** Tubuloglomerular feedback responses in the rat during calmodulin inhibition. Am. J. Physiol. 250(4 Pt 2):F715-9, 1986 Apr.

11. **Bell PD. Franco M. Navar LG.** Calcium as a mediator of tubuloglomerular feedback. Annu. Rev. Physiol. 49:275-93, 1987.

12. **Bell, P.D., Franco-Guevara, M., Abrahamson, D.R., Lapointe, J.Y., and Cardinal, J.** Cellular mechanisms for tubuloglomerular feedback signaling. In: Persson A.E.G., Boberg U. (eds) The juxtaglomerular apparatus. Elsevier Science Publishers New York pp 63-77,1988.

13. **Bell PD. Lapointe JY. Cardinal J.** Direct measurement of basolateral membrane potentials from cells of the macula densa. Am. J. Physiol. 257(3 Pt 2):F463-8, 1989 Sep.

14. **Bell PD, Lapointe JY.** Characteristics of membrane transport processes of macula densa cells. Clin Exp Pharmacol Physiol 1997 Jul;24(7):541-547

15. **Biemesderfer D. Pizzonia J. Abu-Alfa A. Exner M. Reilly R. Igarashi P. Aronson PS.** NHE3: a Na^+/H^+ exchanger isoform of renal brush border. Am. J. Physiol. 265(5 Pt 2):F736-42, 1993 Nov.

16. **Bleich M. Schlatter E. Greger R.** The luminal K^+ channel of the thick ascending limb of Henle's loop. Pflugers Arch. Eur. J. Physiol. 415(4):449-60, 1990 Jan.

17. **Bleich M. Kottgen M. Schlatter E. Greger R.** Effect of NH_4^+/NH_3 on cytosolic pH and the K^+ channels of freshly isolated cells from the thick ascending limb of Henle's loop. Pflugers Arch. Eur. J. Physiol. 429(3):345-54, 1995 Jan.

18. **Boberg, U., Seney, F.D., Persson, A.E.G., and Wright, F.S.,**. Signal for tubuloglomerular feedback control of GFR: responses to both sodium and chloride. Kidney Int., 31: 420, 1987.

19. **Boberg, U., and Wright, F.S.** Distal NaCl concentration as signal for the juxtaglomerular feedback mechanism. In: The Juxtaglomerular apparatus. Amsterdam: Elsevier, p. 89-96,1988.

20. **Boll HU. Forssmann WG. Taugner R.** Studies on the juxtaglomerular apparatus. IV. Freeze-fracturing of membrane surfaces. Cell & Tissue Research. 161(4):459-69, 1975 Aug 27.

21. **Bonsib, S.M. 1987**. The macula densa tubular basement membrane: a plaque of specialized basement membrane. Proc. Xth Internatl. Cong. of Nephr. p315

22. **Bookstein C. DePaoli AM. Xie Y. Niu P. Musch MW. Rao MC. Chang EB.** Na^+/H^+ exchangers, NHE-1 and NHE-3, of rat intestine. Expression and localization. J.Clin. Invest. 93(1):106-13, 1994 Jan.

23. **Braam B. Mitchell KD. Koomans HA. Navar LG.** Relevance of the tubuloglomerular feedback mechanism in pathophysiology. J. Am. Soc. Nephrol. 4(6):1257-74, 1993 Dec.

24. **Briggs, J., Kokko, J., and Jacobsen, H.R.,** Proc. Ixth Int. Cong. Nephrol., 406A.1984.

25. **Burnham C. Karlish SJ. Jorgensen PL.** Identification and reconstitution of a $Na^+/K^+/Cl^-$ cotransporter and K^+ channel from luminal membranes of renal red outer medulla. Biochim. Biophys. Acta. 821(3):461-9, 1985 Dec 19.

26. **Burnstock, G.** A basis for distinguishing two types of purinergic receptor. In: Cell Membrane Receptors For Drugs and Hormones: A Multidisciplinary Approach. New York: Raven, p. 107-118. 1978.

27. **Carroll MA. Sala A. Dunn CE. McGiff JC. Murphy RC.** Structural identification of cytochrome P450-dependent arachidonate metabolites formed by rabbit medullary thick ascending limb cells. J. Biol. Chem. 266(19):12306-12, 1991 Jul 5.

28. **Casellas D. Moore LC.** Autoregulation and tubuloglomerular feedback in juxtamedullary glomerular arterioles. Am. J. Physiol. 258(3 Pt 2):F660-9, 1990 Mar.

29. **Christensen JA. Meyer DS. Bohle A.** The structure of the human juxtaglomerular apparatus. A morphometric, lightmicroscopic study on serial sections. Virchows Archiv. A, Pathological Anatomy & Histology. 367(2):83-92, 1975 Jul 17.

30. **Edwards R.M.** Segmental effects of norepinephrine and angiotensin II on isolated renal microvessels. Am. J. Physiol. 244: F526-F534, 1983.

31. **Forster, R.P., and Maes, J.P.** Effect of experimental neurogenic hypertension on renal blood flow and glomerular filtration rates in intact denervated kidneys of unanesthetized rabbit with adrenal glands demedullated. Am. J. Physiol., 150: 534-540. 1947.

32. **Fowler, B.C., Chang, Y.S., Laamarti, A., Higdon, M., Lapointe, J.Y., and Bell, P.D.** Evidence for apical sodium proton exchange in macula densa cells. Kidney Int. 47: 746-751,1995.

33. **Franco, M., Bell, P.D., and Navar, L.G.,** Evaluantion of prostaglandins as mediators of tubuloglomerular feedback. Am. J. Physiol. 254 (Renal Fluid Electrolyte Physiol. 23): F642-F649, 1988.

35. **Gamba G. Miyanoshita A. Lombardi M. Lytton J. Lee WS. Hediger MA.** Molecular cloning, primary structure, and characterization of two members of the mammalian electroneutral sodium-(potassium)-chloride cotransporter family expressed in kidney. J. Biol. Chem. 269(26):17713-22, 1994 Jul 1.

36. **Garg LC. Knepper MA. Burg MB.** Mineralocorticoid effects on Na-K-ATPase in individual nephron segments. Am. J. Physiol. 240(6):F536-44, 1981 Jun.

36a. **Golchini K, Kurtz I.** NH3 permeation through the apical membrane of MDCK cells is via a lipid pathway. Am J Physiol. 255(1Pt 2):F135-F141,1988 Jul

37. **Goligorsky MS, Iijima K, Krivenko Y, Tsukahara H, Hu Y, Moore LC.** Role of mesangial cells in macula densa to afferent arteriole information transfer. Clin Exp Pharmacol Physiol 1997 Jul;24(7):527-531

38. **Gonzalez E. Salomonsson M. Muller-Suur C. Persson AE.** Measurements of macula densa cell volume changes in isolated and perfused rabbit cortical thick ascending limb. II. Apical and basolateral cell osmotic water permeabilities. Acta Physiol. Scand. 133(2):159-66, 1988 Jun.

39. **Gonzalez, E., Salomonsson, M., Muller-Suur, C., and Persson, A.E.G.** NaCl transport and osmotic water permeability of macula densa cells contained in isolated and perfused rabbit kidney tubules. In The Juxtaglomerullar apparatus. Amsterdam: Elsevier, p. 97-119,1988.

40. **Good DW.** Effects of potassium on ammonia transport by medullary thick ascending limb of the rat. J. Clin. Invest. 80(5):1358-65, 1987 Nov.

41. **Good DW.** Active absorption of NH_4^+ by rat medullary thick ascending limb: inhibition by potassium. Am. J. Physiol. 255(1 Pt 2):F78-87, 1988 Jul.

42. **Good DW. Knepper MA.** Mechanisms of ammonium excretion: role of the renal medulla. Seminars in Nephrology. 10(2):166-73, 1990 Mar.

43. **Goormaghtigh. N**. L'appareil neuro-myo-artérial juxta-glomérulaire du rein; ses réactions en pathologie et ses rapports avec le tube urinifère. C.R.Soc. Biol. 124: 293-296,1937.

44. **Gottschalk CW. Leyssac PP.** Proximal tubular function in rats with low inulin clearance. Acta Physiol. Scand. 74(3):453-64, 1968 Nov.

45. **Greger R.** Coupled transport of Na^+ and Cl^- in the thick ascending limb of Henle's loop of rabbit nephron. Scandinavian Audiology. Supplementum. 14 Suppl:1-15, 1981.

46. **Greger R.** Ion transport mechanisms in thick ascending limb of Henle's loop of mammalian nephron. Physiol. Rev. 65(3):760-97, 1985 Jul.

47. **Guggino SE. Guggino WB. Green N. Sacktor B.** Blocking agents of Ca^{2+}-activated K^+ channels in cultured medullary thick ascending limb cells. Am. J. Physiol. 252(2 Pt 1):C128-37, 1987 Feb.

48. **Gutsche HU. Muller-Suur R. Hegel U. Hierholzer K.** Electrical conductivity of tubular fluid of the rat nephron. Micropuncture study of the diluting segment in situ. Pflugers Arch. Eur. J. Physiol. 383(2):113-21, 1980 Jan.

50. **Haas M. McBrayer DG. Yankaskas JR.** Dual mechanisms for Na-K-Cl cotransport regulation in airway epithelial cells. Am. J. Physiol. 264(1 Pt 1):C189-200, 1993 Jan.

51. **Haas M.** The Na-K-Cl cotransporters. Am. J. Physiol. 267(4 Pt 1):C869-85, 1994 Oct.

52. **Hackenthal E. Paul M. Ganten D. Taugner R**. Morphology, physiology, and molecular biology of renin secretion. Physiol. Rev. 70(4):1067-116, 1990 Oct.

53. **Haberle DA. von Baeyer H.** Characteristics of glomerulotubular balance. Am. J. Physiol. 244(4):F355-66, 1983 Apr.

53a. **Hebert SC.** An ATP-regulated, inwardly rectifying potassium channel from rat kidney (ROMK). Kidney Int. 48(4):1010-1016, 1995 Oct

54. **Hess, R., and Gross, F.** Glucose-6-phosphate dehydrogenase and renin in kidneys of hypertensive or adrenalectomized. Am. J. Physiol., 197:869-872, 1959.

55. **Huang WC. Bell PD. Harvey D. Mitchell KD. Navar LG.** Angiotensin influences on tubuloglomerular feedback mechanism in hypertensive rats. Kidney Int. 34(5):631-7, 1988 Nov.

56. **Hurst AM. Lapointe JY. Laamarti A. Bell PD.** Basic properties and potential regulators of the apical K^+ channel in macula densa cells. J. Gen. Physiol. 103(6):1055-70, 1994 Jun.

57. **Igarashi P. Vanden Heuvel GB. Payne JA. Forbush B 3rd.** Cloning, embryonic expression, and alternative splicing of a murine kidney-specific Na-K-Cl cotransporter. Am. J. Physiol. 269(3 Pt 2):F405-18, 1995 Sep.

58. **Inscho, E.W., Carmines, P.K., and Navar, L.G.** Juxtamedullary afferent arteriolar responses to P1 and P2 purinergic stimulation. Hypertension Dallas 17: 1033-1037,1991.

59. **Inscho EW. Ohishi K. Navar LG.** Effects of ATP on pre- and postglomerular juxtamedullary microvasculature. Am. J. Physiol. 263(5 Pt 2):F886-93, 1992 Nov.

60. **Inscho EW. Ohishi K. Cook AK. Belott TP. Navar LG.** Calcium activation mechanisms in the renal microvascular response to extracellular ATP. Am. J. Physiol. 268(5 Pt 2):F876-84, 1995 May.

61. **Ito S. Carretero OA.** An in vitro approach to the study of macula densa-mediated glomerular hemodynamics. Kidney Int. 38(6):1206-10, 1990 Dec.

62. **Ito S. Juncos LA. Carretero OA.** Pressure-induced constriction of the afferent arteriole of spontaneously hypertensive rat. Hypertension 19 (Suppl. II) : II-164-7, 1992

63. **Ito S. Ren Y.** Evidence for the role of nitric oxide in macula densa control of glomerular hemodynamics. J. Clin. Invest. 92(2):1093-8, 1993 Aug.

65. **Juncos LA. Garvin J. Carretero OA. Ito S.** Flow modulates myogenic responses in isolated microperfused rabbit afferent arterioles via endothelium-derived nitric oxide. J. Clin. Invest. 95: 2741-8, 1995.

66. **Kaissling B. Kriz W.** Structural analysis of the rabbit kidney. Advances in Anatomy, Embryology & Cell Biology. 56:1-123, 1979.

67. **Kaissling B. Kriz W.** Variability of intercellular spaces between macula densa cells: a transmission electron microscopic study in rabbits and rats. Kidney Int.- Supp. 12:S9-17, 1982 Aug.

68. **Kaji DM.** Na+/K+/2Cl- cotransport in medullary thick ascending limb cells: kinetics and bumetanide binding. Biochim. Biophys. Acta. 1152(2):289-99, 1993 Nov.

69. **Kaplan MR. Plotkin MD. Lee WS. Xu ZC. Lytton J. Hebert SC.** Apical localization of the Na-K-Cl cotransporter, rBSC1, on rat thick ascending limbs. Kidney Int. 49(1):40-7, 1996 Jan.

70. **Kaplan MR. Plotkin MD. Brown D. Hebert SC. Delpire E.** Expression of the mouse Na-K-2Cl cotransporter, mBSC2, in the terminal inner medullary collecting duct, the glomerular and extraglomerular mesangium, and the glomerular afferent arteriole. J. Clin. Invest. 98(3):723-30, 1996 Aug 1.

71. **Kashgarian M. Biemesderfer D. Caplan M. Forbush B 3d.** Monoclonal antibody to Na,K-ATPase: immunocytochemical localization along nephron segments. Kidney Int. 28(6):899-913, 1985 Dec.

72. **Keeton TK. Campbell WB.** The pharmacologic alteration of renin release. Pharmcol. Rev. 32(2):81-227, 1980 Jun.

73. **Kikeri D. Sun A. Zeidel ML. Hebert SC.** Cell membranes impermeable to NH_3. Nature. 339(6224):478-80, 1989 Jun 8.

74. **Kikeri D. Sun A. Zeidel ML. Hebert SC.** Cellular NH_4^+/K^+ transport pathways in mouse medullary thick limb of Henle. Regulation by intracellular pH. J.Gen. Physiol. 99(3):435-61, 1992 Mar.

75. **Kinne R. Kinne-Saffran E. Schutz H. Scholermann B.** Ammonium transport in medullary thick ascending limb of rabbit kidney: involvement of the $Na^+:K^+:Cl^-$ cotransporter. J. Membr. Biol. 94(3):279-84, 1986.

76.**Kirk, K.L., Schafer, J.A., and DiBona, D.R.** Optical methods for analysis of function in isolated nephron segments. In: Dinno, M.A., Callahan, A.B. and Rozzell, T.C. (Eds) Membrane Biophysics II: Physical Methods in the Study of Epithelia., New York: Liss. p. 21-36, 1983.

77.**Kirk KL. Bell PD. Barfuss DW. Ribadeneira M.** Direct visualization of the isolated and perfused macula densa. Am. J. Physiol. 248(6 Pt 2):F890-4, 1985

77a. **Klocke RA, Andersson KK, Rotman HH, Forster RE**. Permeability of human erythrocytes to ammonia and weak acids. Am J Physiol. 222(4):1004-1013, 1972 Apr

78.**Koenig B. Ricapito S. Kinne R.** Chloride transport in the thick ascending limb of Henle's loop: potassium dependence and stoichiometry of the NaCl cotransport system in plasma membrane vesicles. Pflugers Arch. Eur. J. Physiol. 399(3):173-9, 1983 Nov.

79.**Krompecher-Kiss,E., and Bucher, O.** Comparison of the activities of some dehydrogenases in the juxtaglomerular complex of kidneys of wistar rats and desert rats (Meriones culati). Histochemistry, 53:265-269, 1977.

80. **Laamarti, A.M. Lapointe JY.** Determination of NH_4^+/NH_3 fluxes across the apical membrane of macula densa cells : a quantitative analysis. Am. J. Physiol. 273 (Renal Physiol.42) : F817-F824,1997.

81. **Laamarti, M.A., Bell PD. Lapointe JY.** Transport and regulatory properies of the apical Na :K :2Cl cotransporter of macula densa. Am. J. Physiol (en révision).

82. **Lapointe JY. Bell PD. Cardinal J.** Direct evidence for apical $Na^+:2Cl^-:K^+$ cotransport in macula densa cells. Am. J. Physiol. 258(5 Pt 2):F1466-9, 1990 May.

83. **Lapointe JY. Bell PD. Hurst AM. Cardinal J.** Basolateral ionic permeabilities of macula densa cells. Am. J. Physiol. 260(6 Pt 2):F856-60, 1991 Jun.

84. **Lapointe JY. Laamarti A. Hurst AM. Fowler BC. Bell PD.** Activation of Na:2Cl:K cotransport by luminal chloride in macula densa cells. Kidney Int. 47(3):752-7, 1995 Mar.

85. **Latta, H., and Maunsbach, A.** Juxtaglomerular apparatus as studied electron microscopically. J.Ultrastruct. Res., 6: 547-561, 1962.

86. **Leung S. O'Donnell M.E. Martinez A. Palfrey H.C.** Regulation by nerve growth factor and protein phosphorylation of Na:K:2Cl cotransport and cell volume in PC12 cells. J.Biol. Chem. 269: 10581-9, 1994.

87. **Lonnerholm G. Wistrand PJ.** Carbonic anhydrase in the human kidney: a histochemical and immunocytochemical study. Kidney Int. 25(6):886-98, 1984 Jun.

88. **Lorenz JN. Weihprecht H. Schnermann J. Skott O. Briggs JP.** Characterization of the macula densa stimulus for renin secretion. Am. J. Physiol. 259(1 Pt 2):F186-93, 1990 Jul.

89. **Lytle C. Xu JC. Biemesderfer D. Forbush B 3rd.** Distribution and diversity of Na-K-Cl cotransport proteins: a study with monoclonal antibodies. Am. J. Physiol. 269(6 Pt 1):C1496-505, 1995 Dec.

90. **Matsunaga H. Yamashita N. Okuda T. Kurokawa K.** Mesangial cell ion transport and tubuloglomerular feedback. Curr. Opin. Nephrol. Hypertens. 3(5):518-22, 1994 Sep.

94. **McManus, J.F.A.** The juxtaglomerular complex. Lancet 2: 394-396, 1942.

95. **McNicholas CM. Yang Y. Giebisch G. Hebert SC.** Molecular site for nucleotide binding on an ATP-sensitive renal K^+ channel (ROMK2). Am. J. Physiol. 271(2 Pt 2):F275-85, 1996 Aug.

96. **Messina A. Alcorn D. Ryan GB.** Intercellular spaces between macula densa cells: an ultrastructural study comparing high pressure perfusion fixation with in situ drip-fixation of rat kidney. Cell & Tissue Research. 250(2):461-4, 1987 Nov.

97. **Mitchell, K.D., and Navar, L.G.** The renin-angiotensin-aldosterone system in volume control. In: Bailliere's Clinical Endocrinology and Metabolism. London: Bailliere Tindall, p. 393-430, 1989.

98. **Mitchell KD. Navar LG.** Tubuloglomerular feedback responses during peritubular infusions of calcium channel blockers. Am. J. Physiol. 258(3Pt 2):F537-44, 1990 Mar.

99. **Mitchell KD. Navar LG.** Modulation of tubuloglomerular feedback responsiveness by extracellular ATP. Am. J. Physiol. 264(3 Pt 2):F458-66, 1993 Mar.

100. **Morgan T. Gillies A.** Factors controlling the release of renin. A micropuncture study in the cat. Pflugers Arch. Eur. J. Physiol. 368(1-2):13-8, 1977 Mar 11.

101. **Mrkic B. Forgo J. Murer H. Helmle-Kolb C.** Apical and basolateral Na/H exchange in cultured murine proximal tubule cells (MCT): effect of parathyroid hormone (PTH). J. Membr. Biol. 130(3):205-17, 1992 Dec.

102. **Mundel P. Bachmann S. Bader M. Fischer A. Kummer W. Mayer B. Kriz W.** Expression of nitric oxide synthase in kidney macula densa cells. Kidney Int. 42(4):1017-9, 1992 Oct.

103. **Navar, L.G., Burke, T.J., Robinson, R.R., and Clapp, J.R.** Distal tubular feedback in the autoregulation of single nephron glomerular filtration rate. J. Clin.Invest., 53:516-525, 1974.

104. **Navar, L.G., Bell, P.D., Thomas, C.E., and Williams, R.H.** Characteristics of glomerular feedback responses to distal nephron microperfusion in the dog. Cardiovasc. Med. 3:137-149,1977..

105. **Navar LG.** Renal autoregulation: perspectives from whole kidney and single nephron studies. Am. J. Physiol. 234(5):F357-70, 1978 May.

106. **Navar LG. Bell PD. Thomas CE. Ploth DW.** Influence of perfusate osmolality on stop-flow pressure feedback responses in the dog. Am. J. Physiol. 235(4):F352-8, 1978 Oct.

107. **Navar LG. Bell PD. Burke TJ.** Role of a macula densa feedback mechanism as a mediator of renal autoregulation. Kidney Int - Supp. 12:S157-64, 1982 Aug.

108. **Navar LG. Rosivall L.** Contribution of the renin-angiotensin system to the control of intrarenal hemodynamics. Kidney Int. 25(6):857-68, 1984 Jun.

109. **Navar LG. Inscho EW. Ibarrola M. Carmines PK.** Communication between the macula densa cells and the afferent arteriole. Kidney Int-Suppl. 32:S78-82, 1991 Jun.

110. **Navar, L.G., Carmines, P.K., Mitchell, K.D., and Bell, P.D.** Role of intracellular calcium in the regulation of renal hemodynamics. In: Proceeding of the 11th International Congress on Nephrology. New York: Spriner-Verlag, vol. 1, p. 718-730, 1991.

111. **Noel J. Pouyssegur J.** Hormonal regulation, pharmacology, and membrane sorting of vertebrate Na+/H+ exchanger isoforms. Am. J. Physiol. 268(2 Pt 1):C283-96, 1995 Feb.

112. **Nørgaard, T.** Quantitative measurement of glocose-6-phosphate dehydrogenase in cortical fractions of the rabbit nephron. Histochemistry, 63:103-113, 1979.

113. **Oberling, C., and Hatt, Y.** Etude de l'appareil juxtaglomérulaire du rat en microscope electronique. Ann. Anat. Pathol. (paris), 5:441-474, 1960.

114. **Obermuller N. Kunchaparty S. Ellison DH. Bachmann S.** Expression of the Na-K-2Cl cotransporter by macula densa and thick ascending limb cells of rat and rabbit nephron. J.Clin. Invest. 98(3):635-40, 1996 Aug 1.

115. **Ogasawara A. Hisa H. Satoh S.** Effects of nifedipine and TMB-8 on renal vasoconstriction induced by hypertonic saline in dogs. Eur. J. Pharmacol 243(1):103-6, 1993 Oct 12.

116. **Osswald H. Nabakowski G. Hermes H.** Adenosine as a possible mediator of metabolic control of glomerular filtration rate. Int. J. Biochem. 12(1-2):263-7, 1980.

117. **Paulais M. Teulon J.** cAMP-activated chloride channel in the basolateral membrane of the thick ascending limb of the mouse kidney. J. Membr. Biol. 113(3):253-60, 1990 Feb.

118. **Payne JA. Forbush B 3rd.** Alternatively spliced isoforms of the putative renal Na-K-Cl cotransporter are differentially distributed within the rabbit kidney. Proc. Natl.Acad. Sci. USA 91(10):4544-8, 1994 May 10.

119. **Payne JA. Xu JC. Haas M. Lytle CY. Ward D. Forbush B 3rd.** Primary structure, functional expression, and chromosomal localization of the bumetanide-sensitive Na-K-Cl cotransporter in human colon. J. Biol. Chem. 270(30):17977-85, 1995 Jul 28.

120. **Persson AEG. Schnermann J. Wright FS.** Modification of feedback influence on glomerular filtration rate by acute isotonic extracellular volume expansion. Pflugers Arch. 381: 99-106, 1979.

121. **Persson BE. Persson AE.** The existence of a tubulo-glomerular feedback mechanism in the Amphiuma nephron. Pflugers Arch. Eur. J. Physiol. 391(2):129-34, 1981Aug.

122. **Persson AE. Hahne B. Selen G.** The effect of tubular perfusion with PGE2, PGF2 alpha, and PGI2 on the tubuloglomerular feedback control in the rat. Can. J. Physiol. Pharmacol. 61(11):1317-23, 1983 Nov.

123. **Persson AE. Salomonsson M. Kornfeld M. Gutierrez AM. Gonzalez E.** Activation of the tubuloglomerular feedback mechanism in an in vitro preparation of the juxtaglomerular apparatus. Acta Physiol. Scand. 146(2):289-90, 1992 Oct.

124. **Ploth DW. Rudulph J. Thomas G. Navar LG.** Renal and tubuloglomerular feedback response to plasma expansion in the rat. Am. J. Physiol. 235: F156-62, 1978.

125. **Pricam C. Humbert F. Perrelet A. Orci L.** Gap junctions in mesangial and lacis cells. J. Cell Biol. 63(1):349-54, 1974 Oct.

126. **Reisin IL. Prat AG. Abraham EH. Amara JF. Gregory RJ. Ausiello DA. Cantiello HF.** The cystic fibrosis transmembrane conductance regulator is a dual ATP and chloride channel. J. Biol. Chem. 269(32):20584-91, 1994 Aug 12.

127. **Robertson C.R. Deen W.M. Troy J.L. Brenner B.M.** Dynamics of glomerular ultrafiltration in the rat. III. Hemodynamics and autoregulation. Am. J. Physiol. 223: 1191-1200, 1972.

128. **Salomonsson M. Gonzalez E. Westerlund P. Persson AE.** The effect of furosemide on the chloride concentration in the macula densa and in cortical thick ascending limb cells. Acta Physiol. Scand. 139(2):387-8, 1990 Jun.

129. **Salomonsson M. Gonzalez E. Westerlund P. Persson AE.** Intracellular cytosolic free calcium concentration in the macula densa and in ascending limb cells at different luminal concentrations of sodium chloride and with added furosemide. Acta Physiol. Scand. 142(2):283-90, 1991 Jun.

130. **Salomonsson M. Gonzalez E. Kornfeld M. Persson AE.** The cytosolic chloride concentration in macula densa and cortical thick ascending limb cells. Acta Physiol. Scand. 147(3):305-13, 1993 Mar.

131. **Schlatter E. Greger R.** cAMP increases the basolateral Cl^- conductance in the isolated perfused medullary thick ascending limb of Henle's loop of the mouse. Pflugers Arch. Eur. J. Physiol. 405(4):367-76, 1985 Dec.

132. **Schlatter E. Salomonsson M. Persson AE. Greger R.** Macula densa cells sense luminal NaCl concentration via furosemide sensitive Na+2Cl-K+ cotransport. Pflugers Arch. Eur. J. Physiol. 414(3):286-90, 1989 Jul.

133. **Schlatter E.** Effect of various diuretics on membrane voltage of macula densa cells. Whole-cell patch-clamp experiments. Pflugers Arch. Eur. J. Physiol. 423(1-2):74-7, 1993 Apr.

134. **Schnabel E. Kriz W.** Morphometric studies of the extraglomerular mesangial cell field in volume expanded and volume depleted rats. Anatomy & Embryology. 170(2):217-22, 1984.

135. **Schnermann J. Wright FS. Davis JM. Stackelberg W von. Grill G.** Regulation of superficial nephron filtration rate by tubulo-glomerular feedback. Pflugers Arch. Eur. J. Physiol. 318(2):147-75, 1970.

136. **Schnermann J. Ploth DW. Hermle M.** Activation of tubulo-glomerular feedback by chloride transport. Pflugers Arch. Eur. J. Physiol. 362(3):229-40, 1976 Apr 6.

137. **Schnermann J. Osswald H. Hermle M.** Inhibitory effect of methylxanthines on feedback control of glomerular filtration rate in the rat kidney. Pflugers Arch. Eur. J. Physiol. 369(1):39-48, 1977 May 6.

138. **Schnermann J. Schubert G. Hermle M. Herbst R. Stowe NT. Yarimizu S. Weber PC.** The effect of inhibition of prostaglandin synthesis on tubuloglomerular feedback in the rat kidney. Pflugers Arch. Eur. J. Physiol. 379(3):269-79, 1979 Apr 30.

139. **Schnermann J.** Localization, mediation and function of the glomerular vascular response to alterations of distal fluid delivery. Fed. Proc. 40(1):109-15, 1981 Jan.

140. **Schnermann J. Briggs JP.** Participation of renal cortical prostaglandins in the regulation of glomerular filtration rate. Kidney Int. 19(6):802-15, 1981 Jun.

141. **Schnermann J., Weber PC.** Reversal of indomethacin-induced inhibition of tubuloglomerular feedback by prostaglandin infusion. Prostaglandins. 24(3):351-61, 1982 Sep.

142. **Schnermann J., Briggs J.** Role of the renin-angiotensin system in tubuloglomerular feedback. Fed. Proc. 45(5):1426-30, 1986 Apr.

143. **Schnermann J., Marver D.** ATPase activity in macula densa cells of the rabbit kidney. Pflugers Arch. Eur. J. Physiol. 407(1):82-6, 1986 Jul.

144. **Schnermann J. Briggs J.P.** Interaction between loop of Henle flow and arterial pressure as determinants of glomerular pressure. Am. J. Physiol. 256: F421-9, 1989.

145. **Schnermann, J., and Briggs, J.P.** The juxtaglomerular apparatus. In: The Kidney: Physiology and Pathophysiology. chap. 35, pp1249-1289, ed. D.W. Seldin & G. Giebish, Raven Press, New York, 1992.

146. **Schwiebert EM., Egan ME., Hwang TH., Fulmer SB., Allen SS., Cutting GR., Guggino WB.** CFTR regulates outwardly rectifying chloride channels through an autocrine mechanism involving ATP. Cell. 81(7):1063-73, 1995Jun 30

147. **Selen F. Muller-Suur R. Persson AEG.** Activation of tubuloglomerular feedback mechanism in dehydrated rats. Acta Physiol. Scand. 117: 75-81, 1983

148. **Seney F.D. Wright F.S.** Signal for tubuloglomerular feedback control of GFR: separate change of sodium and chloride at constant osmolarity. Kidney Int. 29: 388, 1986.

149. **Sikri KL. Foster CL. MacHugh N. Marshall RD.** Localization of Tamm-Horsfall glycoprotein in the human kidney using immuno-fluorescence and immuno-electron microscopical techniques. J. Anat. 132(Pt 4):597-605, 1981 Jun.

150. **Skott O. Briggs JP.** Direct demonstration of macula densa-mediated renin secretion. Science. 237(4822):1618-20, 1987 Sep 25.

151. **Spanidis A. Wunsch H. Kaissling B. Kriz W.** Three-dimensional shape of a Goormaghtigh cell and its contact with a granular cell in the rabbit kidney. Anat. Embryol. 165(2):239-52, 1982.

152. **Spielman WS. Thompson CI.** A proposed role for adenosine in the regulation of renal hemodynamics and renin release. Am. J. Physiol. 242(5):F423-35, 1982 May.

153. **Taugner R. Schiller A. Kaissling B. Kriz W.** Gap junctional coupling between the JGA and the glomerular tuft. Cell & Tissue Research. 186(2):279-85, 1978 Jan 17.

154. **Taugner R. Rosivall L. Buhrle CP. Groschel-Stewart U.** Myosin content and vasoconstrictive ability of the proximal and distal (renin-positive) segments of the preglomerular arteriole. Cell & Tissue Research. 248(3):579-88, 1987 Jun.

155. **Taugner R. Hackenthal E.** The Juxtaglomerular Apparatus. Springer verlag, p215-218, 1989.

156. **Thurau, K.**, Renal hemodynamics. Am. J. Med. 36: 698-719, 1964.

157. **Thurau, K., and Schnermann, J.** Die Natrium-konzentration an den Macula densa Zellen als regulierender Factor für das Glomerulumfiltrat. Klin. Wochenschr. 43: 410-413, 1965.

158. **Thurau K.** Influence of sodium concentration at macula densa cells on tubular sodium load. Ann. NY. Acad. Sci. 139(2):388-99, 1966 Nov 22.

159. **Thurau, K.** Intrarenal action of angiotensin. Handbook of Experimental Pharmacology. New York: Springer-Verlag, vol. 37, p. 475-489, 1974.

160. **Thurau, K., and Mason, J.** The intrarenal function of the juxtaglomerular apparatus. In: Kidney and Urinary Tract Physiology. MTP International Review of Science: Physiology. London: Butterworth, series 1, vol.1, p. 357-389, 1974.

161. **Thurau, K.** Tubulo-glomerular feedback. In: Advances in Physiological Sciences. Kidney and Body Fluids. New York: Pergamon, vol. II, p. 75-82, 1981.

162. **Thorup C. Persson AE.** Inhibition of locally produced nitric oxide resets tubuloglomerular feedback mechanism. Am. J. Physiol. 267(4 Pt 2):F606-11, 1994 Oct.

163. **Tojo A. Gross SS. Zhang L. Tisher CC. Schmidt HH. Wilcox CS. Madsen KM.** Immunocytochemical localization of distinct isoforms of nitric oxide synthase in the juxtaglomerular apparatus of normal rat kidney. J. Am. Soc. Nephrol. 4(7):1438-47, 1994 Jan.

164.**Vander AJ.** Control of renin release. Physiol. Rev. 47(3):359-82, 1967 Jul.

165. **Vigne P. Farre A.L. Frelin C.** Na:K:2Cl cotransporter of brain capillary endothelial cells. J. Biol. Chem. 269: 19925-30, 1994.

166. **Wang, WH, White S, Geibel J, Giebisch G.** A potassium channel in the apical membrane of rabbit thick ascending limb of Henle's loop. Am J Physiol 1990 Feb;258(2 Pt 2):F244-F253

167. **Wang W, Giebisch G.** Dual effect of adenosine triphosphate on the apical small conductance K+ channel of the rat cortical collecting duct. J Gen Physiol 1991 Jul;98(1):35-61

168. **Wang W. Lu M.** Effect of arachidonic acid on activity of the apical K^+ channel in the thick ascending limb of the rat kidney. J. Gen. Physiol. 106(4):727-43, 1995 Oct.

169. **Wang WH. Lu M. Hebert SC.** Cytochrome P-450 metabolites mediate extracellular Ca^{2+}-induced inhibition of apical K^+ channels in the TAL.
Am. J. Physiol. 271(1 Pt 1):C103-11, 1996 Jul.

170. **Watts BA 3rd. Good DW.** Effects of ammonium on intracellular pH in rat medullary thick ascending limb: mechanisms of apical membrane NH_4^+ transport. J. Gen. Physiol. 103(5):917-36, 1994 May.

171. **Weaver DR. Reppert SM.** Adenosine receptor gene expression in rat kidney. Am. J. Physiol. 263(6 Pt 2):F991-5, 1992 Dec.

172. **Weihprecht H. Lorenz JN. Briggs JP. Schnermann J.** Vasomotor effects of purinergic agonists in isolated rabbit afferent arterioles. Am. J. Physiol. 263(6 Pt 2):F1026-33, 1992 Dec.

173. **Welch WJ. Wilcox CS.** Modulating role for thromboxane in the tubuloglomerular feedback response in the rat. J. Clin. Invest. 81(6):1843-9, 1988 Jun.

174. **Welch WJ. Wilcox CS.** Potentiation of tubuloglomerular feedback in the rat by thromboxane mimetic. Role of macula densa. J. Clin. Invest. 89(6):1857-65, 1992 Jun.

175. **Wilcox CS. Welch WJ. Murad F. Gross SS. Taylor G. Levi R. Schmidt.** Nitric oxide synthase in macula densa regulates glomerular capillary pressure. Proc. Natl. Acad. Sci. USA. 89(24):11993-7, 1992 Dec 15.

176. **Woodhall PB. Tisher CC.** Response of the distal tubule and cortical collecting duct to vasopressin in the rat. J. Clin. Invest. 52(12):3095-108, 1973 Dec.

177. **Wright FS. Schnermann J.** Interference with feedback control of glomerular filtration rate by furosemide, triflocin, and cyanide. J. Clin. Invest. 53(6):1695-708, 1974 Jun.

178. **Wright FS. Briggs JP.** Feedback control of glomerular blood flow, pressure, and filtration rate. Physiol. Rev. 59(4):958-1006, 1979 Oct.

179. **Yang T. Huang YG. Singh I. Schnermann J. Briggs JP.** Localization of bumetanide- and thiazide-sensitive Na-K-Cl cotransporters along the rat nephron. Am. J. Physiol. 271(4 Pt 2):F931-9, 1996 Oct.

180. **Zou AP. Imig JD. Ortiz de Montellano PR. Sui Z. Falck JR. Roman RJ.** Effect of P-450 omega-hydroxylase metabolites of arachidonic acid on tubuloglomerular feedback. Am. J. Physiol. 266(6 Pt 2):F934-41, 1994 Jun.